



University of Kentucky
UKnowledge

University of Kentucky Doctoral Dissertations

Graduate School

2003

ORIGINS OF ISOPRENOID DIVERSITY: A STUDY OF STRUCTURE-FUNCTION RELATIONSHIPS IN SESQUITERPENE SYNTHASES

Bryan T. Greenhagen
University of Kentucky, btgree0@uky.edu

[Right click to open a feedback form in a new tab to let us know how this document benefits you.](#)

Recommended Citation

Greenhagen, Bryan T., "ORIGINS OF ISOPRENOID DIVERSITY: A STUDY OF STRUCTURE-FUNCTION RELATIONSHIPS IN SESQUITERPENE SYNTHASES" (2003). *University of Kentucky Doctoral Dissertations*. 440.
https://uknowledge.uky.edu/gradschool_diss/440

This Dissertation is brought to you for free and open access by the Graduate School at UKnowledge. It has been accepted for inclusion in University of Kentucky Doctoral Dissertations by an authorized administrator of UKnowledge. For more information, please contact UKnowledge@lsv.uky.edu.

ABSTRACT OF DISSERTATION

Bryan T. Greenhagen

The Graduate School
University of Kentucky
2003

ORIGINS OF ISOPRENOID DIVERSITY: A STUDY OF STRUCTURE-FUNCTION
RELATIONSHIPS IN SESQUITERPENE SYNTHASES.

ABSTRACT OF DISSERTATION

A dissertation submitted in partial fulfillment of the
requirements for the degree of Doctor of Philosophy in the
Department of Agriculture at the University of Kentucky

by

Bryan T. Greenhagen

Lexington, KY

Director: Dr. Joseph Chappell, Professor

Lexington, KY

Copyright © Bryan T. Greenhagen 2003

ABSTRACT OF DISSERTATION

ORIGINS OF ISOPRENOID DIVERSITY: A STUDY OF STRUCTURE-FUNCTION RELATIONSHIPS IN SESQUITERPENE SYNTHASES.

Plant sesquiterpene synthases catalyze the conversion of the linear substrate farnesyl diphosphate, FPP, into a remarkable array of secondary metabolites. These secondary metabolites in turn mediate a number of important interactions between plants and their environment, such as plant-plant, plant-insect and plant-pathogen interactions. Given the relative biological importance of sesquiterpenes and their use in numerous practical applications, the current thesis was directed towards developing a better understanding of the mechanisms employed by sesquiterpene synthases in the biosynthesis of such a diverse class of compounds.

Substrate preference for sesquiterpene synthases initially isolated from *Nicotiana tabacum* (TEAS), *Hyoscyamus muticus* (HPS) and *Artemisia annua* (ADS) were optimized with regards to a divalent metal ion requirement. Surprisingly, careful titration with manganese stimulated bona fide synthase activity with the native 15-carbon substrate farnesyl diphosphate (FPP) as well as with the 10-carbon substrate geranyl diphosphate (GPP). Reaction product analysis suggested that the GPP could be used to investigate early steps in the catalytic cascade of these enzymes.

To investigate how structural features of the sesquiterpene synthases translate into enzymatic traits, a series of substrate and active site residue contacts maps were developed and used in a comparative approach to identify residues that might direct

product specificity. The role and contribution of several of these residues to catalysis and product specificity were subsequently tested by the creation of site-directed mutants. One series of mutants was demonstrated to change the reaction product to a novel sesquiterpene, 4-epi-eremophilene, and while another series successfully transmuted TEAS into a HPS-like enzyme. This is the first report of a rational re-design of product specificity for any terpene synthase.

The contact map provides a basis for the prediction of specific configurations of amino acids that might be necessary for as yet uncharacterized sesquiterpene synthases from natural sources. This prediction was tested by the subsequent isolation and validation that valencene synthase, a synthase from citrus, did indeed have the amino acid configuration as predicted.

Lastly, an in vitro system was developed for analyzing the interaction between sesquiterpene synthases and the corresponding terpene hydroxylase. Development of this in vitro system is presented as a new important tool in further defining those biochemical features giving rise to the biological diversity of sesquiterpenes.

KEYWORDS: Terpene Synthase, Terpene Cyclase, Isoprenoid Biosynthesis, Phytoalexin biosynthesis, Cytochrome P450.

Bryan T. Greenhagen

July 15, 2003

ORIGINS OF ISOPRENOID DIVERSITY: A STUDY OF STRUCTURE-FUNCTION
RELATIONSHIPS IN SESQUITERPENE SYNTHASES.

By

Bryan T. Greenhagen

Joseph Chappell
Director of Dissertation

Arthur Hunt
Director of Graduate Studies

July 15, 2003

RULES FOR THE USE OF DISSERTATIONS

Unpublished dissertations submitted for the Doctor's degree and deposited in the University of Kentucky Library are as a rule open for inspection, but are to be used only with due regard to the rights of the authors. Bibliographical references may be noted, but quotations or summaries of parts may be published only with the permission of the author, and with the usual scholarly acknowledgments.

Extensive copying or publication of the dissertation in whole or in part also requires the consent of the Dean of the Graduate School of the University of Kentucky.

A library that borrows this dissertation for use by its patrons is expected to secure the signature of each user.

DISSERTATION

Bryan T. Greenhagen

The Graduate School
University of Kentucky
2003

ORIGINS OF ISOPRENOID DIVERSITY: A STUDY OF STRUCTURE-FUNCTION
RELATIONSHIPS IN SESQUITERPENE SYNTHASES.

DISSERTATION

A dissertation submitted in partial fulfillment of the
requirements for the degree of Doctor of Philosophy in the
College of Agriculture at the University of Kentucky

By

Bryan T. Greenhagen

Lexington, KY

Director: Dr. Joseph Chappell, Professor

Lexington, KY

Copyright © Bryan T. Greenhagen 2003

DEDICATION

This dissertation is dedicated to the memory of my grandfather Charles L. Greenhagen Sr. (1922-1996).

ACKNOWLEDGMENTS

I wish to express my gratitude to Joe Chappell for the opportunity and freedom to pursue the research contained in these pages. I also thank my committee members Robert Houtz, Art Hunt, Sharyn Perry, and Peter Spielmann for their support and encouragement, and especially my outside examiner Rod Croteau. My development over the course of my work in the Chappell lab has benefited greatly from interactions with all the Chappell lab members, particularly, Tim Devarenne, Mark Schoenbeck and Shunji Takahashi. I am indebted to our collaborators Robert Coates, Marylin Xiao, Joseph Noel and Paul O'Maille. The assistance of these people has made the following thesis possible and shaped it. I owe an especially deep gratitude to my wife, Jennifer Keeney Greenhagen.

TABLE OF CONTENTS

ACKNOWLEDGMENTS	iii
LIST OF TABLES	viii
LIST OF SCHEMES.....	ix
LIST OF FILES	x
CHAPTER 1 Isoprenoid Biosynthesis and Terpene Cyclase Enzymology.....	1
A. Overview.....	1
B. Terpene Biosynthesis.....	2
C. Origins of terpene diversity	3
D. Terpene biosynthesis in plants is spatially and temporally regulated.....	4
E. Enzymology of Terpene Cyclases	5
F. TEAS as a model	6
G. Thesis Work.....	19
CHAPTER 2 Mechanistic insights into substrate specificity, ionization, and isomerization of prenyl diphosphates revealed by monoterpene synthase activities inherent in sesquiterpene synthases	31
Introduction.....	31
Materials and Methods.....	32
Results.....	35
Discussion.....	38
CHAPTER 3 4-epieremophilene Synthase, a novel product terpene cyclase derived from 5-epi-aristolochene synthase	50
Introduction.....	50
Materials and Methods.....	52
Results.....	53
Discussion.....	57
CHAPTER 4 Conversion of 5-epi-aristolochene into a premnaspirodiene synthase	71
Introduction.....	71
Materials and Methods.....	72
Results.....	74

Discussion.....	75
CHAPTER 5 Variations on a theme, Cloning and Mutational Analysis of Valencene Synthase from <i>Citrus x paradisi</i>	85
Introduction.....	85
Materials and Methods.....	86
Results.....	88
Discussion.....	91
CHAPTER 6 Probing sesquiterpene hydroxylase activities in a coupled assay with terpene synthases	103
Introduction.....	103
Materials and Methods.....	104
Results.....	106
Discussion.....	110
CHAPTER 7 Conclusions and Perspectives.....	123
REFERENCES	126
APPENDIX: Synthesis of 4-epieremophilene	144
VITA.....	145

LIST OF FIGURES

Figure 1.1 Biosynthetic origins of isoprenoids.....	21
Figure 1.2 The isoprene rule helps explain the biosynthetic origins of cholesterol.	22
Figure 1.3 A few representative sesquiterpenoids.....	23
Figure 1.4 Variations of internal addition reactions leading to diverse sesquiterpenoid classes.....	24
Figure 1.5 Regulation and compartmentalization of isoprenoid pathways.....	25
Figure 1.6 Classes of sesquiterpenoid that may have the eudesmyl carbocation as a common intermediate.....	26
Figure 1.7 Eremophilene does not contain contiguous isoprene units.....	27
Figure 2.1 Model of the J-K loop, DDxxD motif, and hydrogen bonding interactions at the mouth of the active site.....	43
Figure 2.2 Dependence of reaction rate on metal concentrations.....	44
Figure 2.3 GC separation of monoterpenes produced by ADS and TEAS.....	45
Figure 2.4 Chiral separation of linalool enantiomers by gas chromatography.....	46
Figure 2.5 Relative turnover rates for GPP and FPP incubated with active site tyrosine mutants.....	47
Figure 3.1 A Van der Waals contact map for TEAS.....	65
Figure 3.2 Reaction product analysis of TEAS and the respective C440 mutants by GC.	66
Figure 3.3 Initial kinetic comparison between TEAS and the C440 mutants.....	67
Figure 3.4 GC-MS identification of the TEAS-T402S/V516I reaction products.....	68
Figure 3.5 Kinetic comparison of TEAS to the TEAS mutants T402S, V516I and T402S/V516I.....	69
Figure 3.6 Docking of the eremophilyl carbocation in a modeled EES (TEAS- T402S/V516I) active site.....	70
Figure 4.1 Structural analysis of chimeric sesquiterpene synthases between TEAS and HPS.....	79
Figure 4.2 A cross-section of the TEAS crystal structure highlighting the location of mutations converting TEAS into a prenaspirodiene synthase (TEAS- M9).....	80
Figure 4.3 Residues in the TEAS structure that were mutated in TEAS-M9.....	81
Figure 4.4 Proposed conformational control of eremophil carbocationic intermediates specified by wildtype and mutant TEAS.....	82
Figure 4.5 Conceptual cartoon representing how structural elements of the synthase enzymes might constrain substrate conformers and thus impose stereochemical control in catalysis.....	83
Figure 4.6 Graphic depiction of stepwise changes in product distribution for mutants leading up to TEAS-M9.....	84
Figure 5.1 The stereo- and regiochemical generation of eremophilanes.....	98
Figure 5.2 Reaction product analysis by GC-MS for CVS incubated at pH 7.5.....	99
Figure 5.3 The pH dependence for citrus valencene synthase.....	100
Figure 5.4 DNA sequence and predicted amino acid sequence for citrus valencene synthase.....	101

Figure 5.5 GC-MS data for ethylacetate extractable sesquiterpene products of <i>citrus</i> valencene synthase at pH 7.	102
Figure 6.1 Capsidiol formation in a coupled assay with 5-epi-aristolochene synthase and 5-epi-aristolochene dihydroxylase.	115
Figure 6.2 Verification of capsidiol as the dominant product of the coupled assay with 5-epi-aristolochene synthase and 5-epi-aristolochene dihydroxylase.	116
Figure 6.3 Optimization of the EAS/EAH coupled assay.....	117
Figure 6.4 5-epi-aristolochene dihydroxylase hydroxylates germacrene A, the sesquiterpene reaction product synthesized by the C440A mutant of EAS.	118
Figure 6.5 Novel reaction products are formed in a coupled assay with Hyoscyamus premnaspirodiene synthase (HPS) and 5-epi-aristolochene dihydroxylase.....	119
Figure 6.6 GC-MS analysis of the reaction products synthesized in the premnaspirodiene synthase/5-epi-aristolochene dihydroxylase coupled assay.....	120

LIST OF TABLES

Table 1.1 Cloned and characterized sesquiterpene synthases.....	20
Table 2.1 Product Distribution from FPP and GPP For Various Sesquiterpene Synthases.....	42
Table 3.1 Alignment of residues in and near the active site of TEAS with other sesquiterpene synthases.	62
Table 3.2 Relative product distributions in TEAS and TEAS mutants T402S and V516I.	63
Table 4.1 Reaction profiles for TEAS, TEAS-M9, and intermediate mutant synthase enzymes. GA: germacrene A; EA: 5-epi-aristolochene; EE: 4-epi- eremophilene; PSD: prenaspirodiene.....	78
Table 5.1 Reaction product profiles for CVS, CVS mutants and CVS-like mutations in TEAS.....	97

LIST OF SCHEMES

Scheme 1.1 Proposed mechanism for 5-epi-aristolochene biosynthesis by TEAS.	28
Scheme 1.2 Similarities between prenyltransfrase and terpene cyclase catalyzed reactions.	29
Scheme 1.3 Mechanism for isomerization of the 2,3 double bond of isoprenoids.	30
Scheme 2.1 Proposed mechanisms for production of sesquiterpenes and monoterpenoids by TEAS and ADS.	48
Scheme 2.2 Selectivity in proton abstraction from GPP and LPP if diphosphate acts as the base.	49
Scheme 3.1 Variation in the biosynthesis of solanaceous phytoalexins from Farnesyl Diphosphate (FPP).	61
Scheme 5.1 A proposed biosynthetic pathway for Nootkatone.	95
Scheme 5.2 Stereochemical alternatives for sesquiterpene synthase reaction pathways.	96
Scheme 6.1 The elicitor-inducible branch pathway for capsidiol biosynthesis in Nicotiana tabacum cells consists of two enzymatic steps.	121
Scheme 6.2 A chemical and mechanistic rationalizations for product of coupled assays.	122

LIST OF FILES

Greenhagen PhD thesis.pdf.....1,558 KB

CHAPTER 1 Isoprenoid Biosynthesis and Terpene Cyclase Enzymology

A. Overview

This dissertation attempts to relate the functional characteristics of sesquiterpene synthases, enzymes that catalyze the cyclization and rearrangement of farnesyl diphosphate, to the 3-dimensional structure of these enzymes. The dissertation work centers on an enzyme initially isolated from tobacco, 5-epi-aristolochene synthase or TEAS, which has been structurally and kinetically well characterized. A chemical rationalization for the stereochemically complex, multi-step reaction catalyzed by TEAS has also been proposed previously by others. In this chapter, the field of isoprenoid biochemistry is introduced; sesquiterpenes, a particular class of isoprenoids, are briefly reviewed; then the pivotal role of sesquiterpene synthases in regulating the amount and type of sesquiterpenes is discussed. Thereafter, discrete steps in sesquiterpene biosynthesis are discussed in sections which correspond to the background for research chapters 2-6. These discussions rely on work in related fields and parallels to work in monoterpenoid biosynthesis (ten carbon terpenoids), prenyltransferases, and microbial sesquiterpene synthases, particularly trichodiene synthase. Trichodiene synthase has also received a considerable amount of attention and is perhaps the most extensively characterized sesquiterpene synthase. The major research objective of this thesis is to understand how variations in sequence space (enzymatic primary structure) define reaction pathways which have enormous possible variations. TEAS was chosen for this investigation because of the extensive background information available about this enzyme and the many parallels that are now recognized as common features among and between plant and microbial sesquiterpene cyclases. It is my thesis that the basis for terpenoid diversification can be further appreciated by examining TEAS relative to other terpene synthases or cyclases.

B. Terpene Biosynthesis

The isoprenoid biosynthetic pathways produce an extraordinarily diverse class of biological active molecules and encompasses the largest class of natural products from plants, commonly called the terpenoids (Fig. 1.1). Chemical structures range from the simple 5-carbon isoprene to the 30-carbon, tetracyclic sterols. Isoprenoids are involved in biological functions as universal as the Q cycle of electron transport (ubiquinone)¹ and as particular as pheromone signaling between specific species of plants and insects²⁻⁵. Isoprenoids in plants also include growth regulators (abscisic acid⁶, cytokinin⁷, gibberellins⁸ and brassinolides^{9,10}), compounds that contribute to the structure and function of membranes (sterols¹¹), serve as photoprotectants (carotenoids¹²), and provide a means for localizing biochemical processes at membrane surfaces (dolichols^{13,14}).

The early biochemical dissection of this pathway was largely driven by the desire to understand cholesterol biosynthesis. A profound clarification came from Ruzicka with the recognition that cholesterol and all other isoprenoids were generated from five-carbon isoprene units¹⁵ (Figure 1.2). Subsequently, the work of Lynen, Bloch, Cornforth, Popjak, and Corey elucidated the classical, mevalonate (MVA) biosynthetic pathway and demonstrated a likely mechanism for the biosynthesis of sterols from the simply isoprene building blocks. More recently, work by Rohmer¹⁶⁻²², Arigoni²³⁻³⁰ and others³¹⁻³⁵ have revealed another mevalonate-independent pathway for the biosynthesis of the isoprene units in plants and bacteria, the methylerythritol phosphate or MEP pathway (reviewed in references^{36, 37,38}.)

The common metabolite in both isoprenoid pathways is isopentenyl diphosphate (IPP), which is formed from the condensation of acetyl-CoA units in the central mevalonate pathway, or the condensation of pyruvate and glyceraldehyde 3-phosphate in the MEP pathway. Diversification then begins with the polymerization of IPP units by prenyltransferase, creating linear intermediates of 10, 15, 20 carbons which can undergo condensation between themselves generating triterpenes (C30) and tetraterpenes (C40), continue polymerization with additional isoprene units (C50+ for dolichols and rubber) or cyclization into elaborate structures known as monoterpenes

(C10), sesquiterpenes (C15), and diterpenes (C20). In plants and microbes, it is largely this later class of compounds that is often referred to as the terpenes and terpenoids.

C. Origins of terpene diversity

Many of the plant and microbial derived mono-, sesqui- and di-terpenes do not seem to participate in essential cellular metabolism and are often referred to as secondary metabolites. These compounds nonetheless appear to be important mediators of inter- and intraspecies interactions⁴ and their distinction as “secondary” does not capture their true biological relevance. While primary metabolites are essential to almost all cells within a species, the array of terpenes associated with any one plant or microbe species can vary, and represents the results of ecological and/or mankind selection. For instance, the fragrance of flowers is generally a complex composition of volatiles that can include mono- and sesqui-terpenes produced in floral organs³⁹. Another example of species specific terpenes is the specific arrays of antimicrobial sesquiterpenoids produced by solanaceous plants in response to challenge by specific pathogens⁴⁰⁻⁴³.

Humans have also derived value from many of the terpenes. For example, many commercially important sesquiterpenoids are referred to as “fine chemicals” because of their value, rarity, and the difficulty of their synthesis (Figure 1.3). Nootkatone is a common additive to drinks that imparts a grapefruit flavor⁴⁴⁻⁴⁶. Alloaromadendrene and patchoulol lend distinct aroma profiles to perfumes. Artemesinin is a highly functionalized sesquiterpeneoid which is effective against quinine resistant *Plasmodium falciparum*, the casual agent of malaria⁴⁷. The anti-inflammatory and potential anti-cancer compound parthenolide from the herb feverfew has recently become the focus of intense pharmacological investigations⁴⁸⁻⁶⁵. While the phytochemical identification of new sesquiterpenoids proceeds at an impressive rate of about three hundred new compounds per year⁶⁶⁻⁷⁵, we do not yet have an understanding that can sufficiently explain the origins of this diversity, nor the knowledge that would allow us to manipulate enzymatic chemistry with a set of rules as developed as that for classical organic chemistry.

A significant portion of terpenoid diversity is due to the exquisite regio- and

stereo-chemical cyclization of the linear intermediates geranyl diphosphate (GPP), farnesyl diphosphate (FPP) and geranylgeranyl diphosphate (GGPP) catalyzed by the corresponding synthases (While the terms mono-, sesqui- and di-terpene cyclases have been useful to describe these enzymes in the past, the general nomenclature of *synthase* for these enzymes is used here, because the enzymes are unified by the class of products they produce and common structural folds, not the specific reactions they catalyze. For instance, (3*S*)-linalool synthase from *Clarkia breweri*⁷⁶ is a geranyl diphosphate lyase.) These enzymes catalyze unique electrophilic reactions that often provide for surprisingly complex synthetic tasks. This electrophilic chemistry arises from the generation and manipulation of carbocations by the terpene synthase enzymes and provides for various intramolecular additions and rearrangements that result in hundreds of possible carbon-carbon bond linkages in final products (figure 1.4).

The diversity of terpenes is further amplified by the modification of the cyclic and acyclic hydrocarbon backbones by the addition of functional groups and other subsequent modifications. These include the introduction of hydroxyl groups^{77,78} and their oxidation to ketones⁷⁹, demethylations⁸⁰, and halogenations^{81,82}, which can affect various chemical properties of the molecules that influence their biological activities⁸³. For instance, dihydroxylation of 5-epi-aristolochene by a cytochrome P450 enzyme produces the anti-fungal phytoalexin capsidiol in solanaceous plants⁷⁷.

D. Terpene biosynthesis in plants is spatially and temporally regulated

One interesting phenomenon of terpene accumulation in plants is that these compounds are either produced in specific tissues, organs or cell types, or their biosynthesis appears to be highly regulated. Excellent examples of the former are the mono- and di-terpenes associated with resins and trichome exudates⁸⁴⁻⁸⁸, and the potent insecticidal sesquiterpenes that accumulate in glandular ducts of plants like cotton⁸⁹. Control of terpene accumulation by regulation of the relevant biosynthetic enzymes is probably best illustrated by the induction of sesquiterpene accumulation in pathogen-challenged solanaceous plants⁴⁰⁻⁴³ (figure 1.5). Unchallenged tissues and cells shunt acetyl-CoA units down the mevalonate pathway for the biosynthesis of sterols, dolichols and other primary isoprenoids, while pathogen- or elicitor-challenged cells

suppress sterol biosynthesis and divert up to 20% of the carbon flow into the biosynthesis of antimicrobial sesquiterpenes⁹⁰. The induction of this new sesquiterpene biosynthetic capacity appears to arise from the upregulation of a completely new branch pathway dedicated to a defense response⁹¹, which is simultaneously associated with a transcriptional and post-transcriptional suppression of the sterol-specific branch pathway⁹². The induction of sesquiterpene biosynthesis has been shown to be predominately mediated by transcriptional control of the corresponding genes^{77,93}.

E. Enzymology of Terpene Cyclases

Progress in understanding the origins of terpenoid diversity over the past fifty years has predominantly focused on the development of comprehensive enzymatic models for terpene synthase catalysis⁹⁴⁻⁹⁸. The stereochemical course of terpene cyclase catalyzed reactions have been extensively studied using stereo-specific, radiolabeled substrates and rationally designed substrate analogs. This has resulted in a wealth of information on the transformations of the 10, 15, and 30 carbon isoprenoid substrates^{94,95,97,99}. Overall, the enzymes have been found to be remarkable for their control of multiple stereochemical transformations along extensive reaction pathways. A dramatic example of such catalytic control is found in the enzyme cycloartenol synthase. Cycloartenol synthase uses the triterpenoid (30 carbon) oxidosqualene as a substrate and forms the first multicyclic intermediate in the biosynthesis of plant sterols¹⁰⁰. In the cyclization process, eleven bonds are broken, eleven new bonds made, and nine chiral centers are specified by the cyclase⁹⁴. The significance of this type of chemical control is evidenced by the absence of any comparable “one-pot” organic synthesis methods and recognition that this biosynthetic reaction yields only 1 of approximately 500 possible stereoisomers (2^9).

The experimental emphasis in terpene biochemistry has shifted somewhat over the last 20 years towards the use a new set of tools to better reconcile the function of terpene synthases with their chemical specialization. In particular, investigations to connect primary amino acid sequence, resultant tertiary structure, and active site chemistry have become possible due to major advances in cloning, heterologous expression, molecular manipulations and X-ray crystallographic techniques. And while

very significant progress in assessing mechanistic features of monoterpene (for general review see ref. 97), sesquiterpene (for general review see ref. 95) and triterpene (for general review see ref. 94) synthases using these new methodologies has occurred, it would be impossible to adequately review the progress for each class of terpene synthase. Therefore, the following sections are focused primarily to those advances with sesquiterpene synthases which are germane to the current thesis work and draw upon advances with monoterpene and diterpene synthases that are directly related to my work.

Table 1.1 is a partial list of cloned sesquiterpene synthase genes and those genes whose gene products, the synthases, have been reasonably well characterized. Equally important, ten terpene synthases from plants, bacteria, and fungi have been structurally characterized by x-ray crystallography¹⁰¹⁻¹¹⁰. Terpene synthases fall into two major categories of tertiary structures that functionally correlate with whether the enzymes initiate catalysis upon the ionization of the allylic diphosphate substrate (Class I) or by proton addition to the substrate (Class II). Class I synthases include monoterpene, sesquiterpene and diterpene synthases, while Class II include diterpene and triterpene synthases. No Class II mono- or sesqui-terpene synthases have been identified to date. The major focus of this thesis will be on the enzymology of the Class I synthases and centers on the sesquiterpene synthases 5-*epi*-aristolochene synthase of tobacco (TEAS) and premnaspirodiene synthase from *Hyoscyamus muticus* (HPS), each of which forms three chiral centers upon cyclization of FPP. (The HPS enzyme was originally referred to as vetispiradiene synthase owing to the vetispirane reaction product generated. However, the correct vetispirane stereoisomer in the biosynthesis of the *Hyoscyamus muticus* phytoalexin solavetivone was originally identified and named premnaspirodiene by Rao, Raju, and Krishna¹¹¹.)

F. TEAS as a model

TEAS was chosen for the current studies based on its ready availability and previous characterization by the Chappell and related laboratories. Particular attributes of the TEAS enzyme making it suitable for study include its relative stability upon purification¹¹², the ease expression in bacteria¹¹³, the availability of crystallographic

models for the enzyme¹⁰¹, and a tractably simple catalytic reaction^{95,114}. Another reason for studying TEAS is the availability of closely related synthases. In particular, earlier comparisons and construction of chimeras between TEAS and HPS helped identify regions of the enzymes that were associated with specific partial reactions in the putative cyclization events of FPP¹¹⁵.

TEAS may be envisioned as catalyzing two discrete sequential reactions (Scheme 1.1). The first (I), involves ionization of FPP, intramolecular addition, and proton elimination forming a stable enzyme-bound intermediate germacrene A. The second reaction (II), involves protonation of germacrene A, a second cyclization, methyl migration, and deprotonation. Reaction I has parallels to the mechanisms of isoprene diphosphate polymerization catalyzed by the well-studied prenyltransferase farnesyl diphosphate synthase and is the subject of Chapter 2 of this thesis. Reaction II involves less well-understood biochemistry which forms the basis of Chapters 3-5.

1. Divalent cation requirements, substrate binding, and formation of the enzyme substrate complex.

All terpene synthases reported up to this time require a divalent cation for optimal activity *in vitro*. Sesquiterpene synthases have been reported to prefer Mg^{2+} *in vitro* and usually exhibit half-maximal velocities at 1-2 mM¹¹⁶⁻¹¹⁸. In most cases examined, Mn^{2+} supports catalysis at low concentrations (<0.1 mM) but has also been found to inhibit at concentrations in excess of 1 mM^{116,118,119}. These values, however, appear to vary with the substrate concentration used. Monoterpene synthases seem to be less selective in their divalent cation requirements in general⁹⁷, while those synthases from gymnosperms appear to represent a unique subclass of terpene synthase which prefers Mn^{2+} (or Fe^{2+}), and have an additional K^+ ion requirement¹²⁰⁻¹²².

Subcellular localization is likely to play an *in vivo* role in metal availability and therefore has ramifications for terpene synthase activities. Monoterpene and diterpene synthases have for the most part been localized to plastids (leucoplasts), while sesquiterpene synthases are believed to be cytosolic enzymes based on a lack of amino-terminal targeting sequences and on cell fractionation studies^{123,124}. Interestingly, the concentrations of cellular Mg^{2+} in cultured tobacco cells has been estimated at 2-3

mM¹²⁵⁻¹²⁷, but most of this is expected to reside in the vacuole¹²⁸. Such results raise questions about how the divalent cation requirement for terpene synthases is actually met *in vivo*.

Additional insights into the mechanistic roles for the divalent metals are evident from the crystallographic studies of TEAS¹⁰¹, pentalenene synthase¹⁰², bornyl diphosphate synthase¹²⁹ and trichodiene synthase¹⁰⁷. The TEAS enzyme without substrate analog contains two bound metal ions but the JK and AC loops are uncoordinated with respect to the rest of the enzyme structure. A third Mg²⁺ ion is subsequently observed in the enzyme structure upon binding of the substrate analog FHP. Only the structure for the apo-form of pentalenene synthase has been determined and it does not appear to contain any divalent metals. In contrast, the apo-form of borneyl synthase may contain a single magnesium ion, while synthase complexed with substrate analog contains three, similar to TEAS. Trichodiene synthase likewise appears to bind one divalent metal in its apo-form and gains two additional metal co-factors upon binding of substrate analogs.

A detailed kinetic analysis of the metal requirement for any terpene synthase is lacking. However, in examining the metal requirement of avian prenyltransferase, King and Rilling determined that the K_d for GPP-Mg⁺² was 140 μM and 30 μM for GPP-Mn⁺²¹³⁰, far below the typical cation concentration needed in optimal synthase assays. Such observations have supported a general notion that the highly charged diphosphate head group found on all allylic diphosphates substrates is probably neutralized in solution by the binding of 2 divalent metal ions, which serve as the true substrate complex for the synthases.

A nearly perfectly conserved DDxxD motif found in terpene synthases appears to direct substrate binding via formation of complexes with the metal ions. The idea that conserved aspartate residues may function in forming salt bridges to phosphate groups by binding divalent cations was first proposed on the basis of sequence homologies found for phosphotransferases¹³¹. A similar function was proposed for the terpene synthases when yeast hexaprenyl diphosphate synthase and PHB:polyprenyltransferase (involved in ubiquinone (coenzyme Q) synthesis) were found to share the sequence (I,L,V)xDDxxD with human and yeast FPPS^{132,133}. FPPS

contains two DDxxD motifs which reside on opposite sides of the mouth to the active site¹⁰³. A single DDxxD motif appears in nearly all type I terpene cyclases. Exceptions to the canonical sequence are found in non-plant cyclases, aristolochene synthase (DDxxE)¹³⁴ and germacradienol synthase (DDxxxD)¹³⁵. X-ray crystallography of FPPS¹⁰³, EAS¹⁰¹, trichodiene synthase¹⁰⁷, bornyl diphosphate synthase¹²⁹ have demonstrated that these aspartates are indeed involved in diphosphate binding via the coordination of magnesium ions. Although sesquiterpene and monoterpenes synthases have only one DDxxD motif, TEAS does contain a DDxxT sequence at the spatially equivalent position of the second DDxxD sequence observed in the yeast FPPS¹⁰¹.

Mutagenesis of the DDxxD motif has revealed that conservative substitution of the last aspartate to glutamate has minimal effects, whereas any alteration of the first aspartate strongly compromises the synthase enzyme activity¹³⁶⁻¹³⁸. Mutation of the first aspartate has also been associated with a significant change in the reaction product profile, usually resulting in less complex products¹³⁶⁻¹³⁸. Moreover, Cane and co-workers have extensively investigated the role of the DDxxD motif in trichodiene synthase, a sesquiterpene synthase of fungal origin^{108,139}, and have documented that when the first aspartate is mutated to glutamate (TS-D100E), the reaction product profile was significantly altered, including a novel product isochamigrene^{136, 140}. Unfortunately, clear interpretation of this mutant is hampered by the mutated trichodiene synthase being severely compromised, having a catalytic turnover rate only 1/10 of the wildtype enzyme and at least a 10-fold lower affinity for its substrate.

With regards to a possible mechanistic role of divalent cations for catalysis in terpene synthases, it is possible that the two divalent cations normally associated with FPP in solution are required for initial substrate binding and that the third provides electrostatic interactions required for ionization of the substrate. The third ion may also serve as a trigger in conjunction with R466 to coordinate loop closure over the active site, thus creating the third metal binding and ensuring that ionization occurs subsequent to protection of the substrate from the solvent.

Scheme 1.1 illustrates a chemical rationalization for the conversion of FPP to 5-epi-aristolochene as it has been proposed to occur in a TEAS mediated reaction^{95,114}. After initial substrate binding, the overall reaction is readily divided into partial

reactions or steps and these fall logically into three separate catalytic events. The first is initiated by the ionization of the diphosphate substituent and ends with a proton abstraction and formation of germacrene A. The second series of partial reactions is initiated by a proton addition to the germacrene A intermediate, which promotes a second round of cyclization events resulting in the biosynthesis of 5-epi-aristolochene. The last catalytic event needing to be considered is the release of the 5-epi-aristolochene product, a hydrophobic molecule, from the enzyme active site into the aqueous environment surrounding the TEAS enzyme. Each of these catalytic transformations thus represents putative but discrete activities of the synthase enzyme and activities that should be amenable to experimental testing. The next three sections of this chapter therefore present background information concerning each of these catalytic events with the aim of providing sufficient justification for an experimental probing of each.

2. Reaction I: ionization / addition / elimination

Several experimental approaches have suggested that subsequent to FPP binding, terpene cyclases catalyze reactions directly analogous to the condensation reaction catalyzed by farnesyl diphosphate synthase, FPPS (Scheme 1.2)^{95,141-143}. Two major lines of evidence support this contention. First, a substrate analog having diphosphate substituents at both ends of the molecule is readily cyclized by FPPS¹⁴³. Second, incubation of FPPS with FPP under somewhat extreme conditions can also give rise to cyclic reaction products¹⁴².

Seminal work on FPPS established that the condensation of isoprenoid diphosphates by these enzymes occurs by a stepwise ionization-addition-elimination mechanism¹⁴⁴⁻¹⁴⁷. A key piece of evidence is that when protons at C2 (or 10-methyl) position are replaced with fluorine, these substrate analogs are turned over at much slower rate than those with hydrogens. The strong electron withdrawing effect of the fluorine is believed to impede the formation of the allylic carbocation at C1 by partially eliminating resonance stabilization. If the catalyzed reaction were a typical displacement type reaction (S_N2), then the substituted fluorine analogs would be expected have little bearing on the rate of displacement¹⁴⁴. Evidence for an initial

ionization catalyzed by monoterpene cyclases has similarly been demonstrated using 2-fluorogeranyl diphosphate and 2-fluorolinalyl diphosphate¹⁴⁸

As already mentioned above, dependence of terpene synthases on divalent cations, solvolytic models^{149,150}, and the evidence for an electrophilic mechanism¹⁴⁴⁻¹⁴⁷ has given rise to the suggestion that the cations serve to neutralize the development of negative charge on diphosphate, thus driving substrate heterolysis. Additionally, X-ray crystallographic data on TEAS have shown that when substrate analogs are bound, amino acids R266 and R441 translate nearer to the diphosphate moiety¹⁰¹. Interestingly, the inward translation of R266 is also coupled to the formation of an apparent hydrogen bond between R266 and the second aspartate of the DDxxD motif¹⁰¹, thus providing a temporal connection between metal binding and the initiation of catalysis.

Ionization of farnesyl diphosphate results in the generation of a highly reactive allylic carbocation which has any number of fates. At this point in the catalytic cascade, some synthases allow isomerization about the C2-C3 double bond, from a trans configuration to a cis configuration. The energetic barrier to rotation of the allylic cation is >12 kcal/mol^{97,151}, which precludes direct formation of the cis configuration. Therefore, much effort has been made to understand the mechanism of C2-C3 bond isomerization. The accepted model involves the ionized diphosphate group migrating to C3 and forming a tertiary allylic diphosphate, thereby allowing free rotation about the newly formed C2-C3 sigma bond (Scheme 1.3). This mechanism has been supported through the use of substrate analogs by both monoterpene and sesquiterpene synthases¹⁵²⁻¹⁵⁵. The question remains, however, as to whether synthases control isomerization via control of the formation of a tertiary diphosphate or instead by controlling the conformation the tertiary diphosphate itself.

Such isomerization gives rise to a large contingent of cis (Z) bond containing molecules such as cadinanes, bisabolanes, amorphanes, and cedranes. Sesquiterpene synthases cloned which produce such terpenoids are (+)delta-cadinene synthase, amorpha-4,11-diene synthase, epi-cedrol synthase, from plants and trichodiene synthase from fungi. An attempt to examine the turnover of nerolidyl diphosphate (NPP), the tertiary diphosphate isomer of FPP, by delta-cadinene synthase has been made¹⁵⁶. Theoretically, one NPP enantiomer which represents the true intermediate

should be selectively turned over at faster rates than FPP, as has been shown for a number of monoterpene cyclases. The 3R form was claimed to be the preferred form, yet the turnover of this enantiomer was ten times slower than with FPP and, while product fidelity was 98% for wild type, the products of (3R)-NPP turnover were significantly diversified, giving only 62% delta-cadinene¹⁵⁶. (the interpretation of the authors was significantly more positive based on the overall conservation of k_{cat}/K_M which was essentially the same for FPP and (3R)-NPP (0.004 s^{-1}) due to a ten fold decrease in apparent K_M and the reduced fidelity was explained as catalytic versatility.)

The addition reaction entails the positioning of the newly formed allylic cation (whether cisoid or transoid) such that double bond pi electrons can flow to the positive center at C1, forming a cyclic carbocation. Cyclization via the intramolecular addition of a carbocationic center to a double bond does not require much activation (zero to a few kcal mol^{-1}) and are highly exothermic ($\Delta E \approx 20 \text{ kcal mol}^{-1}$)^{94,157}.

The high fidelity of the terpene synthases means that these enzymes must select specific reaction coordinates while providing a means of preventing self-alkylation. The observation of aromatic residues surrounding the active site of TEAS and pentalanene synthase initially led to the proposition that the carbocation intermediates were steered via cation-pi interactions¹⁵⁸ involving phenylalanines, tryptophans, and/or tyrosine residues. Chemical models support this contention. For instance, quadrupole stabilization has been proposed as a force in the receptor-mediated binding of acetylcholine based on the observation that a synthetic receptor made of a cage of aromatic rings binds the positively charged neurotransmitter with μM affinity¹⁵⁹.

Following C1-C10 bond formation, a proton on the terminal cis-methyl of the isopropenyl group is specifically eliminated, resulting in the generation of germacrene A. The specificity for this elimination was previously demonstrated by D. Schenk and R. Coates (D. Schenk, Ph.D. thesis, University of Illinois), who observed the loss of deuterium and tritium from terminally-labeled FPP upon incubation with TEAS (Scheme 1.2). While there has been some debate about the role of D525 in this abstraction process, current discussions still favors this role for D525. Lastly, the intermediacy of germacrene A has been substantiated via mutagenesis of an active site residue. Mutation of tyrosine 520 to a phenylalanine resulted in a mutant synthase that

apparently produced only germacrene A¹⁶⁰.

3. Reaction II: protonation / addition / rearrangement / deprotonation

The re-initiation of catalysis by protonation of germacrene A remains an interesting and as yet unresolved issue. Germacrenes are rather unstable molecules in large part because of double bonds facing one another across the A ring. These paired double bonds serve to stabilize transition states that can result in relative easy re-protonation and facile intramolecular cyclization, or rearrangements leading to terminal products such as β -elemene^{161,162}. Indeed, intramolecular cyclization of germacrenes proceeds easily under simple acidic conditions in solution¹⁶³⁻¹⁶⁵. Hence, positioning of a proton in close proximity to the germacrene A intermediate is anticipated as sufficient for TEAS to re-initiate the second round of cyclization reactions.

Based on substrate analog farnesy hydroxyphosphonate (FHP) electron density observed in the 5EAT crystal, Starks et al. proposed that Y520 might provide this proton, via a proton shuttle involving D525 and D444. This suggestion was subsequently tested by mutation of Y520 to phenylalanine, resulting in the Y520F mutant which produced exclusively germacrene A at pH 7.8¹⁶⁰. While such data supported the intermediacy of germacrene A in the reaction mechanism, several lines of evidence have questioned the proposed role of Y520 as the proton donor. The first observation contrary to the proposed role for Y520 was the kinetic data provided by Rising et al.¹⁶⁰. If the role of Y520 in catalysis is simply addition of a proton to germacrene A, then one would expect the Y520F mutant to be kinetically comparable if not superior to the wildtype enzyme. A second, more recent discovery is that 5-epi-aristolochene is actually released by this mutant but was undetected due to the low injector temperature on the GC used to prevent cope-rearrangement of germacrene A to β -elemene. And even more recently, both the Chappell (University of Kentucky) and Noel (Salk Institute) laboratories have both found that 5-epi-aristolochene synthesis by the Y520F mutant is pH dependent. At pHs 7.0 and lower, 5-epi-aristolochene is the major product. Taken together, these recent observations suggest that Y520 may not serve as the proton donor to re-initiate the second round of catalysis and argue that another residue may play this role.

According to the proposed mechanism, germacrene A readily undergoes an intramolecular cyclization, followed by a 1,2 hydride shift forming the eudesmyl carbocation (Scheme 1.1). While there is little direct experimental evidence to support this rearrangement, this rationalization is consistent with the types of non-enzymatic rearrangements observed with germacranes in solution¹⁶³⁻¹⁶⁵. The eudesmyl carbocation at this point in the reaction is subject to a wide range of rearrangement possibilities that could give rise to various structural classes of sesquiterpenoids, including eudesmanes, eremophilanes, vetispiranes, and spirojatamanes¹⁶⁶ (Figure 1.6)

5-epi-aristolochene is eremophilane-type sesquiterpene and is notable because this is the class of terpenoid which was recognized early on as an exception to the “isoprene rule” formulated by Wallach and validated by Ruzicka¹⁵. This rule was instrumental in clarifying how the biosynthesis of sterols and terpenoids was derived from isoprene units. The structure of eremophilanes are partially inconsistent with this rule in that a methyl group is out of place or order (Figure 1.7). It was the NMR study of capsidiol biosynthesis via the incorporation [1,2-¹³C₂] acetate into elicited pepper fruits^{167,168}, which established that the reason for this anomaly is a 1,2 methyl migration. The present knowledge of the absolute configuration of the (+) 5-epi-aristolochene^{114,169}, stereochemical course of the reaction¹⁷⁰, and structure of the synthase¹⁰¹, provides an excellent opportunity to understand how this “anomaly” and diversification of isoprenoid biosynthesis comes about.

The *Hyoscyamus muticus* premnaspirodiene synthase, HPS, catalyzes a very similar reaction to TEAS except for a slight variation in the second to last step of catalysis. Instead of the methyl migration from carbon 7 (FPP numbering) to carbon 2 on the opposite side of the bicyclic structure, carbon 8 on the α -face migrates to form a spirane structure. From homology modeling, HPS appears to have identical residues lining the active site as TEAS, suggesting that product specificity is defined by residues outside the active site. Such a suggestion is consistent with the previous domain swapping results of Back and Chappell¹¹⁵, although they were not able to define the spatial orientation of domains without the benefit of the TEAS crystal structure. The selection of which bonds rearrange to produce the different sesquiterpene classes is defined by the peri-perpendicular rule which requires that the conformation of the

eudesmyl cation and positioning of sp² orbitals, dictated by the geometry of the cyclase active site (allowing requisite anti or syn orbital alignments) and possibly other electrostatic interactions within the active site, direct the subsequent methyl or methylene rearrangement¹⁷¹.

After rearrangement has occurred, a eremophilyl cation (in EAS) or vetispiryl cation (in HPS) eliminates a proton via a stereo-electronically preferred pathway. Schenk and Coates have demonstrated that this occurs syn to the migrating bond, meaning that both migration and elimination occur on the same face of the molecule¹⁷⁰. Tryptophan 273, a highly conserved residue in all terpene synthases, was originally proposed as the amino acid residue within the active site assisting in this deprotonation¹⁰¹. This was rationalized because the proton vicinal to the carbocation on C7 (FPP numbering) is relatively labile, and there is a chemical precedent for the formation of a positive arenium ion by electrophilic aromatic substitutions of indole ring systems¹⁷².

4. PRODUCT RELEASE

The final step in epi-arisochoene synthesis is the release of the hydrophilic product from the relatively hydrophobic pocket. The limiting nature of this step for overall catalysis has been addressed in pre-steady state kinetic studies of several sesquiterpene synthases^{155,173}. These studies demonstrated rapid burst phase kinetics suggestive of rapid product accumulation in the active site, followed by a much slower release of product. Although such an interpretation was in concordance with the earlier determined steady-state k_{cat} values, the validity of this interpretation relied on the subjective assignment of catalytic processes to the observed rate phenomena. Hence, conclusions from the pre-steady-state analyses probably need to be corroborated by additional experimental work. For example, these kinetic studies should be repeated where experimental conditions are perturbed and the outcome on calculated kinetic constants verified.

5. FUNCTIONALIZATION BY “TAILORING” ENZYMES

Terpeneoid diversity is further expanded by functionalization of the hydrocarbon structures formed by the terpene cyclases. A goal of this thesis was in part to begin to understand how cyclases and such “tailoring” enzymes might interact by reconstituting the capsidiol biosynthetic pathway *in vitro*¹⁷⁴. 5-epi-aristolochene is functionalized by a cytochrome P450 enzyme which stereo and regio-specifically inserts two hydroxyl groups⁷⁷. Plant P450 enzymes known to catalyze regiospecific monohydroxylation of carbocyclic structures include limonene 3- and 6-hydroxylases¹⁷⁵, cinnamate 4-hydroxylase¹⁷⁶, tyrosine N-hydroxylase¹⁷⁷, ferulate 5-hydroxylase^{178,179}, taxane 10- and 13-hydroxylases^{180,181}, and several of the enzymes for DIMBOA biosynthesis in maize¹⁸². Flavonoid 3',5'-hydroxylase, however, is the only other plant cytochrome P450 yet documented to catalyze regiospecific hydroxylations at two positions within a ring system, the B ring for several anthocyanin biosynthetic intermediates^{183,184}. Yet, even flavonoid 3',5'-hydroxylase differs from EAH in that it catalyzes the insertion of hydroxyl groups into a planar aromatic ring structure, whereas EAH mediates regio- and stereospecific hydroxylations (i.e., different faces of a ring system) at the C1 and C3 positions of 5-epi-aristolochene. The EAH activity is unique in other aspects also. For example, although the enzyme is able to accept monohydroxylated forms of aristolochene (1- and 3-deoxycapsidiol) as substrate, very little monohydroxylated intermediate is released from the enzyme when 5-epi-aristolochene is supplied as substrate⁷⁷.

A major goal in the Chappell laboratory is to better define as many of the structural, functional, and mechanistic features of the EAH enzyme as possible. For this purpose, studies to examine substrate specificity^{185,186}, studies to define domains or amino acids within putative substrate recognition regions¹⁸⁷ of the enzyme that contribute to regio- and stereoselectivity¹⁸⁸, and even studies to probe how the interaction between terpene synthase enzyme and EAH might influence catalysis are anticipated. As such, facility in performing enzyme activity assays is of importance and is needed to overcome a number of limitations. Probably the most important limitations include difficulties in obtaining suitable substrates and substrate analogs without arduous organic synthesis efforts, finding suitable means for introducing hydrophobic

substrates into aqueous solutions, and providing sensitive and rapid means for measuring EAH enzyme activities.

Reengineering Enzymes

A major thrust of this thesis has been the redesign of 5-epi-aristolochene synthase using a rational strategy guided by structural and genetic data. These efforts included the re-design of synthase specific for a novel terpene, and the complete transmutation of a synthase from one product specificity to another. The relative significance of this work cannot, however, be considered without an appreciation for the broader context of enzyme engineering.

The advent of facile mutagenesis techniques, multiple host expression systems and affinity purification techniques for recombinant proteins has resulted in rapid advances in enzyme engineering over the last decade or so. Some of the enzymes subject to significant reengineering efforts have been proteases¹⁸⁹, glutathione transferase¹⁹⁰, beta-lactamase¹⁹¹ and aminotransferases¹⁹², with aims of optimizing or enhancing inherent catalytic capabilities or adding new catalytic functions to the existing enzymes. Successful examples include optimization of thermostability, pH tolerance, and catalytic rates, and even changing metal ion specificities¹⁹³. Redirecting of enzymatic chemistry or the introduction of new catalytic activities has been more elusive. Nonetheless, glutathione S-transferase has been re-engineered by rational mutagenesis of active site residues to accept alkenal substrates to catalyze Michael additions rather than nucleophilic substitution of aromatic substrates^{194,195}. Another interesting example of altering catalytic activity is the conversion of dopa decarboxylase into an oxidative deaminase by a single point mutation¹⁹⁶.

A long range goal in enzyme re-engineering is to use computational methodologies to reduce the sequence space that needs to be considered and to limit the number of iterative cycles of mutagenesis necessary to achieve a desired outcome. An example of success using this strategy is the recent development of thioredoxin as a catalyst for the histidine-mediated hydrolysis of p-nitrophenylacetate¹⁹⁷. Hayes *et al.* also employed a computational means to generate a limited set of random mutants in beta-lactamase, from which a mutant conferring a 1,280-fold increase in bacterial

resistance to cefotaxime was obtained¹⁹¹.

The major methods for enzyme engineering are point mutagenesis, domain swapping, and directed evolution (DNA shuffling, molecular breeding)¹⁹⁸. Domain swapping has been successfully used to engineer terpene synthases with reaction product diversification¹¹⁵ as well as to map functional domains for other terpene biosynthetic enzymes¹⁸⁸, but this method has not resulted in the creation of new catalytic activities in these enzymes^{115,199}. In contrast, homology based engineering which consists of comparative analyses of closely related enzyme followed by directed mutagenesis has shown good promise in this regard. A human glutathione transferase, for example, was converted from a peroxidase type activity into a steroid isomerase¹⁹⁰.

A major question for the terpene synthases is whether loops would need to be altered (or swapped) in order to control active site chemistry. If so, future directed design could be significantly complicated, whereas if mutations affecting product specificity only reside internally the system is more limited and amenable to design. Indeed, loops were shown to be critical in the classic conversion of trypsin to chymotrypsin¹⁸⁹. A second consideration is whether salt-bridges which secure the ends of the alpha-barrel alpha-helices would need to be altered. Both of these difficulties were considered due to the observation that the active site residues in HPS and EAS were apparently identical. Residue substitutions both in the catalytic pocket and at a distance from the pocket were found necessary to convert aspartate aminotransferase to a valine-specific aminotransferase¹⁹².

Engineering terpene synthases for high fidelity catalytic variants is not as obvious as for some other enzyme systems. The modular nature of polyketide biosynthesis, for example, has provided a powerful scaffold for product diversification strategies which have yielded numerous novel products²⁰⁰. Terpene product diversity has been altered in a few notable instances, but for the most part mutagenesis has resulted in either abbreviation or slight extension of a native reaction pathway^{137,160 201-205}. These mutants are for the most part greatly compromised in their catalytic performance as reflected by distorted kinetic constants. δ -selinene and γ -humulene synthases, which produce 30 different products each, have altered product distributions when mutated at positions analogous to Y520 and D444 of TEAS, yet are rather low

efficiency enzymes¹³⁷. Perhaps more notable successes have been the site-directed mutagenesis of prenyltransferases and the creation of transferases capable of generating prenyl chain differences without compromising catalytic activity²⁰¹⁻²⁰⁵, as well as the conversion of a triterpene synthase, B-amyrin synthase, to a lupeol synthase²⁰⁶.

G. Thesis Work

This thesis examines the origins of isoprenoid diversity as represented by my work presented in the following chapters. First, an alternate substrate is employed which demonstrates that there are probably only minor differences between the monoterpene and sesquiterpene cyclases (Chapter 2). This work also shows how this promiscuous substrate turnover will help to dissect those structural elements of terpene synthases that catalize the enigmatic isomerization reaction. Secondly, a rationally designed mutagenesis approach was developed and used to determine the variations in sequence space which define reaction coordinates in sesquiterpene synthases (Chapter 3). TEAS was also fully transmuted into a premnaspirodiene synthase by mining the sequence comparison of HPS to TEAS and mapping differences onto a structural model (Chapter 4). Chapter 5 illustrates how my experimental understanding of terpene synthase mechanics could be tested by predicting features in a putative synthase, then verifying this by cloning and characterizing valencene synthase from *Citrus x paradisi*. The coupling of terpene synthases with subsequent tailoring enzymes was examined in Chapter 6 as a first step in establishing a system to study the interactions between terpene biosynthetic enzymes. The final chapter of my thesis summarizes my results with respect to the major question of how terpenoids diversity is manifested and closes by proposing the new challenges arising from my work.

Table 1.1 Cloned and characterized sesquiterpene synthases.

Major Product	Source	Year Authors
angiosperm		
valencene	<i>Citrus x paradisi</i>	2003 Greenhagen, this thesis
premnaspirodiene	<i>Hyoscyamus muticus</i>	1995 Back and Chappell ²⁰⁷
germacrene C	<i>Lycopersicon esculentum</i>	1998 Colby et al. ²⁰⁸
germacrene A	<i>Chicorium intybus L.</i>	2002 Bouwmeester ²⁰⁹
epi-cedrol	<i>Artemisia annua</i>	1999 Mercke et al. ²¹⁰
E (beta)farnesene	<i>Mentha x piperita</i>	1997 Crock et al. ²¹¹
beta-caryophyllene	<i>Artemisia annua</i>	2002 Cai et al. ²¹² Mercke et al. ²¹³ , Chang et al. ²¹⁴
amorpha-4,11-diene	<i>Artemisia annua</i>	2000 al. ²¹⁴
(+)delta-cadinene* ¹	<i>Gossypium arboreum</i>	1995 Chen et al. ²¹⁵
(+)5-epi-aristolochene*	<i>Nicotiana tabacum</i>	1992 Facchini and Chappell ²¹⁶
gymnosperm		
gamma-humulene	<i>Abies grandis</i>	1998 Steele et al. ²¹⁷
delta-selinene	<i>Abies grandis</i>	1998 Steele et al. ²¹⁷
(E)-alpha-bisabolene	<i>Abies grandis</i>	1998 Bohlmann et al. ²¹⁸
bacterial		
germacradienol	<i>Streptomyces coelicolor</i>	2003 Cane et al. ¹³⁵
pentalanene*	<i>Streptomyces Uc5319</i>	1994 Cane et al. ²¹⁹
fungal		
(+) aristolochene*	<i>Penicillium roqueforti</i>	1993 Proctor and Hohn ¹³⁴
trichodiene*	<i>Fusarium sportrichioides</i>	1989 Hohn and Beremand ²²⁰

* structure solved

¹ structure unpublished

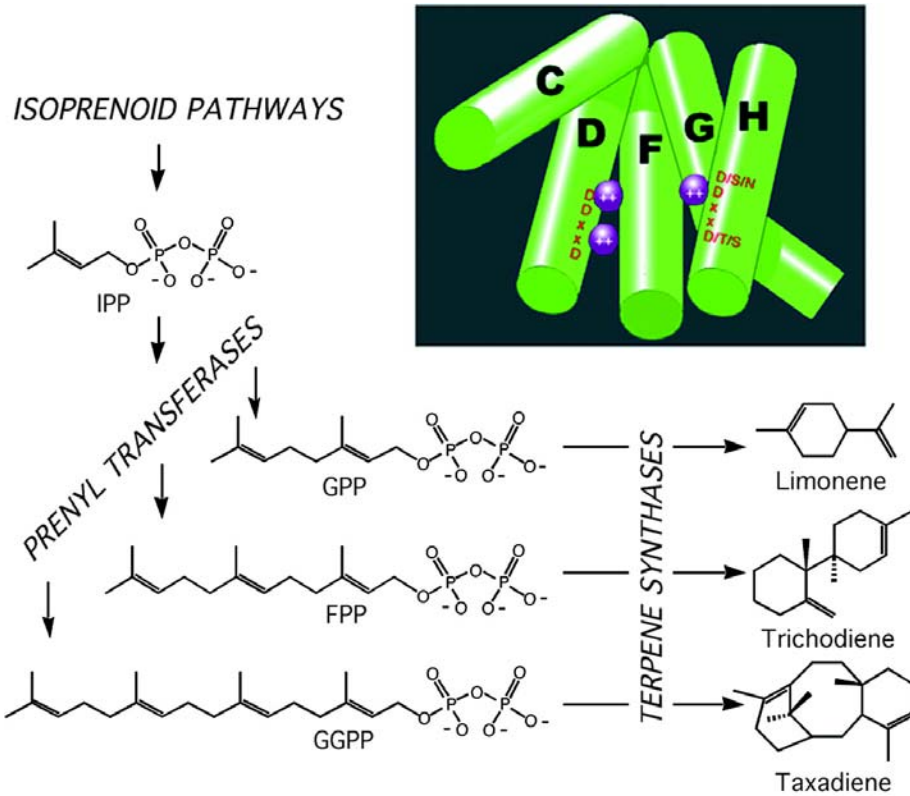


Figure 1.1 Biosynthetic origins of isoprenoids.

Prenyltransferases act to generate different length isoprenoid diphosphates by the addition of IPP. These are then manipulated by terpene synthases (cutaway of terpene synthase fold inset) to form various terpenes.

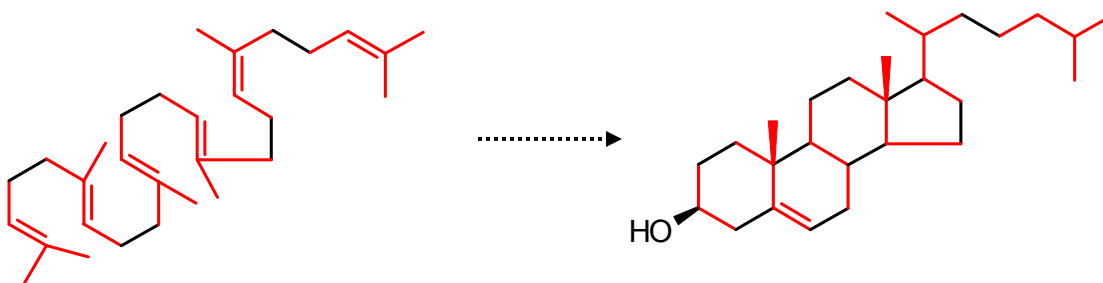


Figure 1.2 The isoprene rule helps explain the biosynthetic origins of cholesterol.

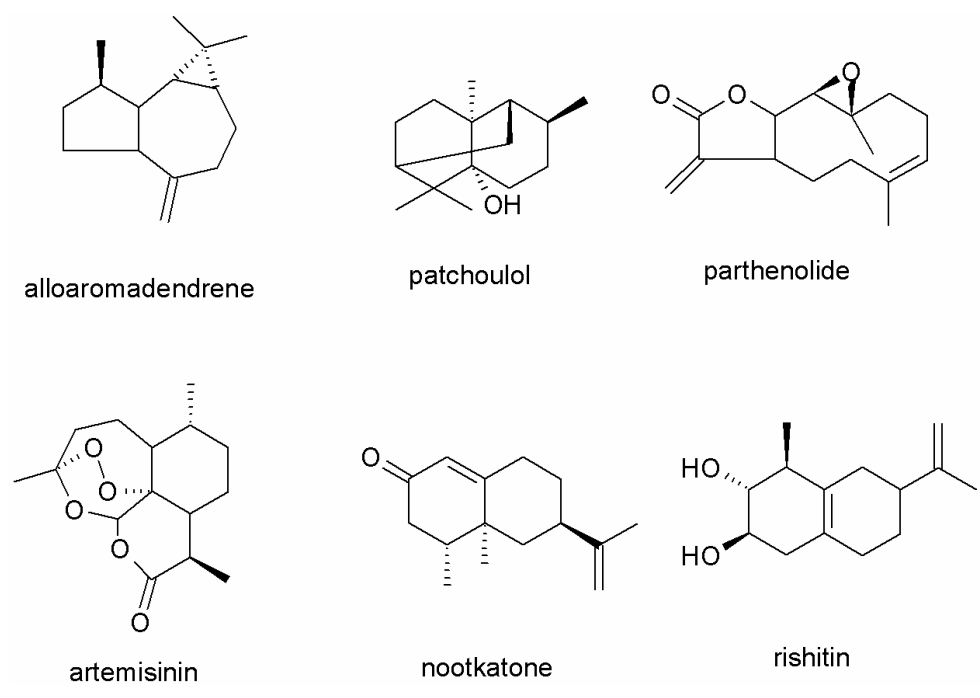


Figure 1.3 A few representative sesquiterpenoids.

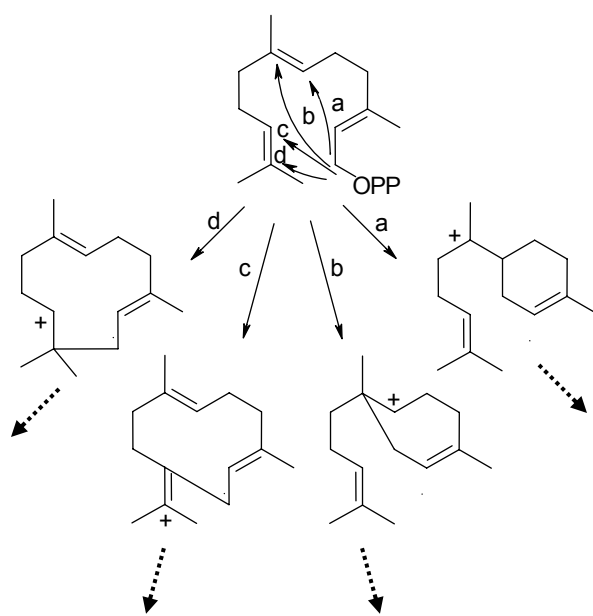


Figure 1.4 Variations of internal addition reactions leading to diverse sesquiterpenoid classes.

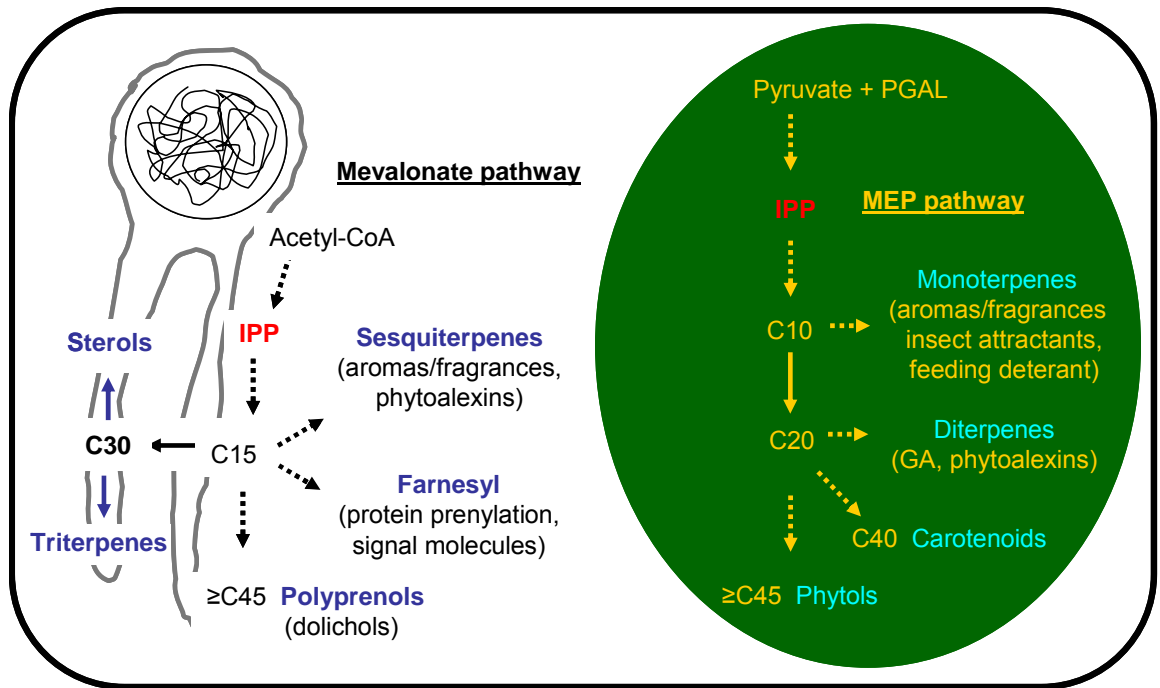


Figure 1.5 Regulation and compartmentalization of isoprenoid pathways.

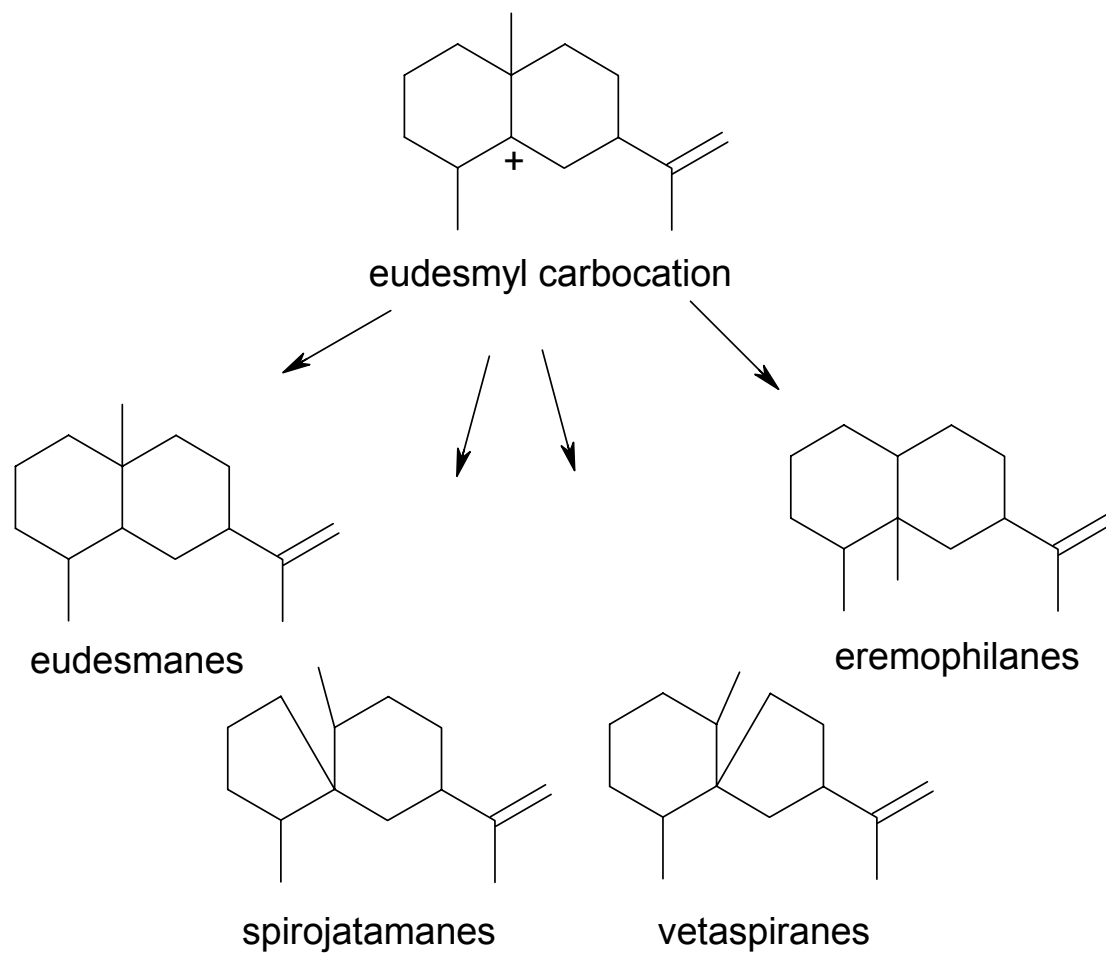


Figure 1.6 Classes of sesquiterpenoid that may have the eudesmyl carbocation as a common intermediate.

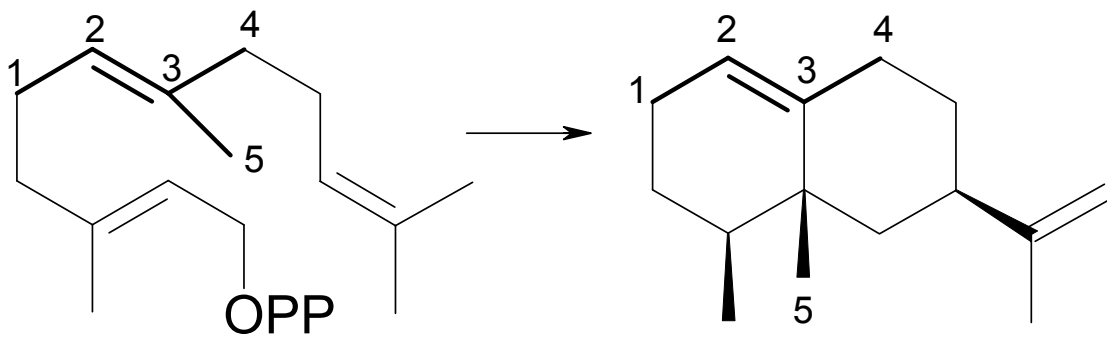
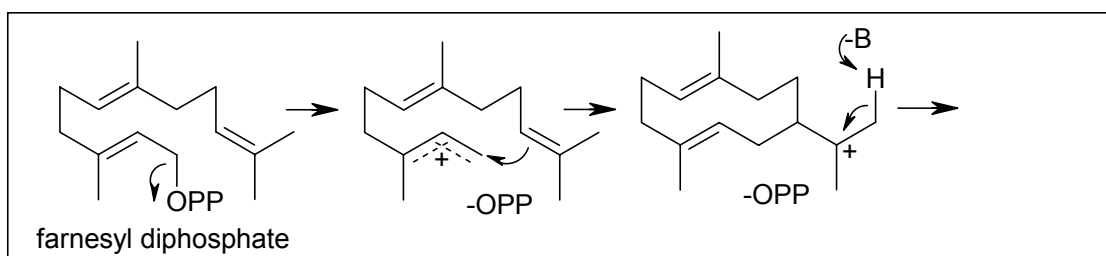
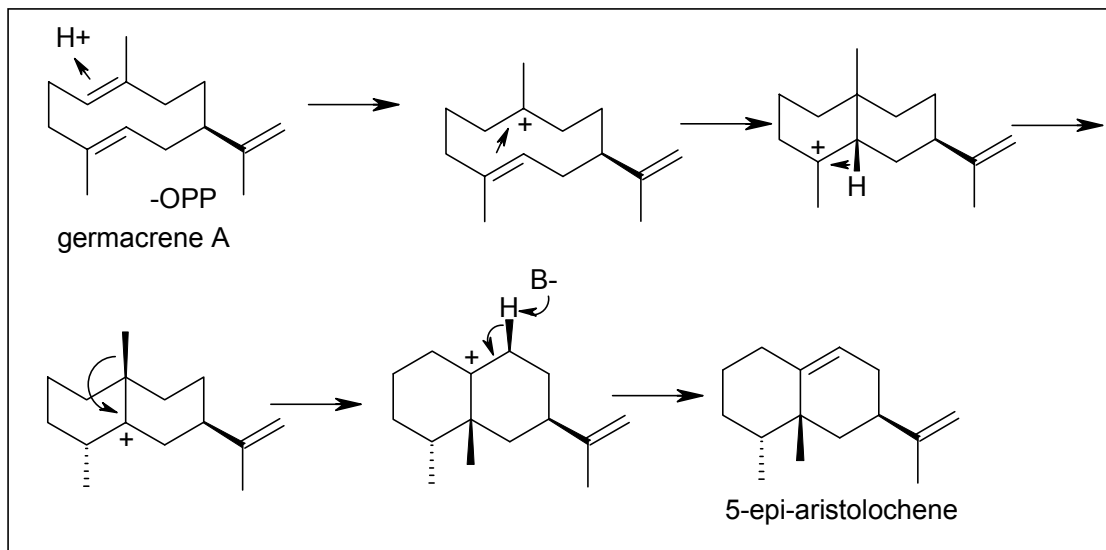


Figure 1.7 Eremophilene does not contain contiguous isoprene units.

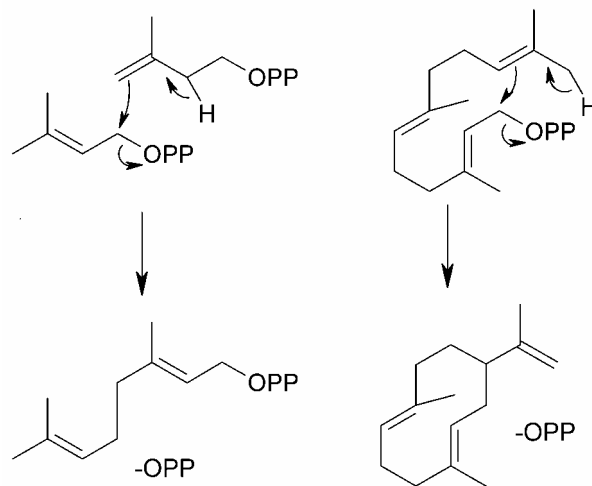


Reaction I

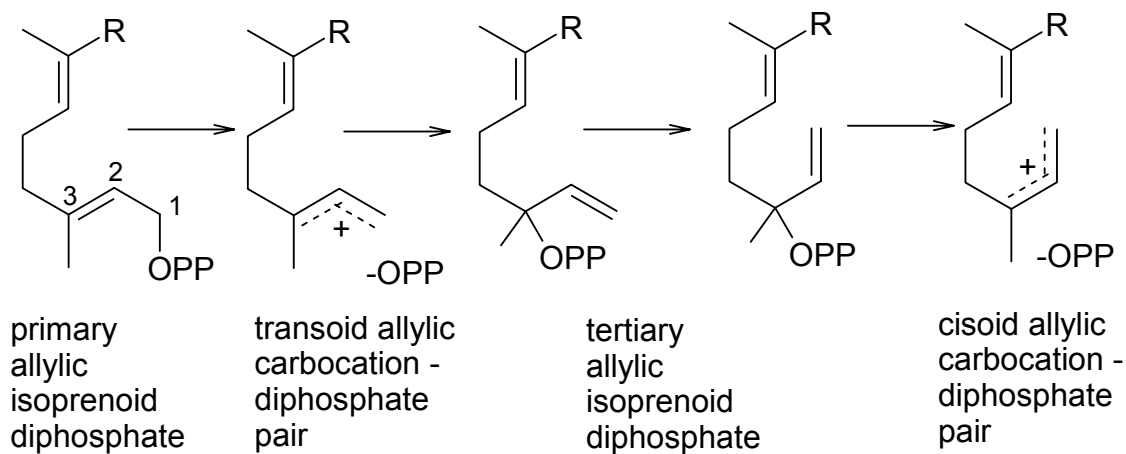


Reaction II

Scheme 1.1 Proposed mechanism for 5-epi-aristolochene biosynthesis by TEAS.



Scheme 1.2 Similarities between prenyltransferase and terpene cyclase catalyzed reactions.



Scheme 1.3 Mechanism for isomerization of the 2,3 double bond of isoprenoids.

CHAPTER 2 Mechanistic insights into substrate specificity, ionization, and isomerization of prenyl diphosphates revealed by monoterpene synthase activities inherent in sesquiterpene synthases

Introduction

Class I terpene synthases initiate catalysis by ionization of allylic isoprenoid substrates and play key roles in diverting carbon into secondary metabolites classified within two major families of terpenes, monoterpenes (10 carbons) and sesquiterpenes (15 carbons)²²¹. Interestingly, the crystal structures of plant monoterpene¹²⁹ and sesquiterpene¹⁰¹ synthases exhibit extensive structural similarities suggesting key structure-function relationships that may be conserved between the two classes of synthase²²¹. However, this apparent functional conservation raises interesting questions about how these enzymes might discriminate between their highly similar substrates, geranyl diphosphate (GPP) and farnesyl diphosphate (FPP). For instance, a number of reports have shown that GPP is turned over by FPP specific synthases^{210,211,217,218}, which the work of Bohlmann *et al.*²¹⁸ suggests could arise as a function of a metal co-factor requirement. Thus, two important issues are: 1. is there a relationship between metal identity and substrate selectivity? and 2. can the turnover of the smaller substrate provide insights into the complex mechanisms by which sesquiterpene synthases convert isoprenoid diphosphates into terpenoids?

Up to this time, the enzymatic activities of sesquiterpene synthases with GPP as substrate have seemed somewhat uninformative, consistently characterized as occurring at relatively low rates and generating simple, usually cyclic monoterpene reaction products^{210,211,217,218}. In contrast, rationally designed substrate analogs have been instrumental in defining steps for terpene synthase catalysis. For instance, a cyclopropyl analog of GPP was used by Wheeler and Croteau to demonstrate migration of the diphosphate substituent to C3 by trapping the analogous tertiary homoallylic diphosphate²²². Likewise, Cane and Tsantrizos provided evidence for the intermediacy of the macrocyclic germacrene A in aristolochene biosynthesis using 6,7-dihydro-FPP which could not undergo a second round of intramolecular cyclization²²³. Other non-

cyclizable analogs have also been used to probe the mechanism of C2-C3 bond isomerization in both monoterpene synthases^{224,225} and a sesquiterpene synthase¹⁵². Although significant evidence and conclusions are possible from these studies, it is important to note that substrate analogs often have considerably different geometries than the normal substrates GPP and FPP. Therefore, these analogs are likely to interact with the active site pocket of the synthase enzymes differently than the natural substrates.

The experiments presented in this chapter demonstrate that once the turnover rate of GPP is optimized for several plant sesquiterpene synthases, 5-epi-aristolochene synthase (TEAS), premnaspirodiene synthase (HPS), and amorpha-4,11-diene synthase (ADS), careful analysis of the reaction products can be used to provide insight into several of the initial catalytic events. In particular, GPP turnover is analyzed with regard to substrate specificity, formation of the ES complex, ionization, and isomerization activities. This information is then used to gain a better appreciation for each of the catalytic steps and to infer mechanisms and enzyme features that control reaction product diversification.

Materials and Methods

Chemicals. [1-³H] farnesyl diphosphate was purchased from New England Nuclear. [1-³H] geranyl diphosphate was purchased from American Radiolabeled Chemicals Inc. Farnesyl diphosphate (FPP) and geranyl diphosphate (GPP) were purchased from Echelon Biosciences Inc. Monoterpene standards beta-myrcene, linalool, geraniol, (*R*)-(+)-limonene, terpineol (principally alpha) were purchased from Sigma Chemical company. All other Chemicals were purchased from either Sigma Chemical Co. or Fisher Scientific Co.

Expression Constructs. TEAS¹⁰¹, ADS²¹⁰, HPS¹⁷³, and EAS-Y520F¹⁶⁰ pET28b (Novagen) expression vector constructs used in this work have been previously described. The EAS-Y527F mutant was prepared similarly to the EAS-Y520F mutant¹⁶⁰. Mutations were verified by automated nucleotide sequencing using the BigDye terminator method (ABI).

Bacterial Expression and Purification of Recombinant EAS, HPS, and ADS.

Recombinant proteins bearing hexa-histidine tags were expressed in *E. coli*, and purified from cell lysates by chromatography over Ni⁺-affinity resin. In brief, BL21 (DE3) cells (Novagen) were transformed with the various expression constructs and selected on solid LB medium containing kanamycin. A colony of bacteria harboring a particular construct was then used to inoculate kanamycin supplemented LB liquid medium to prepare an overnight starter culture. Two mL aliquots of the starter cultures were used to inoculate baffled Erlenmeyer flasks containing 300 mL Terrific broth supplemented with 50 µg/mL kanamycin. These cultures were shaken for approximately 3 hrs. (to OD₆₀₀≈1.2) before expression of the synthase gene was induced by addition of IPTG to 0.1 mM. After five hours of shaking at 200 RPM and 25°C (30°C for ADS), cells were collected by centrifugation (5 min at 5000 x g) and stored at -80°C until used. The cells were thawed and resuspended in 20 mL of cold buffer A (20 mM Tris-HCl, pH 7.9, 0.5 M NaCl, 5 mM imidazole), followed by sonication (75% maximum power, 3 x 30 s pulses) on ice. The lysates were centrifuged at 3900 x g for 20 min, passed through a syringe filter (0.45 µm cutoff) and applied to a 2 mL column of His-Bind Ni²⁺-affinity resin (Novagen) that had been equilibrated with column binding buffer. The columns were washed with 10 mL of buffer A containing 25 mM imidazole, then eluted with 4 mL buffer A containing 125 mM imidazole and dialyzed at 4° C against four changes of 1 L of 50 µM HEPES, pH 7.5, 5 mM MgCl₂, 1 µM DTT. Protein was quantified by the Bradford method using IgG (BIORAD) as a quantitative standard.

Preparation of Divalent Metal-Free Enzymes. Metal-free enzymes were prepared by adding 0.6 g EDTA to 2 mL of enzyme sample and occasional swirling for 1h on ice. After a brief centrifugation at 10,000 x g for 5 min, the supernatant was dialyzed in 6000 dalton FW cutoff dialysis tubing against four changes of 1L of metal free buffer at 4°C (20mM HEPES pH 7.5, 1mM DTT). Activity was negligible in a sesquiterpene synthase activity assay after this procedure, but fully restored in reactions containing 40

mM MgCl₂. After dialysis, enzyme solutions were adjusted to 50% glycerol and stored at -80°C.

Preparation of Isoprenoid Diphosphate Substrates. The substrate stocks were prepared from solid isoprenoid diphosphates, and used to dilute the specific activity of [1-³H] GPP or [1-³H] FPP from different sources. Radiolabeled substrates were normalized by extracting contaminating alcohols, then hydrolyzing aliquots of the preparation to verify the release of the appropriate amount of radioactivity. Stocks of GPP or FPP were prepared in 25 mM ammonium bicarbonate, radiolabel added ([1-³H] GPP or [1-³H] FPP), and these solutions were then gently extracted against pentane in order to remove any contaminating radiolabeled hydrocarbons and alcohols. Small aliquots of each preparation were hydrolyzed with 1.8 M H₂SO₄ at 25°C for two hours, the radiolabeled alcohols partitioned into hexane and an aliquot counted with a liquid scintillation counter to confirm the release of the expected amount radioactivity.

Assays for Monoterpene and Sesquiterpene Synthase Activity. Enzyme assays were modified slightly from the previously reported method, which is based on the conversion of isoprenoid diphosphates substrates into relatively non-polar hydrocarbons and alcohols. Reactions (excepting optimization assays which were modified as described below) were typically 50 µL in size and contained 20 mM Tris-HCl, pH 7.8, 20 mM FPP, 0.1µCi ³H-FPP, 2% glycerol and 50 nM synthase. The reactions were initiated by the introduction of substrate, incubated at 25°C or 30°C for exactly 10 min, terminated by the addition of an equal volume of ice cold 0.2 M KOH, 0.1 M EDTA and then placed on ice. The terminated reactions were then extracted with 200 µL of hexane. Fifty µL of hexane was counted directly in a scintillation counter as a measure of total conversion, while 100 µL was treated with 20 mg of silica to remove any oxygenated species, then the radioactivity in 50 µL of this silica scrubbed hexane was determined. Activities were calculated as conversions of substrate to extractable radiolabel. Metal dependence assays were performed as above except that solutions of divalent metal ion chlorides, MnCl₂ or MgCl₂ were added to the reaction mixtures prior

to substrate. The pH optimization assays were performed using a four buffer system (5 mM each: TRIS, HEPES, PIPES, and MES) adjusted with HCl to indicated pHs.

Product Identification. Reaction product identification was based on a combination of comparative gas chromatography and more absolutely by mass spectrometry. Preparative reactions were performed in 2.5 mL and contained 200 mM Tris-HCl, pH 7.8, 200 μ M FPP, 500 nM EAS or ADS, and 2 μ M MnCl₂ for GPP reactions. Reactions were overlaid with 1 mL of pentane and incubated at 25°C for one hour. The reactions were terminated by vortexing, followed by a second pentane extraction, pooling the extracts, and concentrating the extracts approximately 200-fold on ice under a gentle stream of nitrogen before analysis.

Samples were analyzed by GC using a HP5890 equipped with a capillary HP-5 column (Crosslinked 5% PH ME Silicone, 30 m x 0.32 mm x 0.25 micron film thickness) using He as the carrier gas (flow rate 3.0 mL) and an FID detector at 280°C. The samples were injected at 250°C while the oven temperature was held at 60°C for 30 s, followed by an 8°C temperature ramp to 160°C. Monoterpene products were identified by reference to available standards, a standardized mass spectrum library (NIST), and co-migration with co-injected standards. The only exception was cis-ocimene, which was identified by spectrum matching alone. Chiral phase separation was performed with the same HP5890 gas chromatograph using all the same settings and a J&W CyclosilB column (β -cyclodextrin 30 m x 0.250 mm x 0.25 micron film thickness). Injection port temperature was 250°C, the initial oven temperature held constant at 70°C for 30 s, then ramped to 150°C at a rate of 5°C per min. The assignment of linalool configuration at C3 was made by reference to Jia *et al.*²²⁶ and Lewinsohn *et al.*²²⁷, both of which reported the *S* enantiomer to migrate slower than the *R* form on β -cyclodextrin capillary columns of the same dimensions.

Results

Metal Dependence of Sesquiterpene and Monoterpene Synthase Activities in EAS

During initial efforts to characterize the 5-*epi*-aristolochene synthase (TEAS) activity, a relatively low level of monoterpene synthase-like activity was observed.

Because we suspected that the monoterpene synthase reaction products could be informative, an attempt to optimize and validate the monoterpene synthase activity was made. The monoterpene synthase activity of TEAS is dependent on the amount of synthase enzyme, and very little if any of the activity is evident with denatured enzyme. In addition, the activity profile of TEAS with either substrate was essentially constant within the pH 6.5 to 7.8 range (data not shown). Both of these results are consistent with the measured monoterpene synthase activity arising from bona fide enzymatic activity of TEAS and not a chemically induced solvolysis.

The dependence of substrate turnover by TEAS on manganese and magnesium concentration for FPP and GPP are shown in figure 2.2. Reactions containing Mg^{2+} at concentrations greater than 0.2 mM give reaction rates about one order of magnitude greater for FPP than for GPP. However, when concentrations less than 1 mM of Mn^{2+} were used, GPP was turned over at rates more comparable to FPP. At very low metal concentrations (less than 100 μM), only manganese stimulated substrate turnover for both FPP and GPP. Magnesium did not support significant turnover of either substrate at these lower concentrations. These results parallel previous findings that magnesium dependence of sesquiterpene synthases exhibits saturation kinetics only with FPP²²⁸, while monoterpene synthase tend to utilize either metal⁹⁷.

The concentration of divalent metal ion needed to stimulate catalysis for either GPP or FPP was calculated as the K_A values²²⁹ (half-maximal velocity of activation) for each metal. Due to the inhibition of catalysis of FPP at the higher manganese concentration, the K_A for the manganese dependence was obtained by fitting the initial portion of the Mn^{2+} dependence curve. The estimated K_A for Mn^{2+} was nearly the same for both substrates (≈ 0.031 mM), which is equivalent to the K_d value for the manganese salt of GPP determined by King and Rilling¹³⁰. The K_A for Mg^{2+} was also similar for both substrates (≈ 3 mM), however this is far above the K_d for the magnesium salt of GPP (0.130 mM)¹³⁰.

The maximum velocities of the reactions were metal dependent as well. The V_{max} for the FPP: Mn^{2+} reaction was 2-3 fold greater than the V_{max} for the FPP: Mg^{2+} reaction. The V_{max} for the GPP: Mn^{2+} reaction was also about two fold higher than the GPP: Mg^{2+} reaction. Nonetheless, the V_{max} for FPP was significantly greater than the

V_{\max} for GPP regardless of metal species. Reactions of TEAS with GPP in the presence of optimal MnCl_2 and various concentrations of KCl, which was previously shown to enhance the velocities of some Mn^{2+} dependent coniferous monoterpene synthases²¹⁷, did not influence the overall reaction rates.

EAS and HPS catalyze the synthesis of mostly acyclic monoterpenoids while ADS synthesizes mostly cyclic monoterpenes

Using the optimal conditions established above for the EAS: Mn^{2+} : GPP reaction, the reaction products synthesized by EAS, HPS, and, ADS were examined by gas chromatography and identified by mass spectrometry. The actual GC traces for products synthesized by TEAS and ADS are shown in figure 2.3 and summarized in table 2.1 along with values reported in the literature for several other sesquiterpene synthases as well as the solvolysis products of GPP and LPP.

The monoterpene reaction products generated by the TEAS and HPS enzymes were essentially the same with two acyclic monoterpenoids, myrcene (**1**) and linalool, a tertiary alcohol (**4**), accounting for greater than 90% of the products. In contrast, the ADS monoterpene product profile was dominated by the cyclic alcohol alpha-terpineol (**6**), and linear hydrocarbons myrcene (**1**), and cis-ocimene (**3**). The TEAS products were further examined using chiral phase separation by gas chromatography and the dominant monoterpenyl product, (3*S*)-linalool (**1**), was in approximately 50% enantiomeric excess over its alternative 3*R* form (Figure 2.4). One additional note about the product profiles is that the preparative reactions presented in figure 2.3 and figure 2.4 were performed at room temperature (24°C). When TEAS was incubated with GPP at higher temperatures (i.e. 37°C), the only detectable product was linalool (data not shown).

GPP Turnover Rates in EAS Mutants Y520F and Y527F are suppressed

The reaction product profile of TEAS suggested that the enzyme was essentially carrying out only the initial ionization step, followed by immediate release of acyclic products (see scheme 2.1). If this were the case, then we predicted that site-directed mutants (Y520F and Y527F) of TEAS previously characterized for altered catalytic

activities downstream of the initial ionization step¹⁶⁰ should have similar catalytic rates with GPP as the wildtype enzyme. Surprisingly, the monoterpene synthase activities for both mutants were greatly suppressed and such results are inconsistent with residues Y520 and Y527 solely playing roles independent and downstream of the initial ionization event (Figure 2.5).

Discussion

Scheme 2.1 presents a chemical rationalization for the monoterpene and sesquiterpene synthase activities of TEAS and ADS, and can be used as a guide for interpreting the current results. Mechanistically, TEAS initiates sesquiterpene catalysis by ionization of farnesyl diphosphate (**FPP**), generating a diphosphate anion and the first reactive carbocation intermediate (a transoid farnesyl cation (**7**)). This transoid carbocation (**7**) then undergoes a series of cyclization and rearrangement events leading to **5-epi-aristolochene**. The ADS reaction, similarly is initiated by FPP ionization, but transfers the diphosphate group to carbon 3, forming nerolidyl diphosphate (**NPP**). This allows for rotation about the C2-C3 bond, and formation of a cisoid farnesyl cation (**8**). This cisoid carbocation (**8**) is cyclized and rearranged to **amorpha-4,11-diene**.

If the native TEAS reaction proceeds by direct electrophilic attack subsequent to ionization, without diphosphate migration, one might predict that TEAS would ionize **GPP** and the resultant carbocation would either capture water or eliminate a proton (path **a** or **b**) to form simple acyclic monoterpenes, such as **linalool** or **myrcene**. In contrast, ADS would be expected to ionize **GPP** much like TEAS, but then allow for the formation of a tertiary diphosphate intermediate linalyl diphosphate (**LPP**), followed by rotation around the C2-C3 bond and re-ionization. This second reactive intermediate would then be properly configured to undergo proton eliminations (pathways **a'** or **b'**) to **trans-** and **cis-ocimene**, or to undergo cyclization by attack of the C6-C7 double bond to form cyclic products **α -terpineol**, **terpinen-4-ol**, or **limonene**. Our results are entirely consistent with this scheme. An alternative mechanism for TEAS is that the transoid farnesyl carbocation (**7**) arises indirectly from ionization of **NPP**. If this were so, ADS and TEAS monoterpene product profiles

might instead be expected to be similar. Thus, a mechanism wherein the initial transoid allylic carbocation directly attacks C10 to form germacrene A is supported.

The selectivity towards myrcene formation by TEAS, but nearly equal proportions of myrcene and ocimenes, can be explained if diphosphate is invoked as the base in the proposed mechanisms of monoterpene formation by TEAS and ADS (Scheme 2.2). Subsequent to the ionization of GPP, the path for proton abstraction resulting in ocimene formation (**a**) is much longer and more indirect than the path for proton abstraction resulting in myrcene formation. However, resultant geometries arising from NPP ionization (**a'** and **b'**) are both direct and equidistant. In agreement with the proposed scheme where diphosphate acts as a base, TEAS produces mostly myrcene, while ADS produces relatively equal amounts of both myrcene and ocimenes. This selectivity occurs throughout the literature where sesquiterpene synthases that are believed to proceed an NPP intermediate do not select against ocimene formation relative to myrcene (Table 2.1).

Although these chemical rationalizations make a number of assumptions concerning possible intermediates, they provide a context for interpretation of the data. Specifically, the data suggest that manganese enhances the rate of catalysis with either substrate, that the previous Y520F and Y527F mutants are probably more generally compromised mutants than originally thought, and GPP can be used to map those functional elements within terpene synthases important for formation of the tertiary diphosphate intermediates and isomerization about the C2-C3 double bond.

Manganese stimulates the rate of catalysis

Several sesquiterpene synthases have previously been reported to convert geranyl diphosphate (GPP) into arrays of monoterpenes^{210,211,217,218,230}. Reported turnover rates for GPP relative to FPP have ranged from 3% for (*E*)- β farnesene synthase to 50% each for the grand fir derived cyclases δ -selinene synthase, γ -humulene synthase and (*E*)- α -bisabolene synthase from grand fir^{217,218}. Bohlmann *et al.*²¹⁸ also observed that the monoterpene synthase activity of (*E*)- α -bisabolene synthase was highly sensitive to divalent cation, reporting a four-fold improvement in

monoterpene synthase activity in the presence of 0.5 mM Mn^{2+} relative to saturating concentrations of Mg^{2+} , but a declining rate at concentrations higher than 1mM .

The true substrate for terpene synthases is thought to be a divalent metal ion/isoprenoid diphosphate complex, e.g. $\text{M}^{2+}:\text{XPP}^{231}$. The sigmoidal nature of metal-dependent plots in figure 2.2 are consistent with this assumption, where the apparent K_A values, the activation constants, coincide with (for GPP) or are higher than (for FPP) the K_d values, the metal:substrate dissociation constants. The observed V_{\max} values demonstrate that, regardless of substrate, reaction rates are increased by at least two fold in the presence of Mn^{2+} . This may be attributable to the greater electronegativity of Mn^{2+} ion, which could raise the reaction rates by lowering the energy barrier to substrate heterolysis through electronic interactions with diphosphate. A similar rate enhancement has been observed in solutions at neutral pH where alcohols are produced by solvolysis much faster with Mn^{2+} salts than for Mg^{2+} salts²²⁸. Importantly, in the current interpretation, ionization is the rate-limiting step for catalysis, contrary to the kinetic models constructed from pre-steady state kinetic analyses¹⁷³.

The Y520F and Y527F mutants are pleiotropic

The Chappell and Noel lab groups have previously reported that amino acid residue Y520 was positioned within the TEAS active site pocket to support a key step in the conversion of FPP to 5-epi-aristolochene¹⁶⁰. As predicted, mutation of this residue from tyrosine to phenylalanine resulted in an enzyme activity capable of catalyzing the conversion of FPP to germacrene A, a putative key intermediate in the TEAS catalytic cascade. Because the Y520F mutant was originally thought only to eliminate the protonation of germacrene A, we assumed that these mutants would also turnover GPP at rates comparable to the wildtype enzyme. In contrast to these expectations, both mutant enzymes had significantly suppressed rates of catalysis with GPP. One possible explanation for this suppression is that the mutants in fact were not mutations specific to a particular catalytic step with the TEAS enzyme, but were more general structural requirements for later steps in catalysis and mutation of these residues made the enzyme incompetent to provide the steps beyond the relatively simple addition-elimination reaction which gives germacrene A.

Use of GPP as a probe for the early steps of catalysis

The initial premise for examining the suitability of GPP as a substrate for the sesquiterpene synthases TEAS, HPS and ADS was simply to determine if substrate specificity could be affected by divalent cation preference. Interestingly, magnesium ion has generally been considered the more physiological metal species used *in vivo* by the angiosperm mono- and sesquiterpene synthases, such as EAS^{217,218}. However, previous^{210,211,217,218} and current results suggest that the sesquiterpene cyclases may have difficulties in discriminating between GPP and FPP if presented with both substrates, and that perhaps other physiological considerations such as co-factor and substrate availability are important means for regulating monoterpene versus sesquiterpene synthase activities.

The reaction product profiles of the EAS, HPS and ADS enzymes incubated with GPP suggest that catalytic features of the respective enzymes are preserved and reflected in the reaction products. EAS and HPS catalyzed the generation of linear monoterpene products, while ADS catalyzed the conversion of GPP to several cyclic products. Accumulation of these two different classes of monoterpene products is consistent with the rationalized chemistry for each enzyme, and suggests that GPP utilization could be used in combination with some form of mutagenesis to identify mutations that convert TEAS into an “isomerization” type terpene synthase, and conversely conversion of ADS into a “non-isomerization” type enzyme.

Table 2.1 Product distribution for various sesquiterpene synthases incubated with FPP and GPP.

Distribution of Monoterpenes Drived from isoprenoid diphosphates by Sesquiterpene Synthases and by Chemical Solvolysis

sesquiterpene synthase product	C10 cyclic products										C10 acyclic products			C10 ratios		C15 ratios	
	α -terpineol + terpinen-4-ol	sabinene	α -terpinene + γ -terpinene	terpinolene	limonene	myrcene	E-ocimene	Z-ocimene	linalool	nerol	geraniol	% cyclic	% non-cyclic	cis	trans		
epi-aristolochene					2	40	2	2	54			2	98	nd	98		
prennaspordiene					2	70	2	2	24			2	98	nd	98		
amorpha-4,11-diene	39				11	19		24	6			50	49	98	2		
δ -selinene (3)			6	9.3	41.2	15.1	6	22				57	44	86	13		
(E)- β -farnesene (4)		3	7	15	48	15	7	6				73	28	95	5		
γ -humulene (3)			21	65.4		8.9	5					86	14	98	<2		
epi-cedrol (5)	0.3		10	42	45	5						97	5	99	nd		
non-enzymatic conditions																	
GPP + H ₂ SO ₄	2.6		5	4		18	44	29	77.7	0.9	17	<4	96				
LPP + H ₂ SO ₄	23		2	14	15	23	31	15	59	3.3	11	24	76				
GPP + 100mM Mn ²⁺	3.3				1.2	2.7	1.7		71	0.6	19	5	95				

sulfuric acid derived hydrocarbons are % of total hydrocarbons (only aprox. 3% of total products)

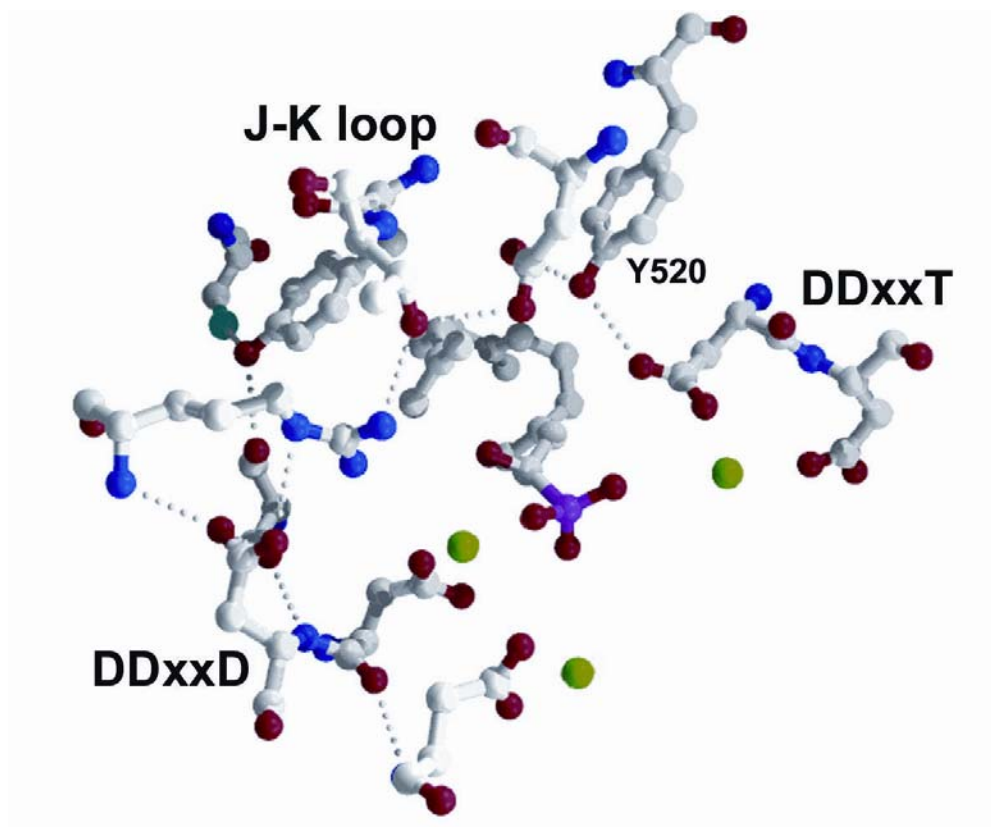


Figure 2.1 Model of the J-K loop, DDxxD motif, and hydrogen bonding interactions at the mouth of the active site.

This model was derived from the 5EAT pdb coordinates and shows farnesyl hydroxyphosphonate (FHP) at center. Green spheres represent magnesium cations. Dotted lines represent possible hydrogen bonds.

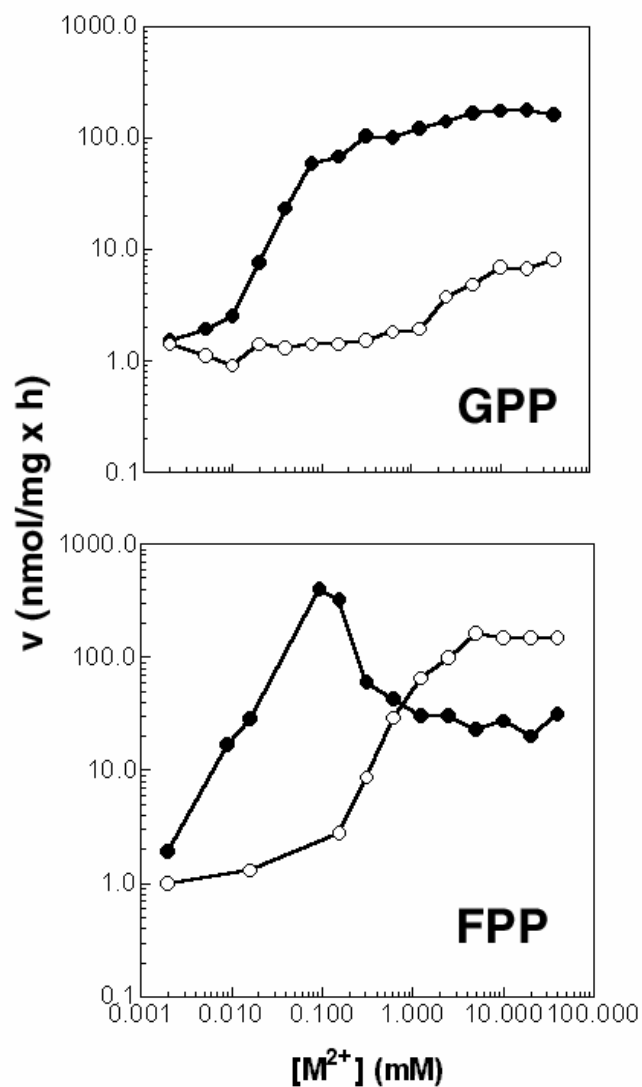


Figure 2.2 Dependence of reaction rate on metal concentrations.

Solid symbols represent data points from incubations with MnCl₂, open symbols represent incubations with MgCl₂. Substrate is indicated in lower right hand of each plot. Scale is log₁₀ on both axes.

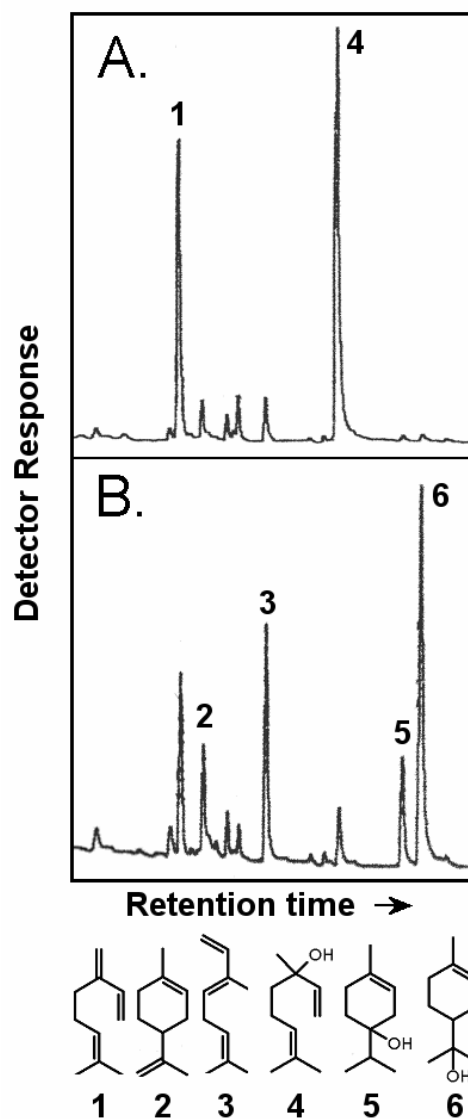


Figure 2.3 GC separation of monoterpenes produced by ADS and TEAS.

Products of incubation of EAS (panel A) and ADS (panel B) with GPP were extracted with pentane and separated by gas chromatography. Compounds were identified by matching GC retention times and mass spectra to standards. Structures identified for major peaks are given and are: 1. myrcene, 2. limonene, 3. cis-ocimene, 4. linalool, 5. terpinene-4-ol, and 6. α -terpineol.

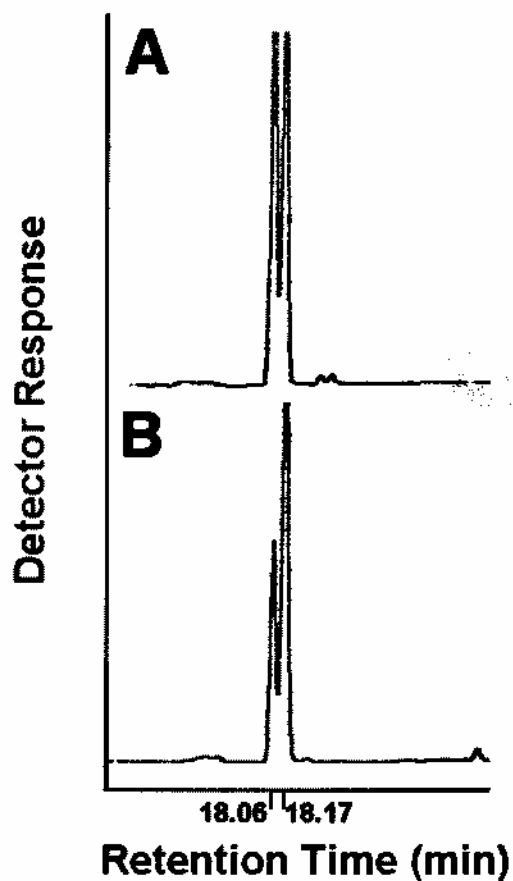


Figure 2.4 Chiral separation of linalool enantiomers by gas chromatography.

A. Racemic linalool dissolved in pentane and separated by chiral phase (β -cyclodextrin) GC. B. Linalool from same pentane extract used to produce GC trace in figure 2.3A separated by chiral phase GC. The peak at 18.17 was assigned the *S* configuration at C3 of linalool by reference to the literature.

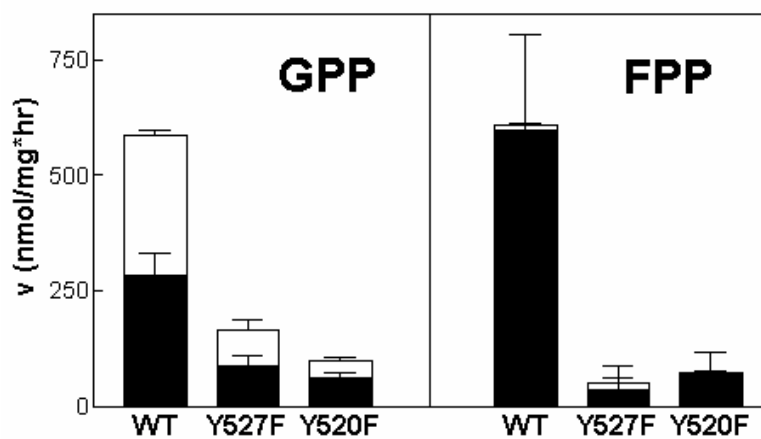
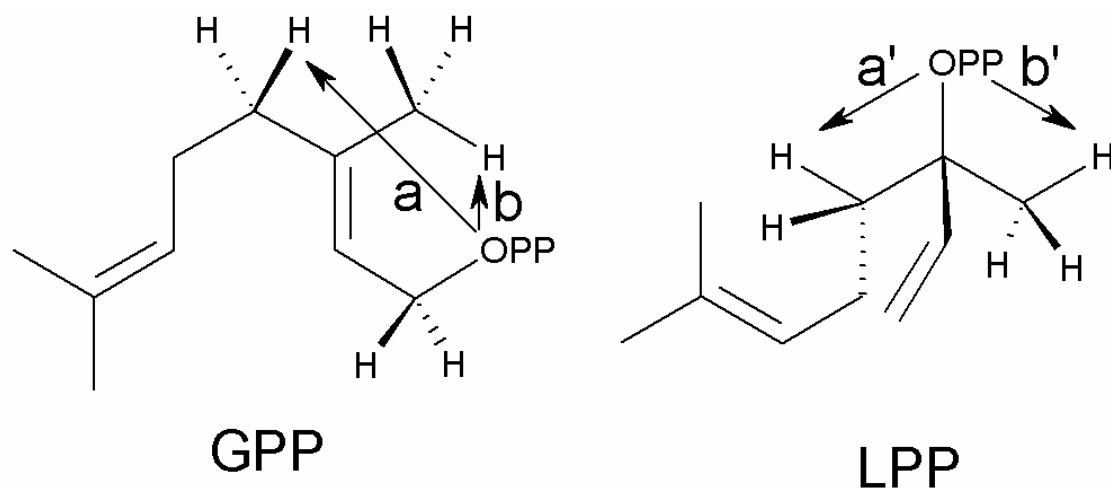


Figure 2.5 Relative turnover rates for GPP and FPP incubated with active site tyrosine mutants.

Dark shaded bars indicate hydrocarbon component of turnover, while unshaded bars indicate oxygenated compounds (removed after treatment of the hexane extract with silica). The hydroxyl group of Y520F and Y527F direct into the TEAS active site. Both the Y527F and Y520F mutants produce significant amounts of germacrene A at pH 7.5.



Scheme 2.2 Selectivity in proton abstraction from GPP and LPP if diphosphate acts as the base.

If diphosphate leaves the primary position of GPP to abstract a proton, the distance for deprotonation from path **a** is greater than path **b** due to the geometry of the 2,3 double bond. Path **a** results in ocimene (**3** in figure 2.3) while path **b** results in myrcene (**1** in figure 2.3). Pathways **a'** and **b'** lead to the same products as paths **a** and **b**, however if diphosphate were to leave the tertiary position (LPP) and abstract a proton, the paths would be more or less equivalent.

CHAPTER 3 4-epieremophilene Synthase, a novel product terpene cyclase derived from 5-epi-aristolochene synthase

Introduction

Sesquiterpene synthases play a key role in sophisticated chemical defense mechanisms that plants have evolved to ward off invading pathogens. In solanaceous plants, sesquiterpenoid phytoalexins, such as capsidiol and solavetivone, are synthesized in response to fungal pathogen attack²³². In mounting this response, the central metabolite farnesyl diphosphate (FPP) is shunted into phytoalexin biosynthetic pathways²³³. Sesquiterpene synthases catalyze the cyclization of FPP into the capsidiol precursor 5-epi-aristolochene or alternatively, the solavetivone precursor premnaspirodiene²³² (Scheme 3.1). Early schemes for the biosynthesis of capsidiol involved many catalytic steps¹⁵. The cloning of terpene cyclases and, more recently, a dihydroxylase involved in capsidiol biosynthesis has demonstrated that only two enzymes are required for capsidiol biosynthesis from farnesyl diphosphate, 5-epi-aristolochene synthase (EAS) and 5-epi-aristolochene dihydroxylase (EAH). To a limited extent EAH will not only accept 5-epi-aristolochene but will also produce solavetivone if presented with premnaspirodiene¹⁷⁴ (see chapter 6).

The apparent plasticity at the cytochrome P450 mediated step, and regulatory control exercised on the terpene synthase suggest that a key step in developing new bioactive sesquiterpenoids is the evolution of product specificity at the level of the terpene synthase. Selection for synthases that efficiently contribute to phytoalexin synthesis may be strong; both EAS and HPS produce their respective sesquiterpenes with high fidelity (>95%)²⁰⁷. In contrast, the constitutively expressed, oleoresin producing sesquiterpene synthases of coniferous species have been found to give rise to broad spectrums of mutli-cyclic sesquiterpenoids²¹⁷. The questions addressed in the next three chapters concern how sequence changes within the angiosperm cyclases, in particular TEAS and *Hyoscyamus muticus* premnaspirodiene synthase (HPS), contribute to the development of new reaction pathways, and therefore, new sesquiterpenoids.

In an effort to determine regions of EAS and HPS (previously, HVS) that contribute to product definition, Back and Chappell constructed a series of fourteen chimeric proteins within which sequence elements from EAS and HPS were exchanged¹¹⁵. Six of these appeared to be bifunctional, giving rise to products similar to those produced by both EAS and HPS¹¹⁵. These results established that the terpene synthases are not modular, as are other important natural product synthases (the polyketide synthases²³⁴) and defined a limited region of 189 amino acids which appear to contain elements affecting product specificity. The crystal structure of EAS¹⁰¹ reveals that this effective region of primary sequence resides in an alpha-barrel structure which surrounds the active site. Site directed mutagenesis to the apparent active site confirmed a single catalytic site for the entire reaction pathway¹⁶⁰. Remarkably, the residues lining this active site are conserved in EAS and in HPS¹⁰¹ and the suggestion has been made that product differentiation is controlled by residues in layers surrounding the active site (Table 3.1). Notably, a similar phenomenon has been demonstrated to be at play in defining the substrate specificity of aspartate aminotransferase¹⁹².

A rational evolution of one cyclase activity (EAS) to the other (HPS) could help us understand how reaction pathways are differentially defined in the respective cyclases. In order to identify targets for mutagenesis, a map of interactions was made in an effort to determine influences at the active site resulting from changes in identity of residues distant from the active site. Van der Waals contacts between each carbon atom of the substrate analog and TEAS residues were determined using pdb file viewing software and plotted (figure 3.1). This set of active site residues is termed the first tier. This operation was repeated for each atom of each R group of each residue in the first tier; the set of residues interacting with 1st tier residues was defined as the second tier. This analysis revealed four non-conserved amino acids residing in the second tier. By inspection of the 3D model, tyrosine 402 (T402) and valine 516 (V516) appeared to influence the positioning of cysteine 440 (C440), a first tier residue. Moreover, in comparison to TEAS, HPS contains a serine at position 402 and an isoleucine at position 516. Considering these respective substitutions in the TEAS enzyme (T402S, V516I) was intriguing because these substitutions would be conservative with respect

to space filling (threonine - serine = valine - isoleucine), except that a methyl group would be re-positioned from one side of C440 to the other, which could influence the projection geometry of C440 into the active site. After an initial assessment of the role of C440 for catalysis, the impact of mutating TEAS to T402S and V516I was examined.

Materials and Methods

Preparation of Enzymes

Mutations were made with a pET-28b vector (Novagen) construct harboring the coding sequence for 5-epi-aristolochene synthase¹⁶⁰ using the standard Quikchange mutagenesis method (Stratagene). Mutagenic primers used were (mutations in bold) CCT AAG CAA TGC ACT AGC AAC TAG CAC ATA TTA CTA CCT CGC GAC and its complement for EAS-T402S, and CCT ATT CTC AAT CTT GCT CGT ATT ATT GAG GTT ACA TAT ATA CAC and its complement for pET-28bEAS-V516I. The EES (pET28b-EAS-T402S/V516I) construct was prepared using pET28b-EAS-V516I as a template with the primers for the T402S mutation. All mutations were verified by automated nucleotide sequencing. Constructs were transformed into BL21 (DE3) cells, cultured and expressed as described previously¹⁷³. The construct provided N-terminal hexahistidine tags which afforded >90% pure protein upon Ni⁺ affinity chromatography in all cases¹⁷³. The wild type and mutant enzymes were further purified to >98% purity using MonoQ column anion exchange chromatography. Protein was quantitated using the Bradford method and IgG as protein standards.

Assay for Cyclase Activity

Small scale reactions were used for rate determinations. These were 50 μ L in size and contained 200 mM Tris-HCl, pH 7.5, 40 mM MgCl₂ and 160 nM enzyme. Substrate was prepared via serial dilutions of [1-³H] FPP diluted with unlabeled FPP (NEN and Sigma). Briefly, 10 μ L of substrate (farnesyl diphosphate) solution (giving 0.7-23 μ M final concentration) was rapidly mixed with 40 μ L of enzyme solution at room temperature (23°C) and allowed to incubate for 1 minute. The reaction was terminated by addition of 150 μ L of a KOH/ EDTA stop solution. Reactions were extracted with 500 μ L of hexane and an aliquot was taken for determination of radiolabeled

hydrophobic product via liquid scintillation counting. Samples were not purified with silica before counting as background was minimal and synthase mutants could possibly produce alcohols. Kinetic constants were determined from direct fits of the Michaelis-Menton equation to the data using Graphpad Prism 2.01 software.

Product Analysis

Preparative reactions were cyclase assays scaled to 2.5 mL and employed 2 μ M enzyme and 80 μ M unlabeled FPP. The reactions were incubated for 1 hr and extracted twice with 2 mL of pentane. Pooled extracts were dried to 50 μ L under a stream of nitrogen gas and analyzed by GC-MS analysis as previously described¹⁷⁴ (See Chapter 6).

Molecular Modeling and Docking (*This work was performed by Dr. Paul O'Maille and Prof. Joe Noel, The Salk Institute for Biological Studies, Structural Biology Laboratory*).

Mutant enzyme structures were built with the program Modeler (version 4.0) using TEAS coordinates (pdb code 5EAT) as template. The five lowest energy structures were subsequently used for docking studies. Presumptive reaction intermediates were constructed using ChemDraw Ultra (version 7.0.1) and MOPAC energy-minimized using Chem3D Ultra (version 7.0.0) (CambridgeSoft). Docking was performed using Genetic Optimization for Ligand Docking (GOLD, CCDC Software). Images were made using Chimera (UCSF).

Synthesis and Verification of 4-epieremophilene (*This was the work of collaborators Marilyn Xiao and Prof. Robert Coates, University of Illinois. Procedures and references given in the APPENDIX*)

Results

C440 mutant reaction products and abundance

The target mutations that were arrived at (T402S and V516I) from the contact map (figure 3.1) both flank a cysteine (C440) which resides at the back of the TEAS active site. No role was originally proposed for this residue¹⁰¹, yet it contacts the

substrate analog in the vicinity of substrate bonds. The relative conformations of which are expected to be critical to defining product specificity. In the crystal structure, C440 contacts C4 and C5 of FHP substrate analog as well as C14, as can be deduced from the contact map (figure 3.1). Significantly, C14 is the methyl that migrates in 5-epi-aristolochene biosynthesis. Additionally, the bond angles between C3-C4-C5 are expected to be critical in defining the boat conformation of the ring A (where ring A is substituted with methyl carbon 15 and ring B has the isopropenyl group) required for 5-epi-aristolochene synthesis vs. the chair conformation necessary for premnaspirodiene synthesis. As a caveat, it is possible that FHP does not bind in the same conformation as FPP in the active site. However, it is likely that the middle (β) isoprene unit is in the vicinity of C440.

In order to determine possible mechanistic influences from C440, this position was mutated to serine and alanine. Crude lysates of *E. coli* harboring and expressing TEAS, TEAS-C440A and TEAS C440S constructs were prepared and incubated with FPP. Products of these reactions were extracted with pentane, separated by gas chromatography, and analyzed by mass spectrometry. From this analysis the dominant product was determined to be germacrene A for both C440S (96%) and C440A (99%) mutants (figure 3.2). Germacrene A was identified as the injector induced thermal (Cope) rearrangement product, β -elemene, by matching to the NIST standard spectrum. Low temperature sample injection revealed a dominant peak identifiable as germacrene A in comparison to a reference spectrum, but less volatile components, such as 5-epi-aristolochene were easily detected at these injector temperatures.

A steady state kinetics analysis was done on TEAS, TEAS-C440S, and TEAS-C440A proteins. The results of this analysis stand in marked contrast to parameters determined previously for the TEAS-Y520F mutant, which produces germacrene A as a dominant product. TEAS-Y520F exhibited a catalytic efficiency (k_{cat}/K_m) which was 3% of wild type ($wt = 0.021 \mu\text{M}^{-1}\text{s}^{-1}$, TEAS-Y520 = $0.0006 \mu\text{M}^{-1}\text{s}^{-1}$). Kinetic constants were calculated for the TEAS-C440S and TEAS-C440A mutants by fitting the data to the Michaelis-Menten equation ($V_0 = V_{max}[S] / K_m + [S]$, figure 3.3). In this analysis k_{cat}/K_m for wild type TEAS is $0.015 \mu\text{M}^{-1}\text{s}^{-1}$, while C440S is $.014 \mu\text{M}^{-1}\text{s}^{-1}$ and C440A is $0.011 \mu\text{M}^{-1}\text{s}^{-1}$, giving 93% and 73% the efficiency of TEAS. Although the standard

error of the curve fitting was up to 18% of the K_m value and 8% of the k_{cat} , it appears that the activity of TEAS-C440S is very near wild type levels, and that TEAS-C440A is only slightly more compromised.

In our collaboration with the Noel Lab (Salk Institute, La Jolla, CA), Dr. Paul O'Maille, has found that C440S, C440A, and Y520F mutants produce significant amounts of 5-epi-aristolochene when reactions are incubated at pHs below neutral. Y520F however exhibited a broad pH titration while the C440S and C440A mutants exhibited sharp transitions between 5-epi-aristolochene and germacrene A at approximately pH 7, reminiscent of titration around a pK_a . Dr. O'Maille has also observed that a similar transition occurs at pH 8.8 for the wild type enzyme, a value near the pK_a of 8.4 for a cysteinyl sulfhydryl group.

Reaction products of the T402 and V516 mutants

TEAS pET vector expression constructs with single targeted mutations, TEAS-T402S and TEAS-V516I, and the double mutant TEAS-T402S/V516I were expressed in *E. coli* and purified to homogeneity. These proteins were incubated with FPP in preparative scale reactions under standard TEAS cyclase reaction conditions at pH 7.5. Figure 3.4 shows the GC profile for the separation of pentane extracted reaction products for the wild type (top) and the double mutant (bottom). The major components in these extracts were identified by comparison to mass spectra of synthetic standards prepared by the Coates Laboratory. Peak A corresponds to the eremophilane sesquiterpene previously characterized as the TEAS reaction product 5-epi-aristolochene. Peak B was identified by comparison to a standard synthesized by the Coates group of the double bond regioisomer of 5-epi-aristolochene, referred to as 4-epi-eremophilene, and identified by Dave Schenk in his recent Ph.D. dissertation¹⁷⁰ (University of Illinois, Urbana, IL) as a minor product of the native TEAS reaction. 4-epi-eremophilene has escaped detection previously because of its low abundance and its poor resolution from the dominant product.

The 4-epi-eremophilene structure has not been published to our knowledge. ³H NMR, ¹³C NMR, IR, and GC-MS data obtained by Marilyn Xiao (of the Coates group) in support of the structure for 4-epi-eremophilene and is provided in an appendix at the

end of this thesis for reference. 4-epi-eremophilene was prepared first by Dave Schenk using an alternate synthetic scheme¹⁷⁰.

Reaction product abundances for the T402 and V516 mutants

The combination of both mutations in TEAS results in slightly more novel product than found in the sum of the single mutations (Table 3.2). TEAS-T402S and TEAS-V516I each produce $\approx 30\%$ 4-epi-eremophilene, while TEAS-T402S/V516 synthesizes 70% at pH 7.5. The putative intermediate germacrene A is the only other major product and varies from significant amounts (16%) in TEAS-V516I to undetectable amounts in T402S. As a caveat, it should be noted that the relative TEAS product abundances, particularly for germacrene A, are very sensitive to pH as has been observed by our collaborators Paul O'Maille and Joe Noel (as described above). TEAS product abundances, however, appear to be invariant at a given pH.

Steady-state kinetic analysis of the T402 and V516 mutants

The catalytic constants of the TEAS mutants are somewhat compromised but remain within the observed range for natural sesquiterpene cyclases (Figure 3.5). Triplicate assays measured hexane-extractable radiolabel recovered from sets of incubations of wildtype and mutants with eight concentrations of [1-³H] FPP, and this was repeated at three concentrations of protein (100-300 nmol, quantitated by IgG standard) to verify turnover rates independent of enzyme concentration. Constants were derived from plots of substrate concentration vs. turnover rate fitted to the Michaelis-Menten equation. The increase in the proportion of 4-epi-eremophilene produced (Table 3.2) roughly parallels a decrease of three to ten fold in the observed k_{cat} values. In all mutants, the K_m drops to less than half of the wild type value, but does not vary considerably from mutant to mutant. The K_m measured for the wildtype enzyme is greater ($8.5 \pm 0.5 \mu\text{M}$) than previously reported ($2\text{-}5 \mu\text{M}$ ^{112,160}) while the K_{cat} (0.105 s^{-1}) is about double (0.048 s^{-1})^{112,160}. Nonetheless, the current comparisons of wildtype to mutant enzymes were performed with preparations and assays prepared in parallel.

Modeling

A computer generated model of the eremophilyl carbocation was made representing the last common intermediate believed to be shared in the reaction pathway to 5-epi-aristolochene and to 4-epieremophilene (Figure 3.6). This molecule was docked into the active site of an energy minimized model of the TEAS-T402S/V516I based on the crystal structure of TEAS. The eremophilyl ligand consistently oriented in the expected direction with the isopropenyl group directing away from the center of the alpha-barrel. A common feature of the minimized fits was that protons abstract at either at C6 for 4-epi-eremophilene synthesis or at C8 for 5-epi-aristolochene synthesis are in close proximity to C440.

Discussion

The objective of the work in this chapter was to discover what residue substitutions are required to convert TEAS into a prenaspirodiene synthase using sequence data from HPS. The strategy employed was to infer the influence of residues outside the active site by mapping Van der Waals contacts within the TEAS structure. Residues potentially influencing the positioning of the β -isoprene unit of FPP were sought since this is the region of the substrate which undergoes product differentiating transformations. Two residues lying six to seven angstroms away from the approximate center of the pocket, T402 and V516, satisfied this criteria and were mutated to their HPS counterparts, serine and isoleucine, respectively. This did not result in the production of detectable prenaspirodiene. However, a regiochemical preference for terminal proton elimination at C6 rather than C8 appears to have been directed via the mutations, and a novel sesquiterpene, 4-epi-eremophilene, is produced as the dominant product (70% at pH 7.5).

These mutations probably could have been arrived at by direct inspection using crystal structure modeling software. However, such interactions quickly become intricate to the degree that direct inspection is far from straightforward. The Van der Waals contact map has been demonstrated here to deconvolute these interactions and direct attention to residue interactions that significantly affect active site chemistry

from a distance. The double mutant TEAS-T402S/V516I exhibits catalytic efficiency well within the range of other characterized terpene synthases (usually measured in $\text{nM}^{-1} \text{s}^{-1}$). Because of its relative robustness and specificity, the double mutant enzyme has been named 4-epi-eremophilene synthase (EES). No counterpart for this enzyme has been reported, nor has this product been identified from natural sources. The hypothesis that the S402/ I516 pair is a conserved structural feature of eremophilane/vetispriane synthases which generate 6,7 double bonds, formed the basis for efforts to clone a new sesquiterpene synthase presented in the chapter 5.

The following model is proposed to explain the change in regioselectivity of the final proton elimination in EES. First, T402 and V516 flank the residue C440. The effect of the EES mutations and the results of C440 mutagenesis suggests that T402 and V516 help define the interaction between the eremophilyl carbocationic intermediate and C440. One hypothesis was that positions 402 and 516 define the rotamer, or freedom of rotation, of the C440 R group. Dr. O'Maille's modeling results do not bear this out, subsequent to energy minimization no alternative to the crystallographically determined rotamer is observed. This does not rule out a dynamic effect. The multifunctional single mutants suggest that when an extra methyl group is introduced (V516I) and when a methyl group is lost (T402S) the active site is less selective for one eremophilyl conformer over the other. However, in the balanced double mutant (EES, T402S/V516) where the location of a methyl group is simply shifted, the available conformers are reduced and this may serve as a generalized argument for selectivity of the final proton abstraction.

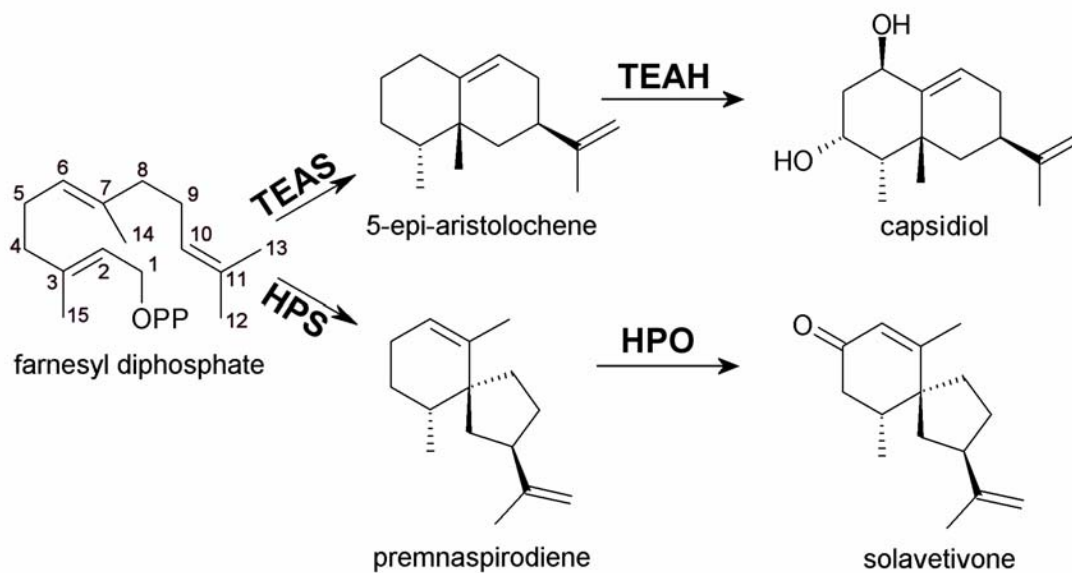
The stereochemical requirements for formation of observed sesquiterpene products must be met through conformational control at the active site. In other words, only certain conformations of carbocationic intermediates will allow for transformations evident in the products. The contact map suggests that T402 and V516 interact with C440 and that C440 may interact with the β -isoprenyl methyl group (C14 of FPP). For methyl migration to occur, the C7 bond to the methyl group (C14) must be in alignment with the empty p orbital on the *si* face of the sp^2 hybridized C3 carbocation. For methylene migration to form premnaspirodiene, the bond between C7 and C8 instead must align with the p orbital on the opposing face (*re*) of C3. How one

conformation is bound and selected thus becomes determinant for product specificity. Examining the contact map, the FHP atoms with the most contact points are the methyl groups (Figure 3.1). C5 is the only non-methyl carbon that interacts directly with more than one other atom. C14 has three contacts, C12 has four, and C13 has two. C15 only has one plotted contact, but actually interacts with two carbonyls (from T401 and T403) which is not shown in this simplified contact map (these are the only non-R group contacts in the active site). I contend, therefore, that the cyclase exerts conformational control by using three-point contacts, in general, to define the positions of methyl groups. Because each methyl is initially a member of a rigid, planar isoprene unit, three-point coordination of methyl substituents could effectively define the conformation of the entire substrate. This is likely to occur in a dynamic fashion as the reaction progresses and possibly assisted by cation-pi interactions.

A second manner of control over product specificity involves a putative catalytic role of C440. The mutations presented here and pH dependence data from the Noel group suggest that C440 plays an active role in acid-base chemistry at the active site. The apparent rescue of 5-epi-aristolchene specificity in C440 and Y520 mutants under acidic conditions suggest that the true donor may be water which is activated by C440 to form hydronium ion. From the results presented here, one interesting piece of genetic data should be introduced. All of the germacrene synthases reported to date have conserved the Y520 residue, but contain an alanine, serine, or glycine substitution at position 440 (Table 3.1). There are other differences in the respective active site residues but none of them are residues with ionizable groups. An additional effect of the EES mutations may have been to reposition a proton abstractor so as to assist in the final elimination. However, a preliminary analysis of a mutant, EES-C440S indicated a product profile containing approximately 50% germacrene A, 20% 4-epi-eremophilene and 30% 5-epi-aristolchene. A better understanding of acid-base chemistry in the active site may clarify these results.

In terms of ecological speculation, mutations resulting in the evolution of EES could be selected for if the resulting sesquiterpene hydrocarbon were functionalized and possessed enhanced anti-microbial activity. If this metabolite, or 4-epi-eremophilene for that matter, gave a selective advantage to a plant against pathogen

attack, a new phytoalexin biosynthetic pathway could conceivably evolve. Questions that follow from this logic include whether further mutation of EES could result in stronger product selectivity. Could the efficiency of the reaction be improved, or is the rate of the reaction limited by the conformational strain required for one stereochemical course (in 5-epi-aristolochene synthesis) over another (in 4-epi-eremophilene synthesis)? One way of addressing these issues is to follow nature's model and determine mutations that convert EES fully to a premnaspirodiene synthase.



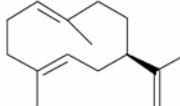
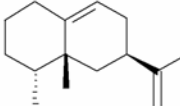
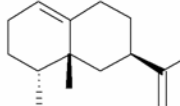
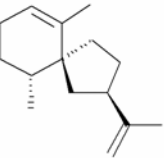
Scheme 3.1 Variation in the biosynthesis of solanaceous phytoalexins from Farnesyl Diphosphate (FPP).

Table 3.1 Alignment of residues in and near the active site of TEAS with other sesquiterpene synthases.

Highlighting indicates residues which are different from those found in TEAS, orange indicates a hydrophobic residue, blue a basic residue, red an acidic residue and purple a polar residue.

synthase product	FIRST TIER								SECOND TIER																				
	264	273	403	404	440	444	JK Loop		20	266	270	298	302	372	376	401	402	407	436	441	445	448	512	515	516	519	529		
5-epi-aristolochene	R	W	T	Y	C	D	Y	D	Y	T	F	R	C	S	D	V	Y	T	T	L	S	R	D	T	L	I	V	T	H
Premnaspirodiene	R	W	T	Y	C	D	Y	D	Y	T	F	R	C	S	D	I	Y	T	S	L	N	R	D	T	L	I	I	T	H
4-epi-eremophilene	R	W	T	Y	C	D	Y	D	Y	T	F	R	C	S	D	V	Y	T	S	L	S	R	D	T	L	I	I	T	H
Valencene	R	W	A	Y	C	D	Y	D	Y	T	F	R	L	S	D	V	Y	S	C	V	A	R	D	G	L	A	I	T	H
Gemacrene A	R	W	A	Y	S	D	Y	D	F	T	F	R	I	V	D	A	Y	T	S	I	S	R	D	T	L	M	I	V	F
Gemacrene B	R	W	G	Y	A	N	Y	D	Y	T	F	R	C	S	D	V	Y	S	G	I	S	R	D	G	L	A	A	L	N
Gemacrene C	R	W	G	Y	A	N	Y	D	Y	S	F	R	C	S	D	V	Y	S	A	I	S	R	D	G	L	V	A	L	T
Gemacrene D	R	W	G	Y	G	D	Y	D	Y	T	F	R	C	S	D	L	Y	T	V	G	S	R	D	G	F	V	I	L	N
delta-cadinene	R	W	G	Y	C	D	Y	D	Y	T	F	R	G	S	D	L	Y	S	I	G	S	R	D	E	L	V	M	L	H
amorpha-4,11-diene	R	W	G	A	G	N	Y	D	F	T	F	R	C	T	D	V	Y	T	G	L	S	R	D	T	L	F	L	Q	R
epi-cedrol	R	W	G	Y	C	D	Y	D	F	T	F	R	C	T	D	V	Y	S	I	A	C	R	D	S	F	S	V	L	N
beta-caryophyllene	R	W	G	Y	A	D	Y	D	F	T	F	R	C	T	D	I	Y	S	S	L	S	R	D	S	L	V	M	L	N
beta-farnesene	R	W	C	I	G	N	Y	D	A	A	H	R	A	G	D	A	F	T	S	M	T	R	D	S	Y	I	C	S	Y
limonene	R	W	S	G	L	D	Y	D	H	G	? R	C	T	D	A	Y	S	I	M	S	R	D	T	L	M	A	M	T	

Table 3.2 Relative product distributions in TEAS and TEAS mutants T402S and V516I.

% of the reaction products formed				
				
	germacrene	epi-aristolochene	epi-eremophilene	premnaspirodiene
EAS	4	96	---	---
EAS -T402S	---	69	28	---
EAS -V516I	16	50	33	---
EAS -T402S/V516I	2	28	70	---

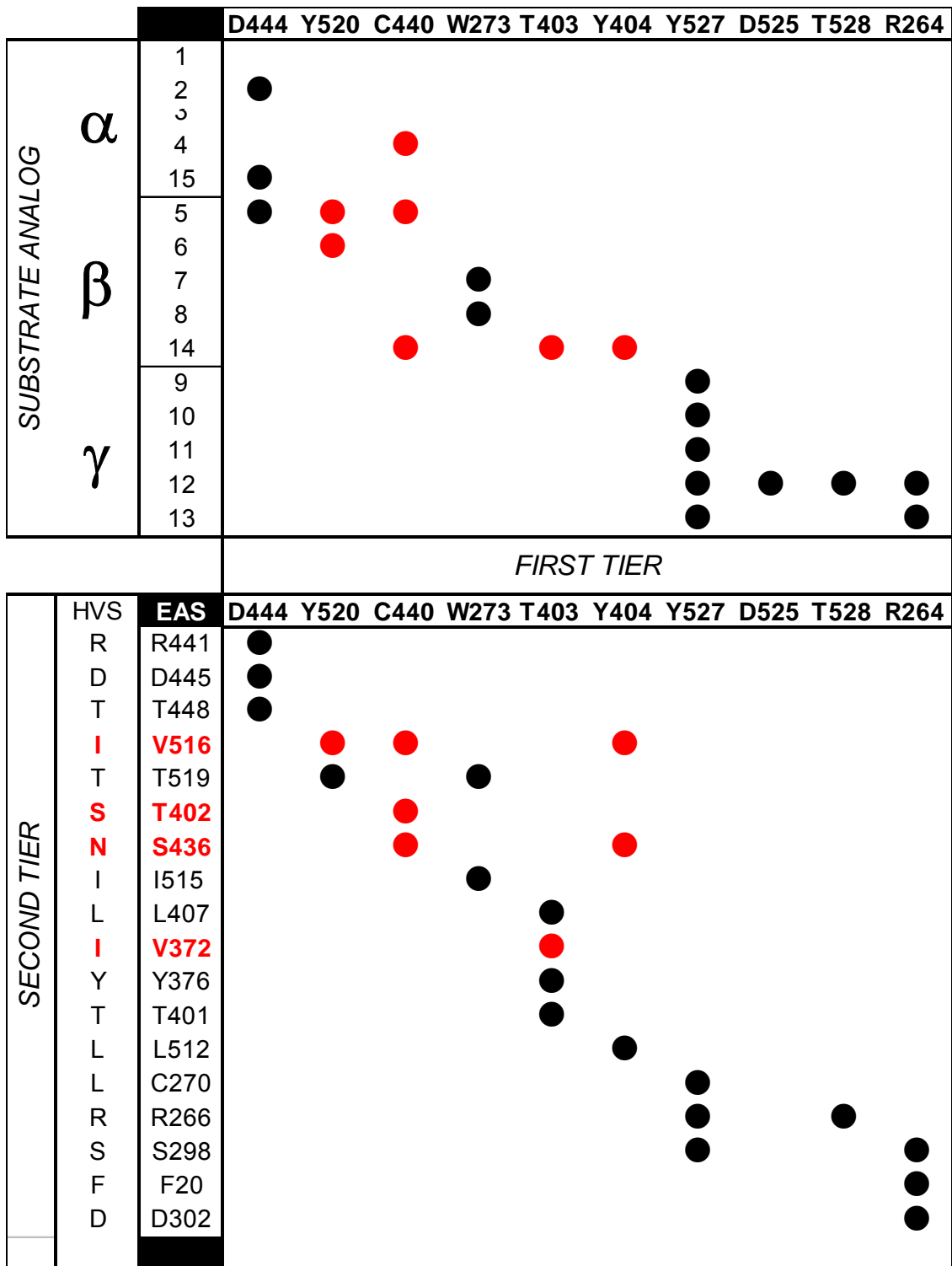


Figure 3.1 A Van der Waals contact map for TEAS.

Each carbon of the proximal (a), medial (b), and distal (c) isoprene units of the substrate analog farnesyhydroxyphosphonate (FHP) were inspected for Van der Waals contacts (represented by dots) with amino acids in the 5EAT pdb model, generating the first tier of active site residues (upper panel). Each atom of the first tier residue R groups was then inspected for contacts with second tier residues, residues surrounding the active site residues and noted in the lower panel. Residues which differ between TEAS and HPS are colored red and their potential interactions with particular atoms of substrate analog traced by the red dots.

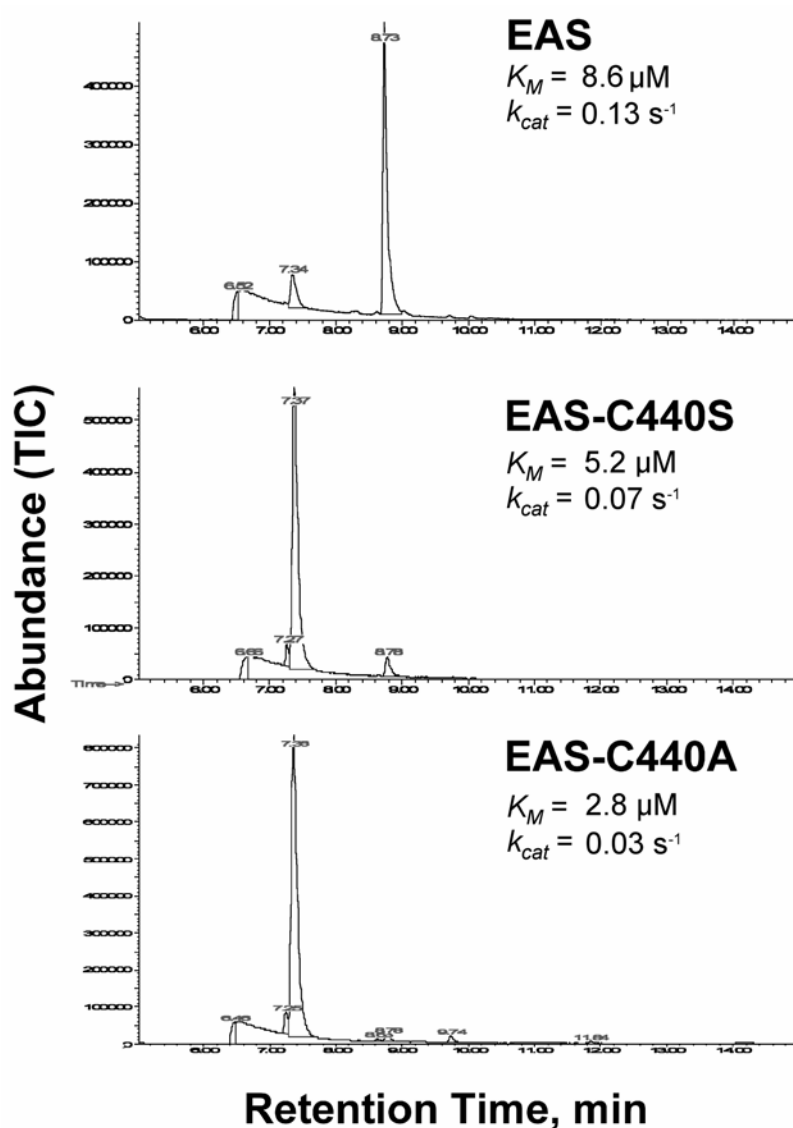


Figure 3.2 Reaction product analysis of TEAS and the respective C440 mutants by GC.

Crude lysates of bacteria expressing TEAS and cysteine mutant enzymes were incubated with FPP, extracted with pentane, the extract concentrated and subjected to GC-MS analysis. The MS for the major peak (8.73) in the wildtype TEAS chromatogram was identical to 5-epi-aristolochene. The MS for the major peak (7.35-7.37) in the TEAS-C440A and TEAS-C440S extracts matched β -elemene, a thermal rearrangement of the germacrene A reaction product. Kinetic constants were derived from fits of the Michaelis-Menten equation as shown in Figure 3.3.

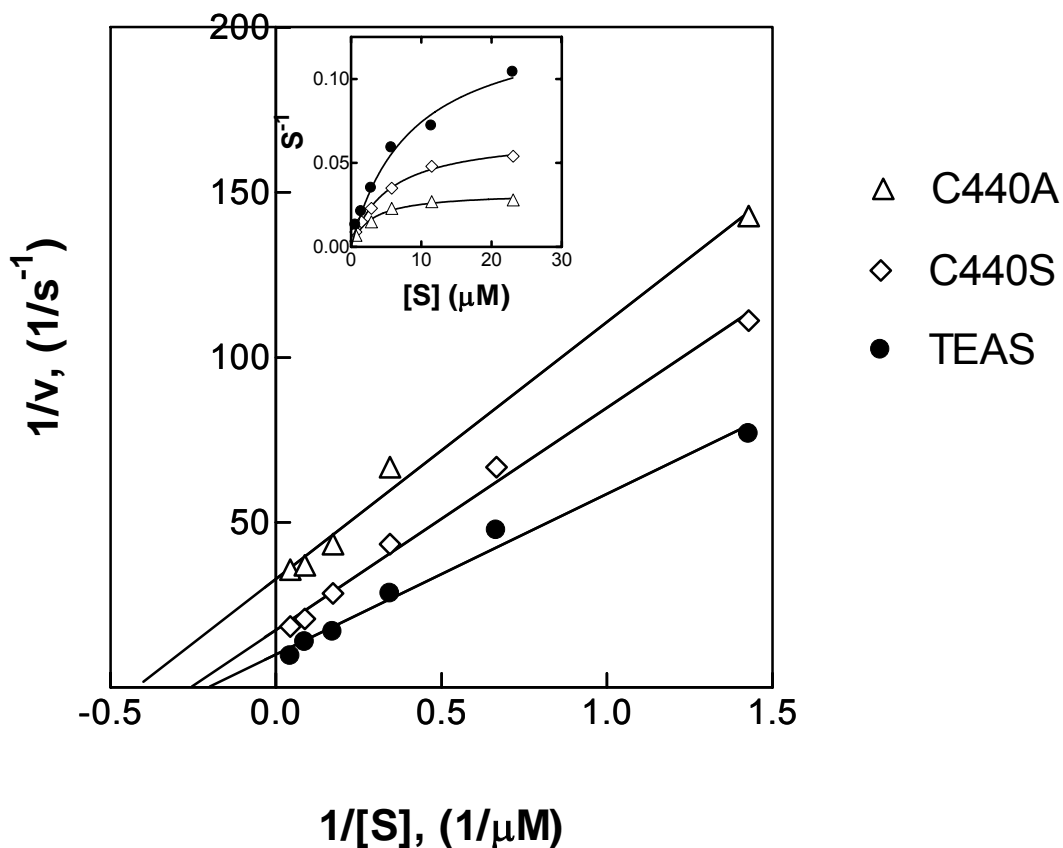


Figure 3.3 Initial kinetic comparison between TEAS and the C440 mutants.

The main graph is a Lineweaver-Burke plot where the slope of the line is the inverse of the efficiency of the wild type and mutant enzymes (K_m / k_{cat}). The inset is the plot of the single rate determinations fit to the Michaelis-Menten equation from which constants in figure 3.2 were derived. The standard errors derived from the fit to the Michaelis-Menten equation were maximally 18% for the K_m determination and 8% for the k_{cat} determination.

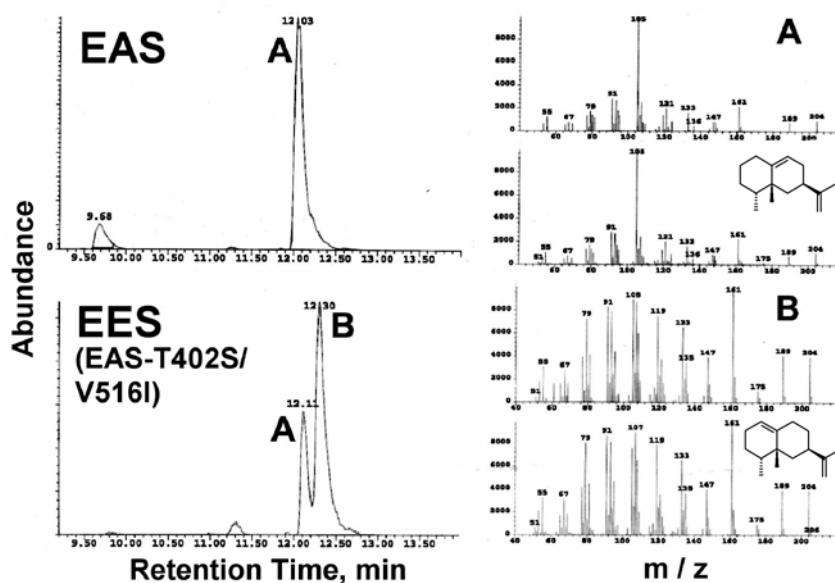
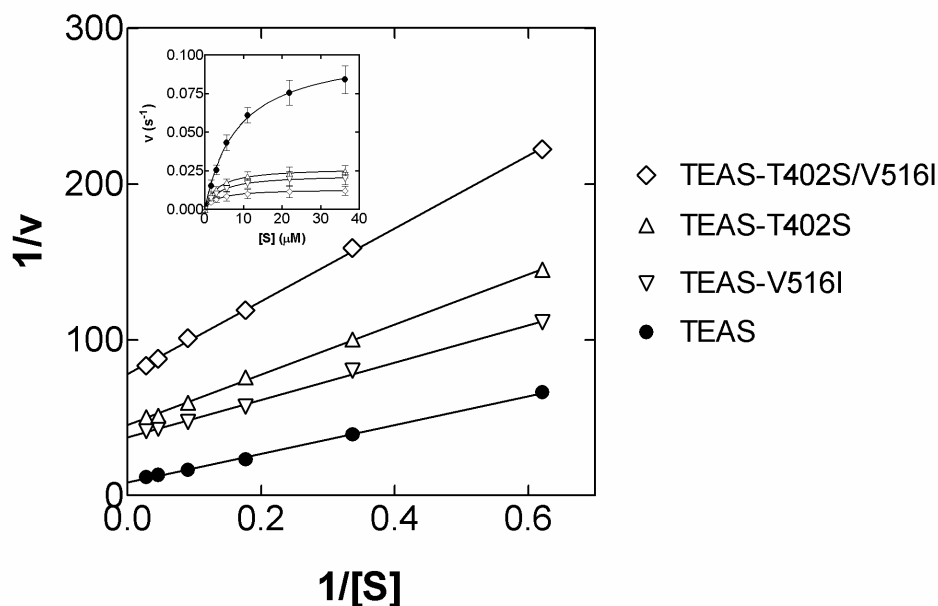


Figure 3.4 GC-MS identification of the TEAS-T402S/V516I reaction products.

Purified TEAS and TEAS-T402S/V516 were each incubated with FPP, the reactions extracted with pentane and aliquots separated by GC. Panels to the left are the resultant GC traces, whereas the MS for peaks labeled in these chromatograms are given to the right. MS standards for 5-epi-aristolochene (panel below A) and 4-epi-eremophilene (panel below B) were used to verify reaction product identities.



	K_m (μM)	k_{cat} (s^{-1})	k_{cat} / K_m
TEAS	8.5 ± 0.52	0.105 ± 0.0024	0.012
TEAS-T402S	3.7 ± 0.19	0.022 ± 0.0003	0.006
TEAS-V516I	3.1 ± 0.15	0.027 ± 0.0003	0.008
TEAS-T402S/V516I	3.1 ± 0.10	0.013 ± 0.0001	0.004

Figure 3.5 Kinetic comparison of TEAS to the TEAS mutants T402S, V516I and T402S/V516I.

The main graph is a Lineweaver-Burke plot of average values where the slope of the line is the inverse of the efficiency of the wild type and mutant enzymes (K_m / k_{cat}). The inset graph is a plot of triplicate measurements, averaged and fit to the Michaelis-Menten equation from which constants given in the lower panel were derived. Errors given for kinetic constants at in the bottom panel are the standard errors derived from the fit to the Michaelis-Menten equation.

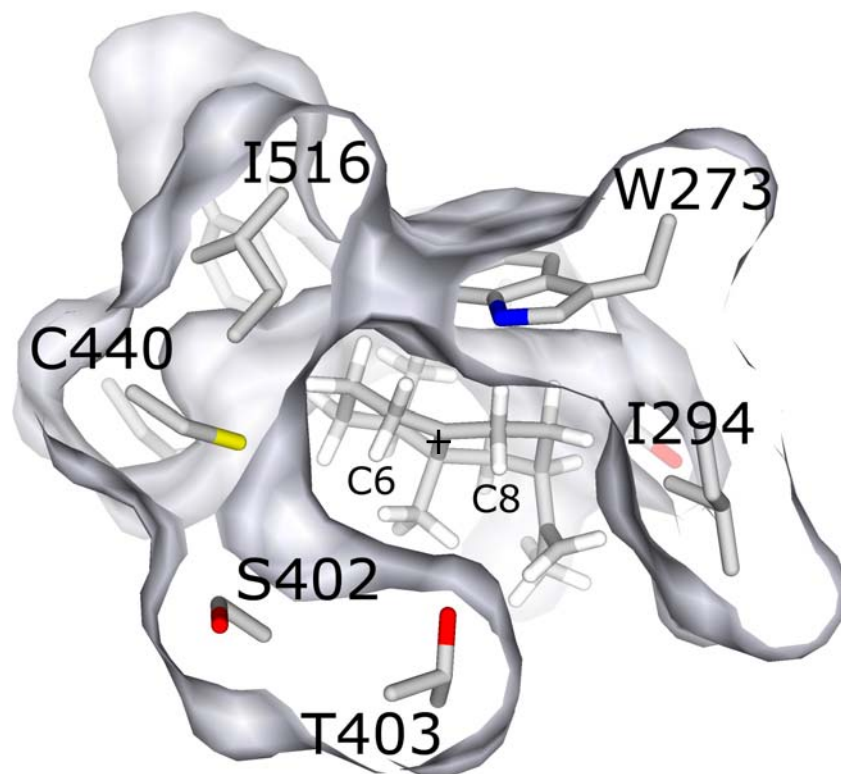


Figure 3.6 Docking of the eremophilyl carbocation in a modeled EES (TEAS-T402S/V516I) active site.

(Modeling, Docking, and Image by Paul O'Maille, Noel Lab, Salk Institute, La Jolla, CA, text and preliminary modeling by BT Greenhagen)

This depiction represents alterations of the 5EAT pdb structure to accommodate the T402S/V515I mutations, then docked with an energy minimized 4-epi-eremophilene carbocation, a putative reaction intermediate. Proton elimination at C8 would form 5-epi-aristolochene, while deprotonation from C6 would result in 4-epi-eremophilene. The proton eliminated from C6 or C8 is on the underside of the molecule (β face of the eremophilyl cation).

CHAPTER 4 Conversion of 5-epi-aristolochene into a premnaspirodiene synthase

Introduction

Most of the sesquiterpenes found in nature are derived from enzymes similar in structure and function to TEAS⁹⁵. Thus, some variation on the TEAS amino acid sequence should provide for the synthesis of each one of the ca. 300 known basic sesquiterpene skeletons. A major effort has been to focus in on sequence elements which have a direct bearing on redirecting reaction pathways from one synthase to the next. The number of permutations of a 550 amino acid protein such as 5-epi-aristolochene is 3.7×10^{715} (20^{550}). Importantly, chimeras of EAS and HPS seem to indicate that at most only about 189 amino acids may be important in driving specificity¹¹⁵, thus reducing the search to 7.9×10^{245} variants. There have not been 10^{254} attoseconds in the history of the universe. However, the structure for 5-epi-aristolochene is known, and only ten residues appear to line the active site, perhaps this is the only sequence space that needs to be considered. Yet, some synthases catalyzing significantly different reactions, such as TEAS and HPS are identical in their apparent active site residues. The intention of the work in this chapter was to determine what amino acid residues are important and to understand how they influence active site chemistry. Natural sources of these enzymes represent an evolutionary distillation of the myriad of sequence and spatial diversity; thus, genetic differences in enzymes like TEAS and HPS should guide us in identifying regions, domains, or individual residues important for product specification. Rational strategies were therefore employed to fully transmute TEAS into a HPS-like synthase (a premnaspirodiene synthase) in an extension of the approach described in chapter 3.

The use of a Van der Waals contact map as described in chapter 3 was fruitful but insufficient to fully reveal the specific sequence differences which define the different product specificities of HPS versus TEAS. When a “third tier” of residues is added to the contact map, instead of becoming extensively complicated, it actually becomes much less informative as surface residues are encountered and influences of third tier residues were more tenuous. In order to canvas a limited volume of sequence

space within which the contact map may have missed important residues (contacts with the peptide backbone were omitted for simplicity), we next identified residues based on spatial proximity to the active site and with reference to results from studies of TEAS:HPS chimeras (Figure 4.1). In hindsight, this approach needed only to employ a hierarchical list of variant residue proximities, but the comparison to the results with chimeric enzymes was informative.

Figure 4.1 presents only those residues which differ between TEAS and HPS and has organized those differences according to which domain of the synthases they are associated. Below this chart is a cartoon depiction of the TEAS enzyme and various chimeric enzymes constructed between TEAS and HPS, along with an indication (in percentage) of how much premnaspirodiene product was produced by each¹¹⁵. The HPS region flanked by HincII- and ClaI sites appeared to contribute to premnaspirodiene, which was enhanced two-fold upon inclusion of the XbaI-HincII segment. Differences in residues from within the HincII-ClaI and XbaI-HincII regions were thus targeted for further analysis and potential mutagenesis. Residues for mutagenesis were then prioritized on the basis of their distance from the active site pocket, followed by a manual inspection of their positions on a 3-D model²³⁵. Any dramatic substitutions were also likely to influence enzyme stability, and therefore necessitated an examination for other compensatory changes. The overall strategy was instructive because it was in part hypothesis driven and in part tinkering, both of which contributed to building a more mechanistic model for how terpene synthases function.

Materials and Methods

The following are essentially the same as in chapter 3 except that additional primers were used to produce further mutations to TEAS.

Preparation of Enzymes

Mutations were made with a pET-28b vector (Novagen) construct harboring the coding sequence for 5-epi-aristolochene synthase¹⁶⁰ using the standard Quikchange mutagenesis method (Stratagene). Mutagenic primers were (mutagenic bases in bold):

S436N: CCA AAA ATT CTT GAA GCT AAT GTA ATT ATA TGT CGA GTT ATC

V372I: GCA ATA GAA AGA ATG AAA GAA ATA GTA AGA AAT TAT AAT
GTC GAG TCA ACA TGG

S295A: CGC GTC ATG CTC GTT AAG ACC ATA GCA ATG ATT TCG ATT GTC
GAT GAC ACC

S436N/I436T/I439L: CCA AAA ATT CTT GAA GCT AAT GTA ACT CTA TGT
CGA GTT ATC GAT GAC ACA GC

T402S/Y406L: CTA GCA ACT AGC ACA TAT TAC TTG CTC GAG ACA ACA
TCG TAT TTG GGC ATG

V291A: GCT CTC TCA AGC TCG CGT CAT GCT CGC TAA GAC CAT ATC AAT
GAT TTC GAT TG

A275T: CGA GTA GTT GAA TGC TAC TTT TGG ACA TTA GGA GTT TAT TTT
GAG CCT CAA TAC

V291A/S295A: GCT CTC TCA AGC TCG CGT CAT GCT CGC TAA GAC CAT
AGC AAT GAT TTC GAT TG

All mutations were verified by automated nucleotide sequencing. Plasmid DNA constructs were transformed into BL21 (DE3) cells, cultured, and protein was expressed as described previously¹⁷³. The construct provided N-terminal hexahistidyl tags which afforded >90% pure protein upon Ni⁺ affinity chromatography in all cases¹⁷³. Protein was quantitated using the Bradford method and IgG as protein standards.

Product Analysis

Preparative reactions were basic cyclase assays scaled to 2.5 mL and employing 2 μM enzyme and 80 μM unlabeled FPP. The reactions were incubated for 1 hr and extracted twice with 2 mL of pentane. Pooled extracts were dried to 50 μL under a stream of nitrogen and analyzed by GC-MS as previously described¹⁷⁴ (See Chapter 6).

Results

The results reported here represent an extension of those in chapter three. Mutations were made sequentially, with each being examined for its premnaspirodiene production specificity. Those mutant cDNAs coding for enhanced premnaspirodiene synthase activity were used for the next round of mutagenesis. Thus, the EES enzyme (TEAS-T402S/V516I) was altered at two sites implicated by the Van der Waals contact map to impinge on the active site V372I and S436N. Introduction of V372I to EES (TEAS-T402S/V516I) resulted in 10% abundance of premnaspirodiene, and addition of S436N to this construct gave 18% premnaspirodiene (Table 4.1). However, enzymes with S436N mutation expressed in bacteria poorly and had relatively low activity. Since S436 is 11.7 angstroms from C7 of FHP, other residues in the vicinity that might compensate for the bulk introduced by the S436N mutation were considered. Due to their proximity, I438T and I439L and were introduced into the TEAS-T402S/V516I/V372I/S436N mutant. This restored overall activity to approximately wild type levels as judged from the relative abundance of GC signals in the pentane extract of reactions. Most importantly, this mutant (M6) improved the yield of premnaspirodiene giving a nearly equal distribution of 5-epi-aristolochene (23%), 4-epi-eremophilene (24%) and premnaspirodiene (27%).

The M6 mutant, however, did not match the product abundance previously found for the TEAS chimera with the XbaI-Stop segment of HPS (77%). Two more residues residing in the XbaI-Stop segment, which are within 11 angstroms of the active site were introduced to determine if any further improvement could be derived from this sequence segment. Activity was barely detectable after the addition of an I443V mutation (10.36 angstroms distant) and was not pursued further. However, introduction of Y406L shifts premnaspirodiene to the dominant product (43%) with good activity. The M7 mutant (TEAS- T402S / V516I / V372 I / S436N / I438T / I436L / Y406L) was mutated to A408T, the last residue within 12 angstroms in of the HincII-Clal segment but this mutation had no effect on product specificity.

The next closest residue change is S295A that resides in the yet unexplored Ndel-XbaI segment, deemed important (about 33% premnaspirodiene contribution) for product specificity from the chimera studies. However, although the mutation is

somewhat subtle, all activity was lost. Mutations were made to M7 that incorporated the next two closest residues in this section, A275T and V291A in a combinatorial fashion with the S295A mutant. The addition S295A nearly eliminated enzymatic activity in all combinations. However, the addition of both A275T and V291A converted M7 into an enzyme which catalyzed the production of premnaspirodiene as the only major product (70% of total). Judging from the ion abundance in extracts from M9, the enzyme does not seem to exhibit significant loss of activity relative to wild type.

Discussion

A prevailing notion in the field of structure-function relationships is that association between an enzymatic residue or motif can be directly associated with a function. Classic enzymology of proteases, for instance, was able to assign very specific roles to specific residues within the enzyme, for instance three residues of the catalytic triad in chymotrypsin fit well with mechanistic functions involved in breaking peptide bonds. For the first step in Class I terpene synthase catalysis, ionization, such direct structure-function associations can be made. Kinetic and structural evidence strongly supports the role of the DDxxD in chelating divalent metal ions and assisting in ionization. Likewise, the role of arginine residues, such as R264, appears relatively straightforward; upon binding it translates into the active site to assist in stabilizing the negative charge developing on diphosphate from the initial ionization of the substrate. However, subsequent to ionization, direct interactions which dictate the transformations of allylic carbocations are far from clear. A compelling hypothesis is that cation- π interactions between carbocationic intermediates and aromatic residues (phe, tyr, trp) provide for quadrupole stabilization and guide the reaction pathway. However, this is a difficult concept to test directly and many sesquiterpene synthases have exactly the same set of aromatic residues in the active site (W273, Y520, and Y/F527 using TEAS numbering). The latter observation emphasizes that the identity of these residues are not predominant determinants of product specificity. Hence, our goal was to identify a limited set of residues sufficient to convert TEAS to an HPS-like, premnaspirodiene

synthase then to use that information to derive a mechanistic model for structure-function relationships in terpene synthases.

Nine mutations were sufficient to transmutate TEAS into a premnaspirodiene synthase. These mutations occur in a disk of space approximately 7.5 Å deep and 13.5 Å in radius that is perpendicular to the axis of the alpha barrel structure and just behind the active site defined by the alpha-barrel (Figure 4.2 and 4.3). The approximate volume of the TEAS alpha barrel domain is about 54,000 Å³, yet the space in which the M9 mutants reside is only about 4,000 Å³. Because most sesquiterpene cyclase/isomerase type enzymes have active sites that are nearly identical, it is possible that product diversity arising from these sesquiterpene synthases is entirely defined within this space. This observation could lend itself to computational strategies for reengineering terpene cyclases^{191,197,236}.

The M9 mutant, and those leading up to it, demonstrate that the determinants of product specificity are at least as subtle as the difference between TEAS and HPS, do not require exchange of loop residues, or changes to the salt bridges which secure the ends of the alpha-helices together at each. The nature of the substituted residues is also interesting, polar amino acids are introduced in two cases (A274S, I438T), whereas a relatively large change in size introduced in another (S436N). For the most part, changes represent subtle gains or losses of a methyl group (V516I, T402S, V291A, V372I). An important caveat is that while this combination of residues is sufficient to cause the transmutation, further work will be required to determine if each substitution is necessary, for instance by reverting each residue in the M9 set of substitutions back to its original identity. Another interesting question is whether more than one combination of residue substitutions is capable of converting TEAS into an HPS-like cyclase.

The residue substitutions in the TEAS-M9 mutants suggest a model for how active site stereochemistry is controlled through interactions distant from the active site. Any transformation along the reaction pathway, whether it is a hydride shift, a methyl migration, or an alkyl migration, will be limited by the orbital alignment of the relevant bonding centers (Figure 4.4). Thus, active site geometry provides physical boundaries to possible catalytic outcomes. The idea of the active site acting as a rigid template

alone is not sufficient to account for how multiple conformations are imposed to drive one set of transformations rather than another. Because the apparent active sites of TEAS and HPS are identical and the crystal structures of plant terpene synthases are nearly identical around the active site^{101,129}, we posit that the active site is a dynamic set of templates. The nature of the TEAS-M9 mutations suggests a way this may occur. Active site residues may be identical if their positions relative to one another are variable. Interactions outside the active site may allow or disallow helix-helix transitions thus imposing barriers to available intermediate conformations at the active site as shown in figure 4.5. The additive effect of the mutations (figure 4.6) and the locations of each TEAS-M9 mutation at similar positions along the axis of the alpha-barrel (figure 4.2) are in agreement with this model. In this way, by manipulating the farnesyl tail through three point contact of methyl groups (as discussed in chapter 3) various conformations could be controlled via the available translations between the alpha-helices surrounding the active site. The transition from 5-epi-aristolochene specificity to 4-epi-eremophilene specificity, to premnaspirodiene specificity (figure 4.6) can be explained by the proposition that a new intermediate conformer is allowed by EES (TEAS-T402S/V516I) (figure 4.4). This model also explains the results from previous experiments with chimeras; each of the sequence segments exchanged was within a section of this “redefining ring” of mutations. Partial redefinitions allowed a wider range of allowed conformations and thus, manifest bifunctionality. The same phenomenon is observed in the point mutants, which correlate with these sequence segments. For example, M6 (Table 4.1) produces products with three mechanistic variations in nearly equal abundance.

Table 4.1 Reaction profiles for TEAS, TEAS-M9, and intermediate mutant synthase enzymes. GA: germacrene A; EA: 5-epi-aristolochene; EE: 4-epi-eremophilene; PSD: premnaspirodiene.

aka	Cyclase	%			
		GA	EA	EE	PSD
wt	TEAS	4	98	ND	ND
	TEAS-T402S	ND	69	28	ND
	TEAS-V516I	16	50	33	ND
EES	TEAS-T402S/V516I	2	28	70	ND
M3	TEAS-T402S/V516I/V372I	10	21	48	10
M4	TEAS-T402S/V516I/V372I/S436N	16	16	33	18
M6	TEAS-T402S/V516I/V372I/S436N/I436T/I439L	16	23	24	27
M7	TEAS-T402S/V516I/V372I/S436N/I438T/I439L/Y406L	16	26	19	43
M9	TEAS-T402S/V516I/V372I/S436N/I438T/I439L/Y406L/A274T/V291A	14	3	8	71

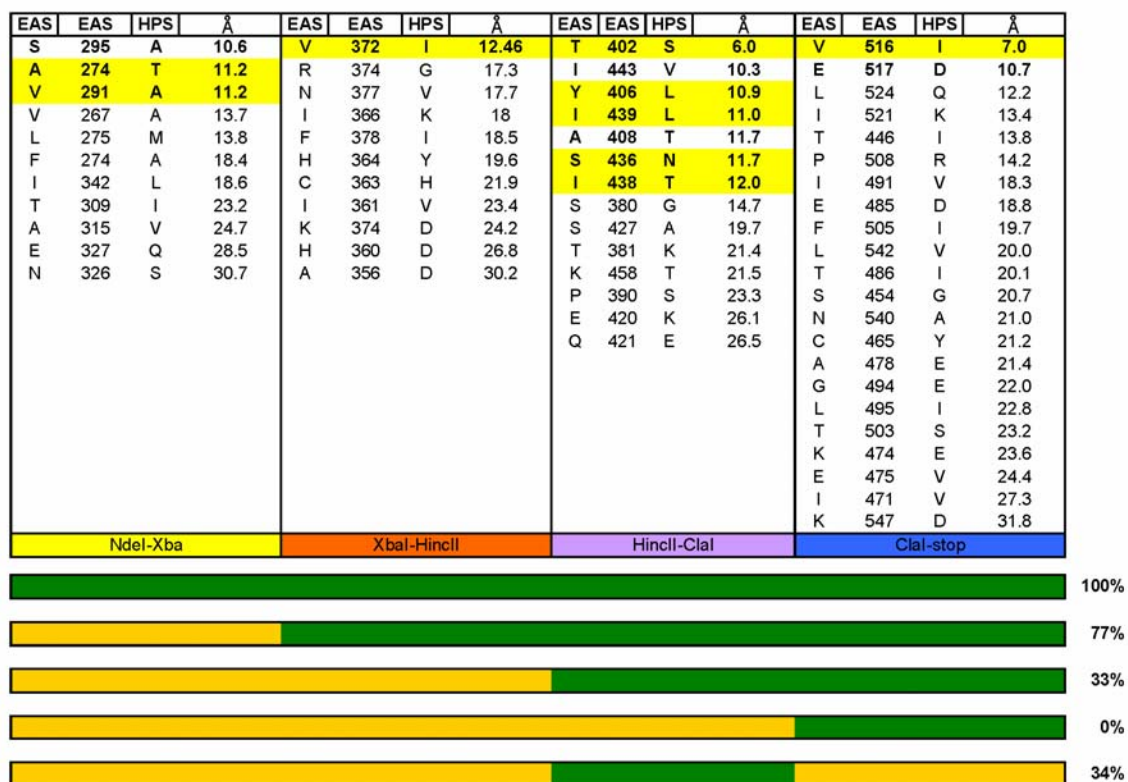


Figure 4.1 Structural analysis of chimeric sesquiterpene synthases between TEAS and HPS.

A diagrammatic representation of the four carboxy-terminal segments of synthase coding sequences that when exchanged in chimeras produced altered reaction products (lower diagram). Orange bars represent TEAS sequence, while green represent HPS specific sequence, and the % of apparent prenaspirodiene reaction product is given¹¹⁵. Residues which differ between TEAS and HPS in each of the respective segments is noted above in the table. Columns represent (left to right): TEAS amino acid identity, TEAS amino acid position, corresponding amino acid in HPS, distance from the approximate center of the active site in angstroms. Residue substitutions of TEAS which improved reaction product specificity for prenaspirodiene are highlighted in yellow.

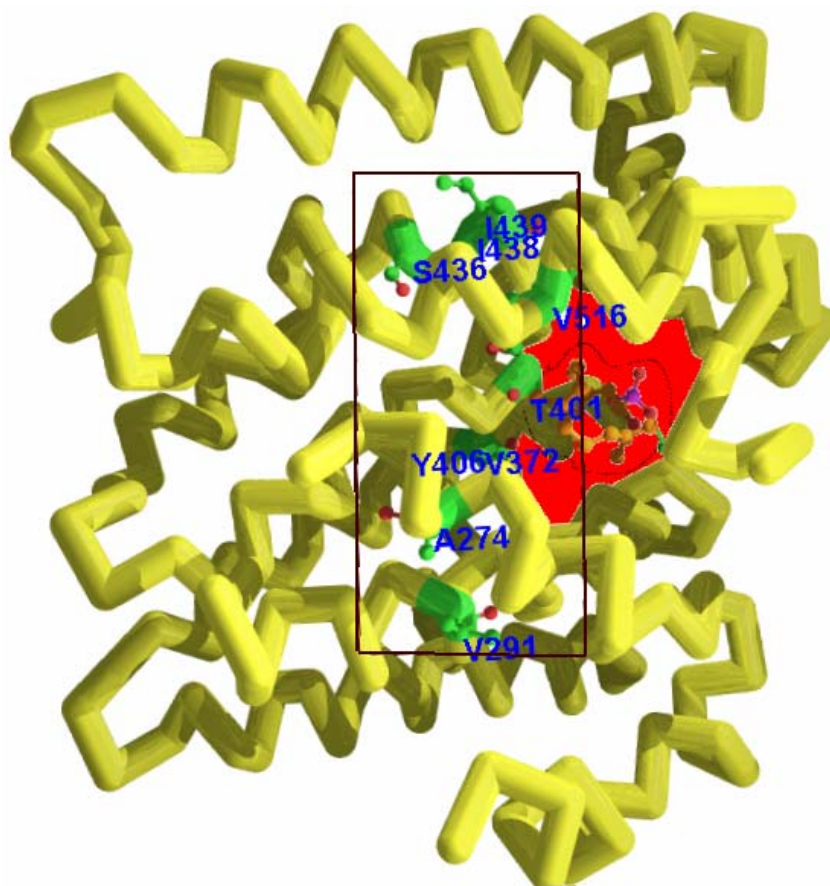


Figure 4.2 A cross-section of the TEAS crystal structure highlighting the location of mutations converting TEAS into a premnaspirodiene synthase (TEAS-M9).

In this rendition of the TEAS structure, the axis of the active site, alpha-barrel domain is approximately parallel to the page. The barrel is sealed to the left and opens to the interior active site to the right (red highlight). The TEAS model has been cut transversely along the alpha-barrel axis to reveal mutations in TEAS-M9 (highlighted in green). The box drawn over this region is about 4.5 Å wide and 27 Å tall.

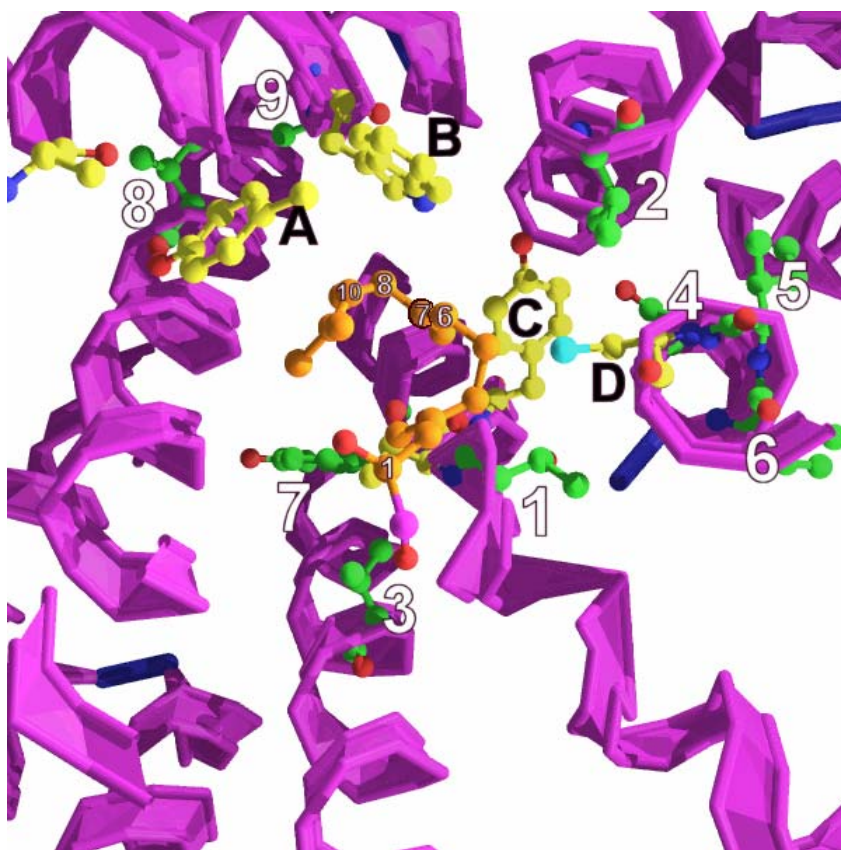


Figure 4.3 Residues in the TEAS structure that were mutated in TEAS-M9.

This view depicts the TEAS active site alpha-barrels perpendicular to the page with the active site opening towards the reader. Active site residues conserved in TEAS and HPS are highlighted in yellow and labeled alphabetically: A. Y527 B. W273 C. Y404 D. C440. TEAS residues which were mutated to make TEAS-M9 are colored green and numbered according to the sequence in which they were mutated: 1. T402S 2. V516I 3. V372I 4. S436N 5. I438T 6. I439L 7. Y406L 9 V291A. The hydroxy-phosphonate FPP analog resolved in the initial TEAS structure is shown in orange.

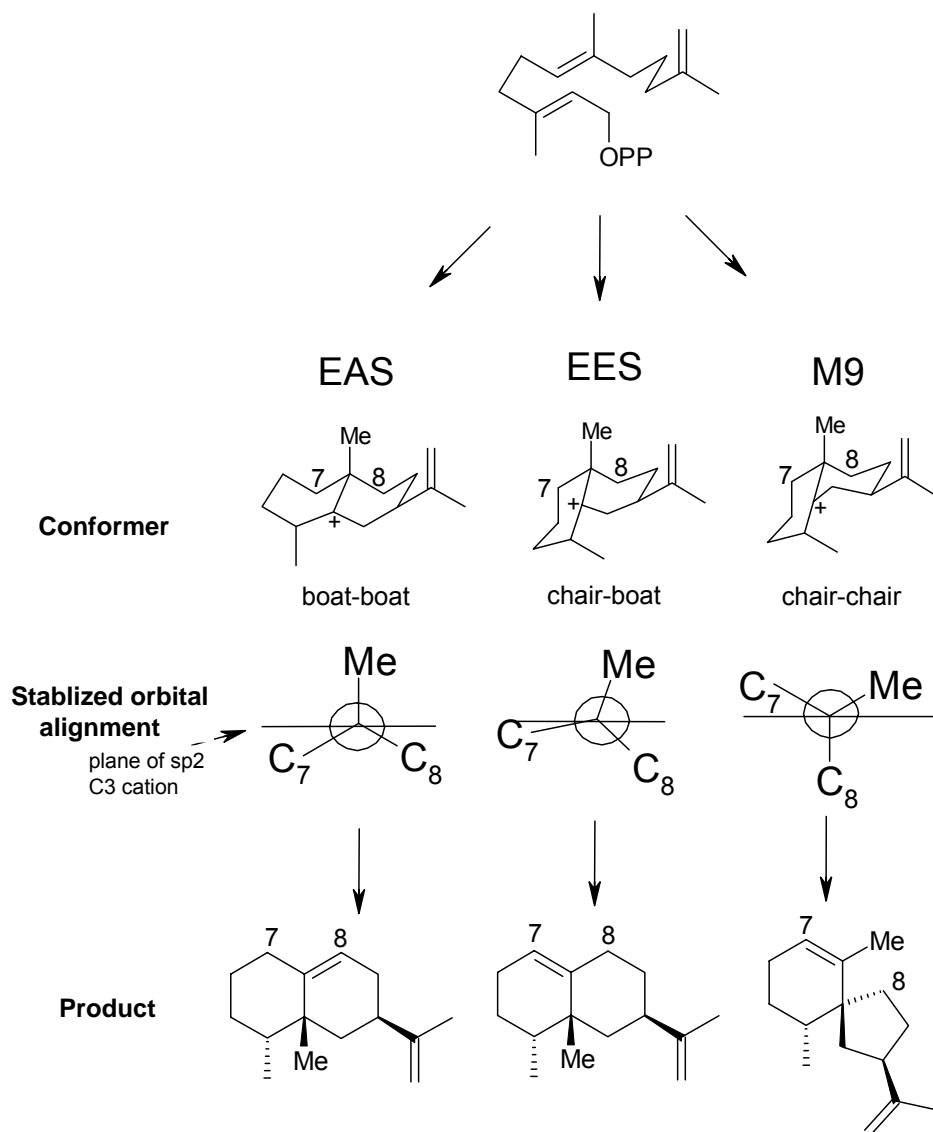


Figure 4.4 Proposed conformational control of eremophyl carbocationic intermediates specified by wildtype and mutant TEAS.

Trans, trans farnesyl diphosphate is the common substrate that must be folded into a particular conformer in order to account for the biosynthesis of the indicated reaction products (EA, EE and PSD). The conformers depicted approximate orbital alignments given in Newman projections. Those groups whose bonds are perpendicular to the plane of the sp² hybridized carbocation at C3 are properly positioned to subsequent migration. Relative deviations from stable perpendicularity of the methyl in the chair-boat configuration for EES may contribute to lower turnover rates in that enzyme.

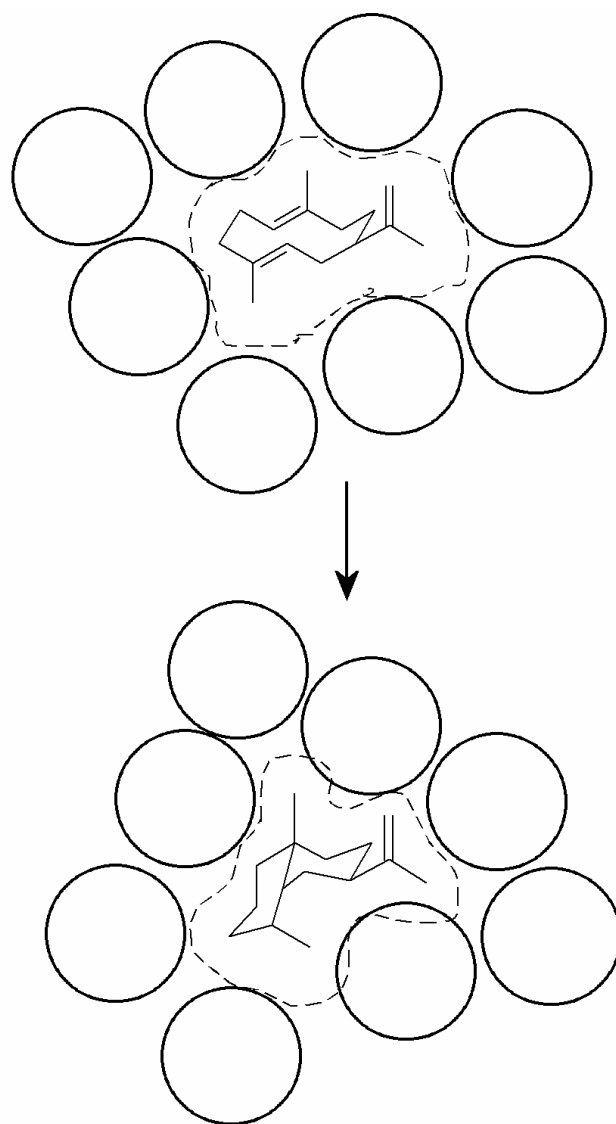


Figure 4.5 Conceptual cartoon representing how structural elements of the synthase enzymes might constrain substrate conformers and thus impose stereochemical control in catalysis.

Circles represent alpha-helices of the alpha-barrel structure with the axis of the barrel perpendicular to the page. Conformational control is exerted by three-point constraints on methyl groups dictated by spatial arrangement of the alpha helices. In this model, active site residues may be identical, yet the relative positioning of the alpha-helices controls the catalytic reaction pathways. Also schematically depicted is the transmutation of TEAS into an HPS-like enzyme via 9 site-specific mutations.

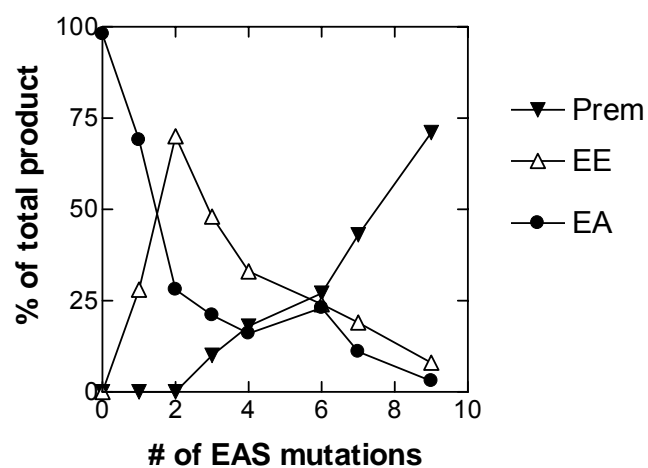


Figure 4.6 Graphic depiction of stepwise changes in product distribution for mutants leading up to TEAS-M9

The sequence of mutations used in this plot correlates with those in Figure 4.3 and the reaction products for the respective mutants as presented in Table 4.1. Prem = premnaspirodiene, EE = 4-epieremophilene, EA = 5-epi-aristolochene.

CHAPTER 5 Variations on a theme, Cloning and Mutational Analysis of Valencene Synthase from *Citrus x paradisi*

Introduction

One consequence of our structure-function studies is a prediction of particular amino acid residues in specific positions of naturally occurring terpene synthases. Therefore, a continuing goal is to isolate terpene synthases with slight but distinct catalytic twists relative to TEAS. A theoretical array of eremophilane isomers is shown in (Figure 5.1). Of these, eremophilene and valencene are commonly identified in nature but the corresponding synthases have not been previously cloned. These two molecules have 1,10 double bonds (6,7 FPP numbering), as opposed to the 10,11 (7,8 FPP numbering) double bond found in 5-epi-aristolochene, the reaction product of TEAS, and we have supposed that features controlling this product specificity should be reflected in the primary sequence of the synthase proteins.

The most common strategy for cloning plant sesquiterpene synthases is to probe a cDNA library with a fragment from a known cyclase^{210,213,215} or to use degenerate primers based on regions of homology within a class of terpene synthases^{209,212,217,218,237}. Large scale sequencing efforts have recently uncovered a more complete array of putative terpene synthase genes within a plant species. In many cases, the catalytic function or product specificity cannot be deduced by a simple alignment or similarity score assignment. As a refinement of this approach, the first two tiers of residues derived from the TEAS contact map (Figure 3.1) were aligned with other terpene synthases in an attempt to tease out functional information. For example, the change in double bond regioselectivity resulting from the T402S/V516I mutations to TEAS (from 1,10 to 10,11) led to the speculation that a serine at position 402 and isoleucine at position 516 might be indicative of synthases which deprotonate from C6 (FPP numbering). In screening genetic database resources, an EST from a citrus sequencing project (*Citrus x paradisi*) denoted as “putative terpene synthase” under accession number AF411120 contained active site residues thought to be indicative of the C6 deprotonation.

Grapefruit is distinguished by the presence of the sesquiterpenoid nootkatone (Scheme 5.1) which is a key component of its unique flavor profile⁴⁴⁻⁴⁶. Nootkatone arises from the introduction of a ketone at the 2 position of valencene. From a chemical viewpoint, valencene is closely related to 5-epi-aristolochene and premnaspirodiene. Most importantly for comparative structure-function studies, valencene is a stereoisomer of 4-epi-eremophilene (Figure 5.1), the product of the synthetic 4-epi-eremophilene synthase, EES. On these grounds, the grapefruit EST looked promising as a possible valencene synthase and a valuable addition to our ongoing comparative structure-function analyses.

Materials and Methods

RT-PCR (*Performed by Yonsoo Yeo, Chappell Lab, University of Kentucky*)

RNA was isolated from the juice vesicles of freshly harvested red grapefruit by standard methods using TRIZOL® (Invitrogen). RNA was reverse transcribed using Superscript II RNase H- and a reverse primer complementary to the 3' end (up to and including the stop codon) of the reported sequence, AF411120. PCR using *Pfu* turbo taq polymerase (Stratagene) employed the same reverse primer and one complementary to the 5' end up to and including the start codon. A fragment of the expected size was amplified (\approx 1.7kD by 1.0% agarose gel electrophoresis).

Construction of E. coli expression vector

A construct was engineered to provide an N-terminal hexahistidyl tag for purification after expression of the putative valencene synthase cDNA in *E. coli*. Primers were used to re-amplify the AF411120 cDNA from the start to stop codons and incorporate ExoRI and XhoI restriction sites by PCR. The PCR product was digested with EcoR1 and XhoI and purified using QIAquick PCR purification kit (Qiagen). The pET-28a(+) expression vector was cut with EcoR1 and XhoI, dephosphorylated with calf intestine alkaline phosphatase (Invitrogen) to prevent self ligation, and purified with the QIAquick kit. The PCR product was ligated into the cloning region of pET-28a(+)

vector using a commercial ligation mix (Clonables, Novagen), to generate the vector pET-28a(+)-CVS.

DNA sequencing

DNA was sequenced by the BigDye terminator system on a ABI 310. Sequence was obtained from start to stop codons in duplicate and was rectified with the reported sequence for Citrus x paradisi putative terpene synthase mRNA accession number AF411120. One nucleotide was found to be altered in the recovered cDNA, the nucleotide 1544 bases 5' downstream of the ATG start site was an A (instead of a G) making codon 492 for arginine rather than aspartate.

Expression and Purification of H₆-CVS

The pET28-CVS vector construct was transformed into BL21 (DE3) cells, expressed and purified as in chapter 3. In short, expression of the CVS insert cDNA was induced by IPTG addition and the expressed CVS protein purified by nickel affinity chromatography.

Product Identification

Products were subjected to GC-MS essentially as described in chapter 3. Briefly, reactions of 2.5 mL were run with purified enzyme and substrate, and pentane extractable products were evaluated by GC-MS.

pH profile experiments (*Enzyme prepared by Bryan Greenhagen, assays performed by Dr. Paul O'Maille, Noel Lab, Salk Institute for Biological Studies*)

Cyclase reactions were conducted in glass vials under a standard set of conditions: 100 nM enzyme, 20 mM MgCl₂, 50 μM FPP (Echelon; Salt Lake City, Utah), and 100 mM buffer at various pH values. The buffer for a particular pH range was generally chosen within one pH unit of the buffer's pK_a (pH 5-5.5, acetate; pH 6-7, MES; pH 7.5-9, Tris; pH 9.5-10, ethanolamine; pH 10.5, CAPS). Reactions were allowed to proceed at room temperature for 30 min prior to overlaying with ethylacetate. Vortexing for 10 sec was sufficient for product extraction and the needle

sampling depth was programmed to remove sample only from the organic phase. Reaction products were analyzed using an HP 6890 gas chromatograph with a 5973 mass spectrometer (Agilent Technologies, Palo Alto, CA). Separations were performed on (5%-phenyl)-methylpolysiloxane column (J&W Scientific, Folsom, CA) of 30 m x 0.25 mm i.d. x 0.25 m thickness. Helium was the carrier gas (flow rate of 2 mL/min). A splitless injection (injection volume of 1uL) was used, and a temperature gradient of 10 °C/min from 50 °C (5-min hold) to 180 °C (4-min hold) was applied. GC/MS data was analyzed using HP-Chemstation software (version B.01.00) and peak areas of terpenoid products were quantitated by manual integration.

Sequence Analysis

All sequence analysis was done using the tools available from NCBI web site (<http://www.ncbi.nlm.nih.gov/>) or using ClustalX.

Site-directed mutagenesis

Site directed mutagenesis was performed according to the manufacturers recommendations (QuikChange, Stratagene) using the following oligonucleotides with pET-28-TEAS-V516I (Chapter 3) or pET-28-CVS as a template. Mutagenic Primers were: **CVS-I516V**: CGA TTC TTA ATC TTG CTC GTG CAG TTG ATT TTA TTT ACA AAG AGG; **CVS-C402T**: GTT ATG ACG AAT GTG TAA GCA GTA TAA GCA GTA CTT GTT AGT GCA ATA GG; **TEAS-T401S/T402C/T403A**: CTA AGC AAT GCA CTA GCA AGT TGC GCA TAT TAC TAC CTC GCG AC.

Results

Bacterial expression of CVS

Hundreds of terpene synthase-like genes are detected in general Genbank data base searches with the TEAS gene or protein sequence. To narrow down this field to a more manageable number, the list of candidate genes were screened for those showing variations relative to TEAS in their second tier residues (Table 3.1). One sequence

resulting from this refinement was an EST sequence reported from a Citrus sequencing project. Although this sequence was already labeled as “terpene synthase-like”, signature sequences within tier two suggested that it might catalyze a reaction deprotonating a reaction intermediate at C6 (FPP numbering). Furthermore, nootkatone and valencene, two terpenes found in citrus fruits possess a C6-C7 double bond suggesting that a suitable terpene synthase for the biosynthesis of these compounds might exist.

The citrus terpene synthase-like cDNA of 1710 nucleotides was isolated from fresh grapefruit via RT-PCR using non-degenerate primers, inserted into an appropriate expression vector, and the bacterially expressed protein was purified. The conceptual translation of the isolated cDNA called for a protein of 548 amino acids having a molecular weight of 63,646 daltons. The bacterially expressed citrus protein was approximately 30% pure as determined by coomassie-stained SDS-PAGE, and migrated as a 64kD polypeptide.

The purified protein was incubated with FPP at pH 7.5 and the pentane extractable products examined by GC-MS (Figure 5.2). The two compounds observed in the GC trace had spectra matching β -elemene and valencene, and the cDNA was therefore named *Citrus* valencene synthase, CVS.

The enzymatic product co-migrated with a sample of authentic valencene and gave a nearly identical mass spectrum. Given the origin of the citrus mRNA (acidic fruit vesicles) we surmised that the CVS enzyme may have a somewhat different pH dependence than TEAS. In collaboration with Dr. O’Maille, I provided him with purified enzyme that he used to examine the reaction product profile over a range of pH values, reported in Figure 5.3. The pH optimum for the reaction from this plot is 6.8. At this pH value valencene is the only identifiable product (Figure 5.5)

Sequence Analysis

Both strands of *Citrus* valencene synthase (CVS) cDNA were sequenced twice; which is presented along with the predicted amino acid sequence in Figure 5.4. The DNA sequence is nearly identical to that deposited by D. Xia and E. Louzada in the GenBank database under accession number AF411120. Only one base pair

variation from the EST sequence was noted and resulted in an amino acid substitution of arginine for aspartate at position 492 relative to the start methionine. The sequence for CVS is consistent with the original hypothesis that first and second tier residues would be conserved in synthases which catalyze the generation of 6,7 double bonds in their reaction products, similar to those in EES. Surprisingly, the closest verified terpene synthase amino acid sequence is delta-cadinene synthase from cotton (*Gossypium arboreum*, 50% identity/69% similarity). In contrast, CVS is approximately 45% identical and 68% similar to both TEAS and HPS.

Initial Mutational Analysis

If our simple assumptions concerning the role of second tier residues is correct, then we would predict that mutations of the appropriate positions within CVS would convert it from a synthase producing a C6-C7 double bond to one synthesizing a C7-C6 double bond.

T402 in TEAS is a one of three consecutive threonine residues which line the active site yet only T403 points into the active site. T403 interacts with the methyl (C14) which migrates to form a chiral center at C2 (FPP numbering) opposite of that in 5-epi-aristolochene (see contact map in chapter 3, figure 3.1). It was reasoned that this motif, in conjunction with a change at position 516, might be sufficient to convert TEAS into a valencene synthase enzyme. Analysis of pentane extracts from preparative reactions with crude lysate from TEAS-T401S/T402S/T403A/V516I expressed in *E. coli* did not detect any valencene, and only germacrene A seemed to be produced (Table 5.1).

The mutation of CVS into TEAS-like enzyme was also considered. That is, a comparison of tier 1 and tier 2 residues between the two enzymes (Table 5.1) suggests select mutations might convert CVS into a TEAS-like synthase. Mutation of CVS to the TEAS residue identities at position 402 and 516 resulted in a synthase (CVS-C402S/I516V) that had a conversion rate of FPP to valencene less than 25% of wildtype enzyme, but approximate a doubling of germacrene A synthesis (Table 3.1).

The CVS-I516V single mutant had very little effect on product specificity.

Discussion

The primary intention of the work described in this chapter was to mine sequence data for new insights into structure-function relationships of terpene synthases as part of a larger comparative study of terpene synthases. In brief, previous successes with comparative analyses, such as the generation of the novel synthase EES by site-directed mutagenesis (Chapter 3), have been facilitated by comparisons between synthases that catalyzing well defined reaction pathways which differ by single partial reactions. The work described here represents another extension to this strategy.

The work presented in this chapter stems from the observation that two mutations to EAS are sufficient to change cyclase product double bond regioselectivity (Chapter 3). It was reasoned that the EES motif (S402 /I516) might be a conserved structural element in eremophilane / vetispirane producing plant cyclases that form double bonds by deprotonation from C6 (FPP numbering). To evaluate this contention, another eremophilene synthase was sought. There are two known eremophilanes for which no synthase has been reported, eremophilene and valencene (Figure 5.1). EST database sequences for plants known to produce these compounds were therefore screened. An EST entry from red grapefruit was noted and found to predict a cysteine at position 402 and an isoleucine at position 516. With the help of Dr. Yonsoo Yeo in the Chappell lab, the respective cDNA was cloned. This cDNA was engineered into a pET expression vector, expressed, recovered, and found to encode valencene synthase enzyme activity.

Intermediacy of Germacrene A

As seen in figure 5.3, a transition between valencene and germacrene A occurs at approximately pH 8.2. We interpret this as a titration point for the protonation of germacrene A. This pH value is close to the pK_a value for cysteine (pH 8.4), which was implicated as being involved in the second protonation step of the chemical cascade

catalyzed by TEAS. The previous results (Chapter 3) demonstrated that when C440 of TEAS was mutated to serine or alanine, a robust germacrene A synthetic activity resulted. In combination with the sequence data provided here (Figure 5.4), it is apparent that germacrene A synthases only differ from CVS by the presence of C440 in the active site while Y520, previously implicated as involved in the same protonation step¹⁶⁰, is conserved (Table 3.1). That germacrene A production is observed and pH dependent is also consistent with its intermediacy in the reaction catalyzed by CVS.

Initial Mutagenesis

Mutagenesis was utilized as means to address the validity of a strategy based on the predicted identity of assumed active site residues. As a test of this strategy, the alteration of CVS to the EAS residues at positions 402 and 516 was predicted to alter double bond regioselectivity and convert CVS into an (-) aristolochene synthase. The enantiomer, (+) aristolochene, is produced by bacterial species¹³⁴, however (-) aristolochene from natural sources has not been reported. Neither the single mutant CVS-I516V nor the double mutant CVS-C402S/V516I exhibited the predicted activities. In fact, initial screens for product revealed a significant increase in the proportion of germacrene A generated (Table 1). Likewise, when EES was altered to the CVS residues corresponding to T401-T403 of CVS (TEAS numbering), the only major product was germacrene A. These results may be explained by two possible models: 1. the active site architecture is altered so that the proton donor is not positioned properly for proton donation; or 2. a dynamic mechanism is at play where the intermediate germacrene A is not brought in to proper stereoelectronic alignment for the proton donation (i.e. proper anti-cyclization geometry is denied).

Mechanism

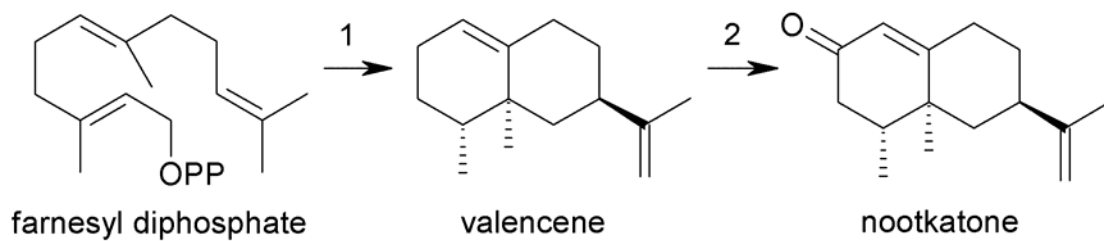
The reaction pathway for CVS is expected to proceed in the same manner as proposed for TEAS and HPS up to the formation of germacrene A (Scheme 5.2). In short, FPP is ionized in a divalent metal dependent manner, forming a allylic

carbocation. The distal double bond of FPP undergoes electrophilic attack at C10 by the carbocation at C1 forming an (*R*)-germacrenyl carbocation. Elimination from a terminal methyl group occurs to give (*R*)-germacrene A. At this point CVS differs from EAS and HPS. A conformer of germacrene A should be bound such that the *re* rather than *si* face (as is the case for EAS and HPS) of C7 (FPP numbering) should be facing parallel to the *re* face of C2 (figure 5.1). This is an initial requirement for the proper stereochemistry of cyclization and rearrangement of the C14 methyl. Cyclization is activated via donation of a proton in a proposed cysteine mediated fashion, to the *si* face of C6, anti to the developing C7,C2 bond. This produces an (*S*)-eudesmyl carbocation diastereomeric to the (*R*) form necessary in HPS or EAS catalysis. In a conformation aligning the *p* orbital on the *re* face of the carbocationic C2 with the C14-C7 bond, methyl migration occurs forming a eremophilyl carbocation. Ring conformations of this species now control elimination, possibly along with an appropriately placed proton acceptor, possibly W273 (TEAS numbering). Deuterium labeling experiments should provide a means to determine what conformation is required in this process¹⁷⁰.

There are other interesting stereochemical differences between the mechanism proposed for TEAS, HPS, and EES. Valencene is assumed to derive from a methyl migration across the alpha face of an eudesmyl carbocation followed by deprotonation from C6. The prenaspirodiene synthase deviates from this pathway in that a methylene group migrates across the same face and deprotonates from C6 syn to the migrating methylene¹⁷⁰. For 5-epi-aristolochene formation, the C14 methyl would migrate across the opposite, beta face of the molecule, but deprotonate from C8 syn to the migrating methyl group (FPP numbering)¹⁷⁰. The synthetic 4-epi-eremophilene synthase affords perhaps the most interesting point of comparison with valencene synthase; the only difference in the two presumed reaction pathways is that the migration of C14 occurs on opposite faces of the eudesmane carbocation. An obvious question remaining to be addressed is how might these alternate processes be controlled by the cyclase.

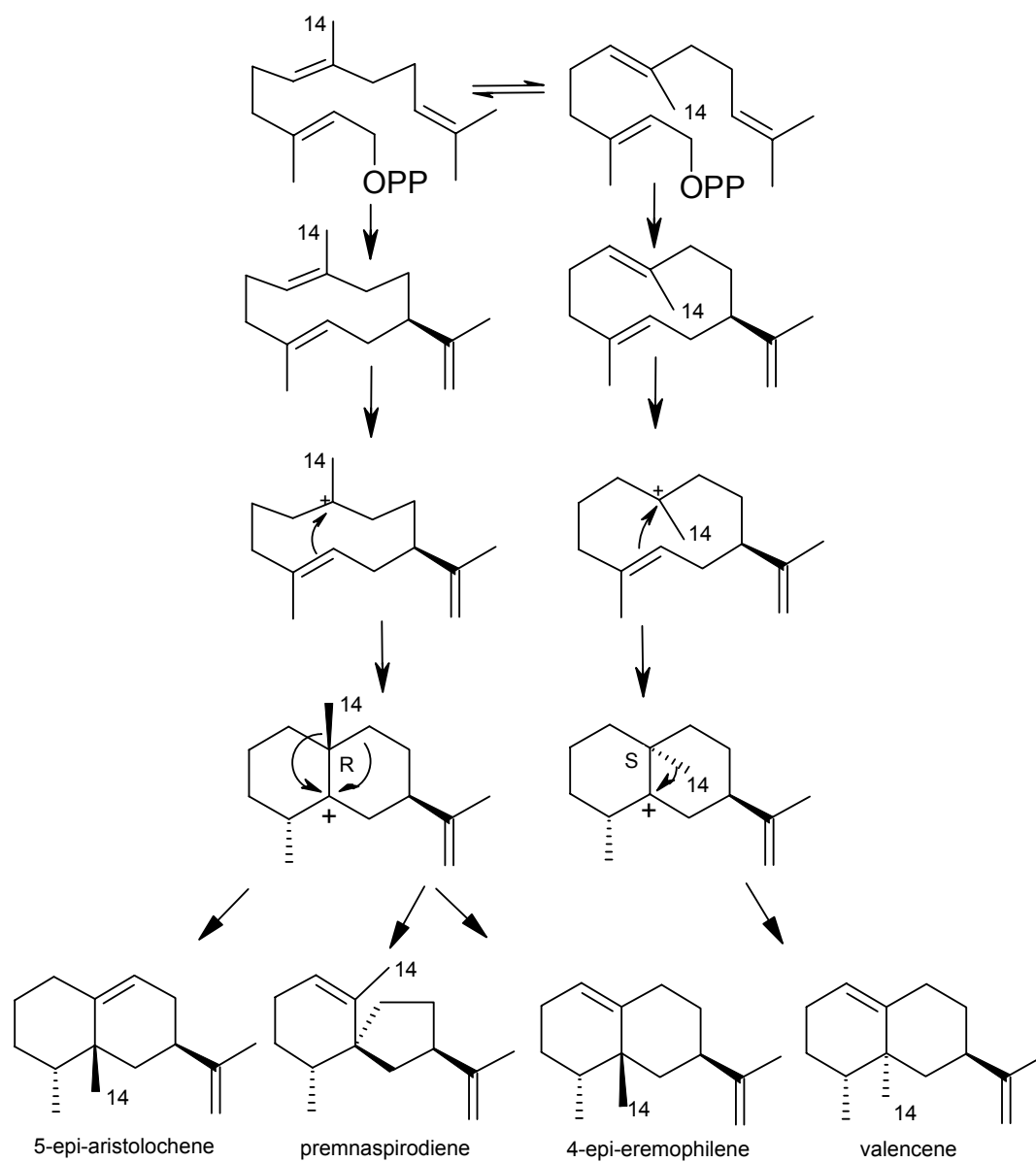
A map illustrating germacrene A conformers that give rise to a theoretical set

of eremophilane double bond regioisomers is given in figure 5.1. The synthetic possibilities diverge first upon the attack of the distal double bond; second as a consequence of double bond geometric relationships; and third as a consequence of double bond formation. As discussed elsewhere in this thesis, in order to define a specific reaction pathway, the active site must: A. limit the conformation of the three isoprene units (which are rigid, planar but connected by conformationally free carbons at C4,5,8, and 9); and B. enforce relative bond geometries (ring conformations) which provide stereoelectronically preferred carbon and hydrogen migrations and proton eliminations. Now, given our current conceptual understanding of these synthases, is the full set of these eremophilane isomers (figure 5.1) available via reconstruction of the basic terpene synthase fold?



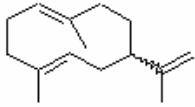
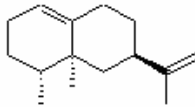
Scheme 5.1 A proposed biosynthetic pathway for Nootkatone.

This scheme proposes that *Citrus x paradisi* nootkatone biosynthesis involves two steps mediated by **1.** Valencene Synthase (CVS) **2.** Valencene Oxidase (CVO).



Scheme 5.2 Stereochemical alternatives for sesquiterpene synthase reaction pathways.

Table 5.1 Reaction product profiles for CVS, CVS mutants and CVS-like mutations in TEAS.

	 Germacrene A	 Valencene	UnID
CVS	35	64	1
CVS-I516V	32	57	11
CVS-S402T/I516V	66	27	7
TEAS-T401S/T402S/T403A/V516I	99	0	1

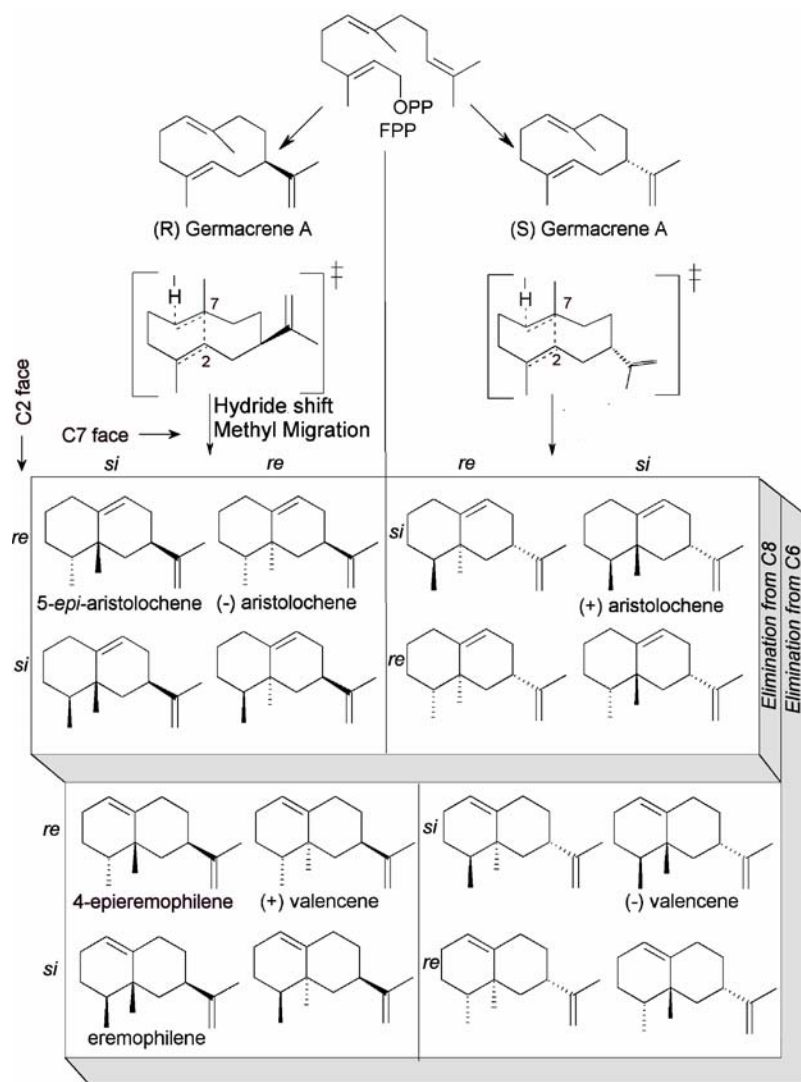


Figure 5.1 The stereo- and regiochemical generation of eremophilanes.

Stereospecificity diverges first in the attack of C10,C11 double bond attack on the *si* face, giving rise to (10*R*)-germacrene A subsequent to proton elimination, or attack of the *re* face, yields the (10*S*) enantiomer. The second key to development of chirality in products is the conformation of germacrene A before the second cyclization event. In the table of eremophilanes, the face of C7 of germacrene A facing inwards is given right to left, while the face of C2 is given from top to bottom. The tiers of the product array represent the two alternatives for direct proton elimination from the eremophilyl carbocation resulting from methyl migration subsequent to cyclization.

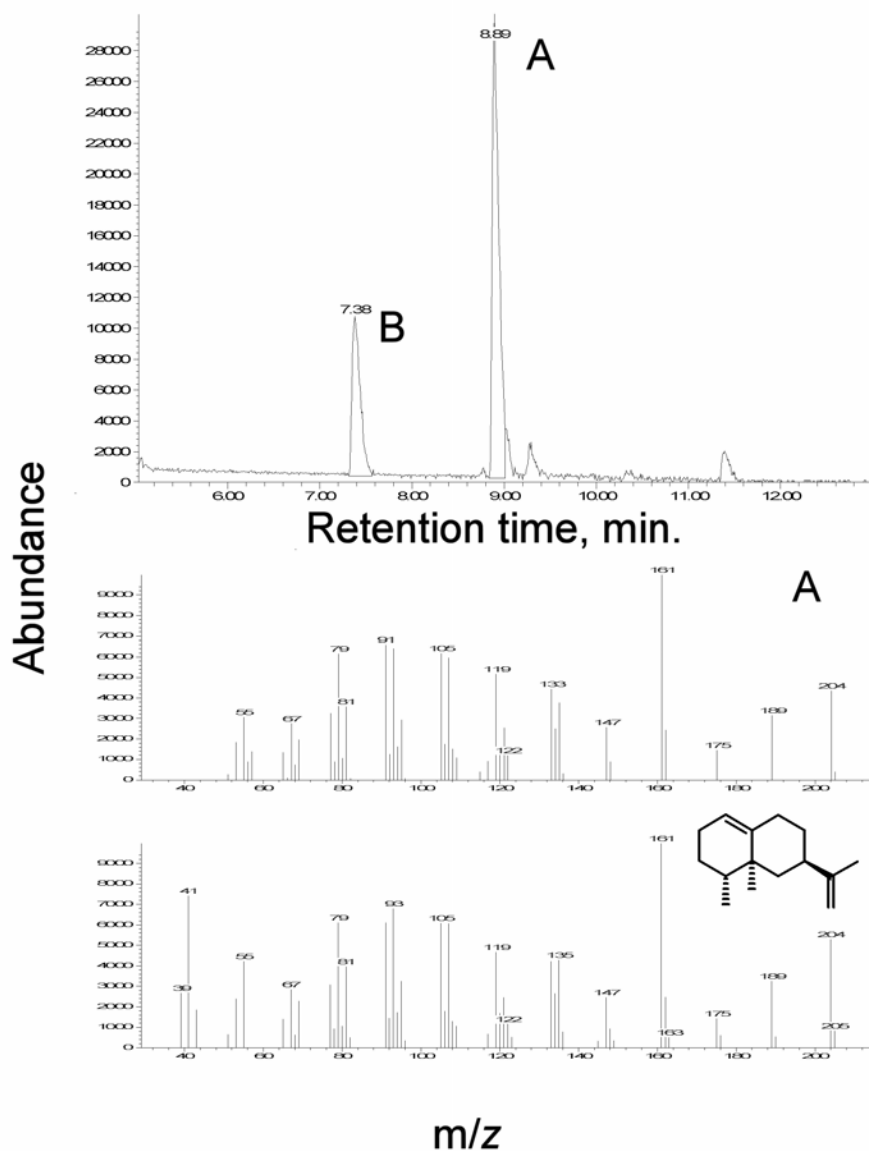


Figure 5.2 Reaction product analysis by GC-MS for CVS incubated at pH 7.5.

Lysate of *E. coli* harboring pET-28-CVS was incubated with FPP at pH 7.5, and an aliquot of the pentane extract examined by GC-MS. The mass spectrum (scanning m/z 50-250) of peak A is given below the GC trace and compared to the mass spectrum for authentic valencene (scanning m/z 35-250). The mass spectrum of peak B is identical to that for β -elemene, the thermal induced rearrangement product of germacrene A.

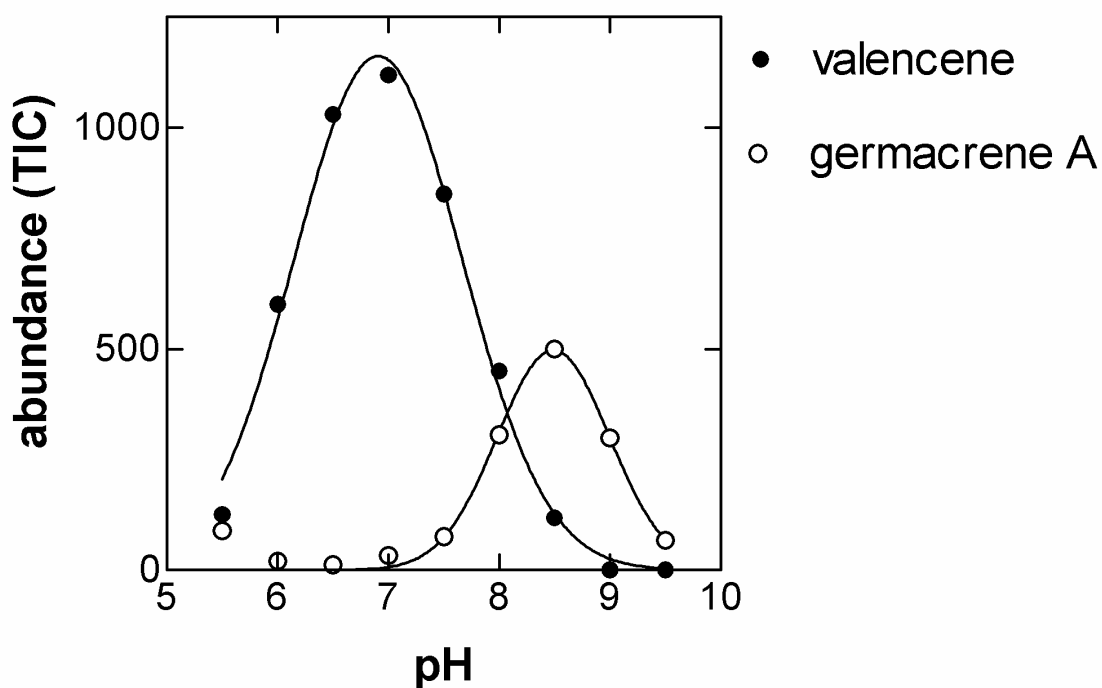


Figure 5.3 The pH dependence for citrus valencene synthase.

Purified CVS was incubated with FPP at various pH values, ethylacetate extracts evaluated directly by GC-MS analysis without concentration of the extract. The pH optimum for valencene synthesis is pH 6.8. The transition between valencene and germacrene A as the major product occurs at pH 8.2. The GC-MS data at pH 7 is given in Figure 5.5.

M S S G E T F R P T A D F H P S L W R N
1 ATGTCGCTCGGAGAAACATTCGTCTACTGCAGATTCCATCCTAGTTTATGGAGAAAC
+1 H F L K G A S D F K T V D H T A T Q E R
61 CATTTCCTCAAAGGTGCTTCTGATTCAAGACAGTTGATCATACTGCAACTCAAGAACGA
+1 H E A L K E E V R R M I T D A E D K P V
121 CACGAGGCACTGAAAGAAGAGGTAAGGAGAATGATAACAGATGCTGAAGATAAGCCTGTT
+1 Q K L R L I D E V Q R L G V A Y H F E K
181 CAGAAGTTACGCTTGATTGATGAAGTACAACGCCTGGGGTGGCTTATCAGCTTTGAGAAA
+1 E I E D A I L K L C P I Y I D S N R A D
241 GAAATAGAAGATGCAATACTAAAATTATGTCCAATCTATATTGACAGTAATAGAGCTGAT
+1 L H T V S L H F R L L R Q Q G I K I S C
301 CTCCACACCGTTCCCTTCATTTTCGATTGCTTAGGCAGCAAGGAATCAAGATTTTCATGT
+1 D V F E K F K D D E G R F K S S L I N D
361 GATGTGTTTGAAGTTCAAAGATGATGAGGGTAGATTCAAGTCATCGTTGATAAACGAT
+1 V Q G M L S L Y E A A Y M A V R G E H I
421 GTTCAAGGATGTTAAGTTTGTACGAGGCAGCATACATGGCAGTTCCGGAGAACATATA
+1 L D E A I A F T T T H L K S L V A Q D H
481 TTAGATGAAGCCATTGCTTTCCTACTACCCTCACCTGAAGTCATTGGTAGCTCAGGATCAT
+1 V T P K L A E Q I N H A L Y R P L R K T
541 GTAACCCCTAAGCTTGGGAAACAGATAAAATCATGCTTTATACCGTCTCTTCGTAACCC
+1 L P R L E A R Y F M S M I N S T S D H L
601 CTACCAAGATTAGAGGCGAGGTATTTTATGTCCATGATCAATTCACCAAGTGATCATTTA
+1 Y N K T L L N F A K L D F N I L L E P H
661 TACAATAAACTCTGCTGAATTTTGCAAAGTTAGATTTAACATATTGCTAGAGCCGCAC
+1 K E E L N E L T K W W K D L D F T T K L
721 AAGGAGAACTCAATGAATTAACAAAGTGGTGGAAAGATTTAGACTTCACTACAAAACATA
+1 P Y A R D R L V E L Y F W D L G T Y F E
781 CCTTATGCAAGAGACAGATTAGTGGAGTTATTTTTGGGATTTAGGGACATACTTCGAG
+1 P Q Y A F G R K I M T Q L N Y I L S I I
841 CCTCAATATGCATTTGGGAGAAAGATAATGACCCAATTAATACATATTATCCATATA
+1 D D T Y D A Y G T L E E L S L F T E A V
901 GATGATACTTATGATGCGTATGGTACACTGAAGAAGTCAAGCTCTTACTGAAGCAGTT
+1 Q R W N I E A V D M L P E Y M K L I Y R
961 CAAAGATGGAATATTGAGGCCGTAGATATGCTTCCAGAATACATGAAATGATTACAGG
+1 T L L D A F N E I E E D M A K Q G R S H
1021 ACACTCTTAGATGCTTTTAAATGAAATGAGGAAGATATGGCCAAGCAAGGAAGATCACAC
+1 C V R Y A K E E N Q K V I G A Y S V Q A
1081 TGCGTACGTTATGCAAAAGAGGAGAATCAAAAAGTAATGGAGCATACTCTGTTCAAGCC
+1 K W F S E G Y V P T I E E Y M P I A L T
1141 AAATGGTTCAGTGAAGTTACGTTCCAACAATGAGGAGTATATGCCTATTGCACTAACA
+1 S C A Y T F V I T N S F L G M G D F A T
1201 AGTTGTGCTTACACATTCGTCATAACAAATTCCTTCCTTGGCATGGGTGATTTTCAACT
+1 K E V F E W I S N N P K V V K A A S V I
1261 AAAGAGGTTTTGAATGGATCTCCAATAACCTAAGGTTGTAAGGAGCAGCATGATGATGATC
+1 C R L M D D M Q G H E F E Q K R G H V A
1321 TGCAGACTCATGGATGACATGCAAGGTCATGAGTTGAGCAGAAGAGAGACATGTTGCG
+1 S A I E C Y T K Q H G V S K E E A I K M
1381 TCAGCTATGAATGTTACACGAAGCAGCATGGTGTCTCTAAGGAAGAGGCAATTAATAATG
+1 F E E E V A N A W K D I N E E L M M K P
1441 TTTGAAGAAGAAGTTGCAATGCATGGAAGATATTACGAGGAGTTGATGATGAAGCCA
+1 T V V A R P L L G T I L N L A R A I D F
1501 ACCGTCGTTGCCGACCACTGCTCGGGACGATTCTTAATCTGCTCGTGAATGATTTT
+1 I Y K E D D G Y T H S Y L I K D Q I A S
1561 ATTTACAAGAGGACGACGGCTATACGCATTCCTTACCTAATTAAGATCAAATGCTTCT
+1 V L G D H V P F *
1621 GTGCTAGGAGACCAGTTCATTTTGA

Figure 5.4 DNA sequence and predicted amino acid sequence for citrus valencene synthase

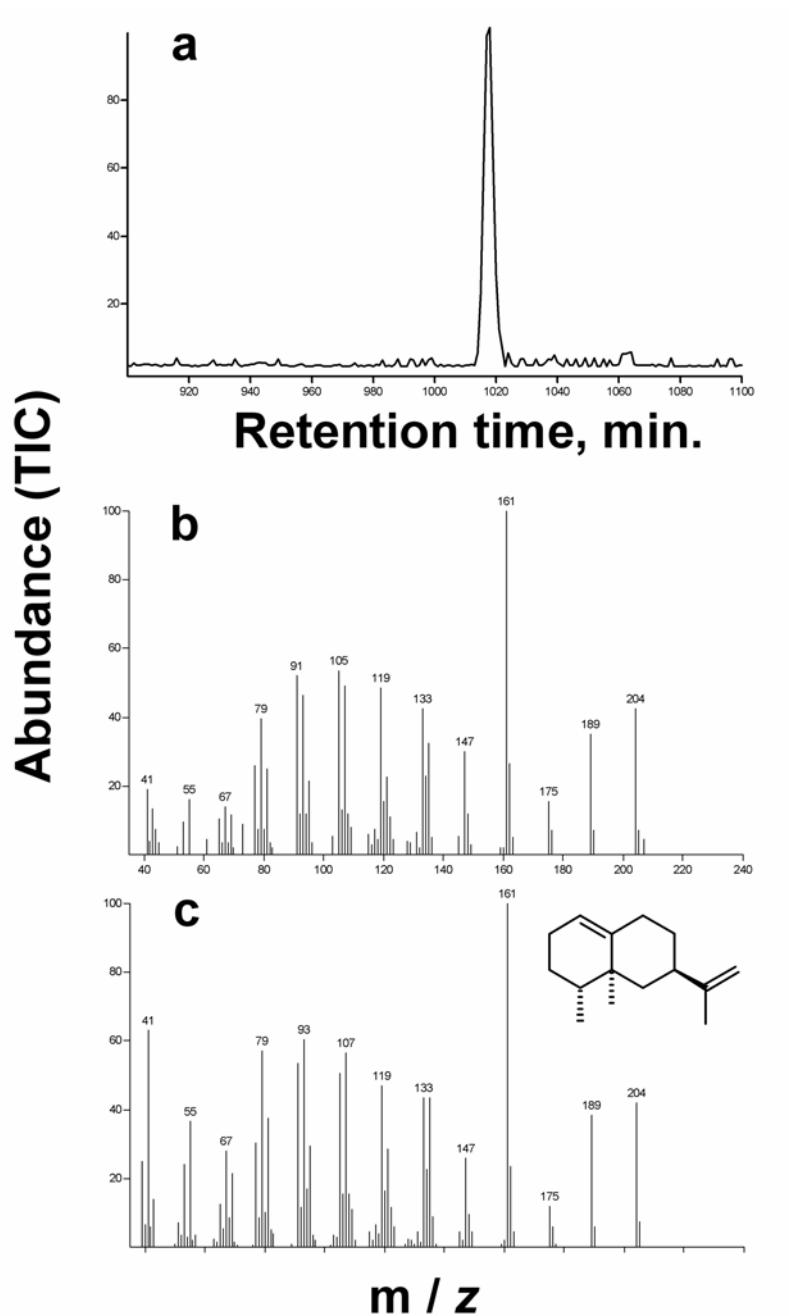


Figure 5.5 GC-MS data for ethylacetate extractable sesquiterpene products of *citrus* valencene synthase at pH 7.

This is the GC-MS data from the pH dependence assay showing in Figure 5.4. The GC trace is given in panel **a** and the mass spectrum of the major peak is given in **b**. The NIST standard spectrum for valencene is given in **c**.

CHAPTER 6 Probing sesquiterpene hydroxylase activities in a coupled assay with terpene synthases

(Special note: The work reported in this chapter has been published in the Archives of Biochemistry and Biophysics (2003) 409: 385-394 and represents the culmination of a collaborative project within the Chappell laboratory between Bryan Greenhagen, Paul Griggs, Shunji Takahashi and Lyle Ralston)

Introduction

5-epi-aristolochene dihydroxylase (EAH) is a cytochrome P450 enzyme responsible for the introduction of two hydroxyl groups into 5-epi-aristolochene resulting in the phytoalexin capsidiol⁷⁷ (Scheme 6.1). The intention of the work in this chapter was to better define as many of the structural, functional and mechanistic features²³⁸ of the EAH enzyme as possible. For this purpose, studies to examine substrate specificity^{186,239}, studies to define domains or amino acids within putative substrate recognition regions²⁴⁰ of the enzyme that contribute to regio- and stereo-selectivity¹⁸⁸, and even studies to probe how the interaction between the terpene synthase enzyme with EAH might influence catalysis are anticipated. As such, facility in performing EAH enzyme activity assays will be of importance and are needed to overcome a number of limitations. Probably the most important limitations include difficulties in obtaining suitable substrates and substrate analogs without arduous organic synthesis efforts, finding suitable means for introducing hydrophobic substrates into aqueous solution and providing sensitive and rapid means for measuring EAH enzyme activities. The aim of the current work was therefore to assess the utility of a coupled, in vitro assay. Using readily available terpene synthase enzymes and microsomes from yeast over-expressing functional EAH²⁴¹, the current work sought to validate a synthase/hydroxylase coupled assay, then to explore the utility of this assay for coupling different synthases to the EAH hydroxylase, thus testing the suitability of different sesquiterpene substrates for hydroxylation by EAH.

Materials and Methods

Chemicals. Standard laboratory reagents were purchased from Fisher Biotech (Fair Lawn, NJ), Sigma Chemical Company (St. Louis, MO), and Aldrich Chemical Co. (Milwaukee, WI). Authentic standards of capsidiol, 1-deoxycapsidiol, 3-deoxycapsidiol and 5-*epi*-aristolochene were prepared as described earlier²⁴¹ and kindly provided by Dr. Robert M. Coates, Department of Chemistry, University of Illinois.

Terpene synthase and dihydroxylase sources. 5-*epi*-aristolochene synthase (EAS)²⁴² and vetispiradiene synthase (HVS)²⁴³, now re-named premnaspirodiene synthase from *Hyoscyamus muticus* (HPS) to properly recognize Rao, Raju and Krishna who first chemically characterized this spirane hydrocarbon¹¹¹, have been previously described. The C440A mutant of EAS used in these studies generates germacrene A as its dominant (>95%) reaction product but is not catalytically compromised as is the Y520F mutant described earlier by Rising et al.²⁴⁴. A complete characterization of the C440 mutant will appear elsewhere. All the sesquiterpene synthases were obtained from bacteria over-expressing the respective genes as described previously^{244,245}. In short, the synthase genes were cloned in pET (Novagen) expression vectors in frame with hexa-histidine purification tags, the clones introduced into the BL21(D3) (Novagen) line of *E. coli.*, and expression of the synthase genes induced by addition of 0.1 mM IPTG to cultures with an A₆₀₀ of 1.0. The bacterial expressed synthase proteins were purified from bacterial lysates by Ni⁺ affinity chromatography according to Mathis et al.²⁴⁵ and the purity of the preparations verified by SDS-PAGE. Synthase preparations of 95% purity or better, based on Coomassie Blue staining, were routinely obtained.

5-*epi*-aristolochene dihydroxylase (EAH) was obtained as a microsomal preparation from yeast over-expressing the corresponding cDNA²⁴¹. In brief, the pYeDP60 yeast expression vector was engineered with the EAH cDNA and this construct introduced in the WAT11 line of yeast^{241,246}. The WAT11 cell line contains an *Arabidopsis thaliana* NADPH-cytochrome P450 reductase as a replacement for an endogenous reductase gene²⁴⁷. A single transformed yeast colony was selected and grown at 30°C for approximately 24 h in liquid SGI media (1 g/L bactocasamino acids;

7 g/L yeast nitrogen base; 20 g/L glucose; and 20 mg/L tryptophan) before an aliquot of this culture was diluted 1:50 into 250 mL of YPGE media (10 g/L bactopectone; 10 g/L yeast extract; 5 g/L glucose; and 3% (V/V) ethanol). Upon depletion of the glucose stock, determined using Diastix reagent strips (Bayer, Elkhart, IN), expression of EAH gene was initiated by the addition of galactose to a final concentration of 2%. The cultures were maintained at 30°C for an additional 16-20 h before collecting the cells by centrifugation at 7,000g for 10 min. The pelleted cells were then washed with 100 mL of TES buffer (50 mM Tris-HCl pH, 7.5; 1 mM EDTA; 0.6 M sorbitol), centrifuged as above, resuspended in 100 mL of TES-M (TES supplemented with 10 mM β -mercaptoethanol), and allowed to incubate at room temperature for 10 min. The cells were then again collected by centrifugation, and the pellet resuspended in 2.5 mL of extraction buffer (1% bovine serum albumin (fraction V), 2 mM β -mercaptoethanol, and 1 mM phenylmethylsulfonyl fluoride dissolved in TES buffer). Glass beads (0.5 mm in diameter, Biospec Products, Inc., Bartlesville, OK) (cleansed by rinsing in ethanol, dilute acid, then copious amounts of water) were added until they occupied approximately 90% of the resuspended cell volume and the cells disrupted by vigorously shaking the mixture in a cold room for 10 min at 30 s intervals separated by 30 s intervals on ice. The cell extract was decanted into a centrifuge tube and combined with 3 washes of the glass beads, each with 5 mL of extraction buffer. Microsomes were prepared by differential centrifugation at 10,000g for 10 min at 4°C to remove cellular debris followed by centrifugation at 100,000g for 70 min at 4°C. The final microsomal pellets were resuspended in 1.5 mL of TEG-M buffer (50 mM Tris-HCl, pH 7.5; 1 mM EDTA; 20% glycerol; and 1.5 mM β -mercaptoethanol) and stored frozen at -80°C until used in the coupled assays.

Synthase/hydroxylase Coupled Assays. Typical assays were performed with a pre-incubation of the synthase enzyme in 50 μ L containing 200 mM Tris-HCl, pH 7.5, 40 mM MgCl₂, 0.5 μ Ci ³H-FPP, 25 to 30 μ M FPP and 500 nM of purified synthase enzyme for 30 min at room temperature. Microsomal protein was then added up to a maximum of 150 μ g, along with 50 μ M NADPH where indicated, and the final volume adjusted to 75 to 80 μ L with 200 mM Tris-HCl, pH 7.5, 40 mM MgCl₂. After an

additional 30 min incubation at room temperature, the reaction was terminated by the addition of 40 to 75 μL of ethyl acetate, vortexed briefly, centrifuged for 10-60 s, and 10 to 20 μL of the organic extract used for TLC analysis. Aliquots of the organic extracts, along with authentic standards for FOH (radioactive and non-radioactive), 1-deoxycapsidiol (non-radioactive only), 5-*epi*-aristolochene (radioactive and non-radioactive) and capsidiol (non-radioactivity), were separated on silica TLC plates using cyclohexane: acetone (1:1) as the solvent. TLC plates were routinely scanned for radioactivity with a Bioscan system 200 Imaging Scanner (Lablogic, Sheffield, UK), and the radioactive zones scraped and counted by liquid scintillation in order to calculate reaction product yields. Standards were localized on the plates by either developing a portion of the plate with vanillin- H_2SO_4 reagent²⁴⁸ or determining the amount of radioactivity associated zones as above. For more analytical experiments, 1 μL aliquots of 5- to 10-fold concentrated ethyl acetate extracts were evaluated by GC and GC-MS along with standards of 5-*epi*-aristolochene, 1- and 3-deoxycapsidiol and capsidiol. GC-MS analyses were routinely performed with an HP-GCDplus equipped with a DB-5ms capillary column (30 m x 0.25 mm, 0.25 μm phase thickness) and run with He as the carrier gas at 1 mL/min. Splitless injections were done at an injection port temperature of 250°C with the oven temperature programmed to remain at 100°C for 1 min, then to increase at 4°C per min to 270°C. The Electron Ionization Detector was set to scan the mass range from 40-240 m/z.

Results

Validation and optimization of the terpene synthase/terpene hydroxylase coupled assay

In earlier work by Ralston et al.²⁴¹, an in vitro assay for measuring 5-*epi*-aristolochene hydroxylating (5EAH) activity was described. That assay consisted of microsomes isolated from yeast expressing the EAH cDNA incubated with synthetic 5-*epi*-aristolochene or 1-deoxycapsidiol, and measured the conversion of these two substrates to capsidiol by GC and GC/MS. Although this assay was suitable to document the biochemical activity of the encoded P450 enzyme, it was limited in several important aspects. First, only limited amounts of these substrates were available because they were prepared by relatively laborious synthetic means. Second,

the reactions required detection of reaction products by GC, which required relatively large incubation volumes to generate sufficient reaction products for detection. Each assay was also time consuming since a GC analysis was required for each sample. Lastly, addition of these hydrophobic substrates to the assays required simultaneous additions of organic solvents and/or detergents. The detergents and organic solvents were necessary to solubilize and introduce the hydrophobic substrates into the aqueous incubations, but their effects on the hydroxylase enzymes and presentation of substrate to the enzyme were difficult to determine. Given these complications, we sought an alternative assay, which would be rapid, sensitive and capable of providing substrates and substrate analogs without requiring organic synthesis efforts.

Our earlier work with wildtype terpene synthases^{242,243} and mutant enzymes capable of generating novel reaction products²⁴⁴ suggested that an alternative assay for hydroxylase activities might take advantage of these resources. Hence, initial experiments were performed to assess the potential of coupling EAS activity with the EAH activity (Fig. 6.1). EAS enzyme was obtained from bacteria over-expressing the corresponding cDNA and purified to near homogeneity by affinity chromatography²⁴⁵. The source of hydroxylase enzyme was isolated microsomes from yeast over-expressing the EAH cDNA. The hydroxylase concentration in these preparations was approximately equivalent to 120 pmoles of heme binding protein per mg of microsomal protein (0.7% of total microsomal protein) as approximated from difference absorbance maximum at 450 nm of the reduced enzyme in the presence of CO. The assay for hydroxylase activity thus consisted of pre-incubating the EAS with radiolabeled FPP for 30 min prior to the addition of yeast microsomes. As an additional control, microsomes were added with and without NADPH and the mixtures incubated a further 30 min. The reactions were then terminated and extracted simultaneously by the addition of ethyl acetate and aliquots of the organic extract separated by TLC. Authentic standards of capsidiol (zone A), 1 & 3-deoxycapsidiol and farnesol (zone B), and aristolochene (zone C) were also run in a neighboring lane, and located either using a developing reagent²⁴⁸ or by detection of the radioactivity incorporated into the standard. Each lane of the TLC plate corresponding to the experimental samples was then scanned for radioactivity.

Greater than 93% of the radiolabeled products, corresponding to 787 nmoles, generated in incubations without NADPH addition co-migrated with *5-epi-aristolochene* and about 6% co-migrated to the position of farnesol. Addition of 50 mM NADPH to the incubations caused a significant reduction (~60%) in the amount of radioactivity co-migrating with *5-epi-aristolochene*, but a very significant increase in the amount of label associated with zone A and an approximate tripling of radioactivity associated with zone B were observed. Assuming the reduction of radioactivity associated with zone C in the presence of NADPH corresponds to *5-epi-aristolochene* converted to capsidiol (zone A) and a mono-hydroxylated form of *5-epi-aristolochene* (zone B), then this would correspond to ~440 nmoles of capsidiol. Interestingly, greater than 379 nmoles of reaction product appears to migrate to the position of capsidiol and another 120 nmoles to that of the mono-hydroxylated forms (for a total of 500 nmoles of product), suggesting some sort of synergism in the coupled assay incubated with NADPH.

Confirmation of the authenticity of the various reaction products measured in the TLC assays was obtained by GC/MS (Fig. 6.2). Incubation of the synthase and microsomal preparations without NADPH resulted in the generation of a single new peak (peak A) on the gas chromatogram, which was not evident in the control chromatograms (synthase plus microsomes without FPP, data not shown). The mass spectra for peak A is identical (greater than 99% correspondence) with authentic *5-epi-aristolochene* and matches that previously reported²⁴². Incubation of the synthase and hydroxylase preparations with NADPH resulted in a dramatic reduction in the *5-epi-aristolochene* peak, and the appearance of a new peak, peak B. The mass spectrum observed for peak B was identical to that for authentic capsidiol as reported earlier²⁴¹. The MS for several minor (less than 5% of the total products) peaks with retention times between 25 and 27 min were also examined and were consistent with mono-hydroxylated forms of aristolochene (1- and 3-deoxycapsidiol).

The coupled assay was further optimized using the radioactive/TLC procedure described above for several parameters (Fig. 6.3), except the TLC zones corresponding to the standards were scraped from the plates and the radioactivity determined by liquid scintillation spectrophotometry. The amount of capsidiol formed was clearly dependent

on the amount of synthase or microsomal protein added to the assays (compare panels A and B). A ratio of at least 1 μg of pure synthase protein (15 pmoles) per 10 μg of microsomal protein (corresponding to 12 pmol of newly expressed heme-binding protein) appears to represent the optimal amounts for both of these enzymes in terms of capsidiol generation. Incubations of the synthase and hydroxylase longer than 30 minutes did not increase the amount of capsidiol recovered (panel C). The pre-incubation period for the synthase with radiolabeled FPP was important for full activity. Without any pre-incubation period or only a 10 min pre-incubation period, capsidiol biosynthesis was only 26% or 47%, respectively, of the standard 30 min pre-incubation assay. Longer pre-incubations did not enhance capsidiol synthesis further. The optimal concentration of FPP for these coupled assays was determined to be 18.5 μM , which is approximately double the K_m value for the synthase enzyme²⁴⁴, while the optimal concentration for NADPH was 50 μM .

Coupled assays with other synthases

One of the ways in which the coupled assays could provide utility is in examining substrate specificity of the hydroxylase by using terpene synthases that synthesize different sesquiterpene hydrocarbons. To initially assess this possibility, a cysteine to alanine mutation at amino acid position 440 of EAS was tested in the coupled assay (Fig. 6.4). The C440A-EAS mutant synthase catalyzes the conversion of FPP to a single, dominant (>95%) reaction product, germacrene A. Importantly, the C440A mutant is unlike the previous characterized mutant (Y520F)²⁴⁴, which also produces germacrene A, and is not catalytically compromised relative to the wildtype enzyme. Regardless, addition of the C440A mutant synthase to the coupled assay resulted in greater than 500 nmoles of FPP turned over to ethyl acetate extractable reaction products (sum of all the radioactivity associated with the peaks in zones E and F). Approximately 5% of these products were further metabolized in the presence of NADPH to a molecular species that co-migrated with capsidiol (zone D). Under identical conditions, wildtype EAS catalyzed the turnover of approximately 850 nmoles of FPP, greater than 40% of which was converted to capsidiol in the presence of NADPH (Fig. 6.1). GC-MS analysis revealed NADPH dependent peaks with retention

times and apparent parent ions (220.1 and 236.2) consistent with mono- and di-hydroxylated sesquiterpenes, respectively. Definitive assignments, however, were confounded by relatively weak signals and what appeared to be thermal-induced rearrangements of the germacrene skeleton as described by de Kraker et al.²⁴⁹.

The coupled assay was further evaluated using prenaspirodiene synthase from *Hyoscyamus muticus* (HPS) (renamed from vetispiradiene synthase (HVS) since the spirane hydrocarbon was first described by Rao, Raju and Krishna¹¹¹) which is a sesquiterpene synthase related to 5-epi-aristolochene and germacrene A synthase, yet catalyzes the synthesis of a bicyclic, spirane-type sesquiterpene (see Scheme 6.2). Like the EAS coupled assay, incubation of HPS and hydroxylase containing microsomes without NADPH resulted in radioactive products that migrated to the front of the TLC, consistent with the product(s) being un-modified hydrocarbon(s) (Fig. 6.5). Addition of NADPH to the incubations did not cause a significant reduction in the amount of radioactivity migrating near the solvent front, but did result in a significant increase of radioactivity found at a lower position on the TLC plate. Because these results indicated that the EAH enzyme was capable of metabolizing the spirane hydrocarbon generated by the action of the prenaspirodiene synthase, the reaction products of the HPS/EAH incubations were also examined by GC-MS (Fig. 6.6). Incubations without NADPH contained a dominant new compound (peak C) relative to control incubations (no FPP) whose spectrum matched that for prenaspirodiene²⁵⁰. In contrast, extracts of incubations done in the presence of NADPH contained not only the spirane compound (peak C), but also 3 new peaks (D, E and F) and several other minor peaks. Spectral characteristics of peaks D-F were consistent with these compounds being derived from prenaspirodiene. In fact, the spectrum for peaks D and E were consistent with mono-hydroxylated forms (parent ion of 220), while the spectrum for peak F matched that for solavetivone (parent ion of 218), a ketone, with a confidence value greater than 98%.

Discussion

Very significant progress has been made in mapping catalytic features of cytochrome P450 enzymes, especially those associated with isoprenoid metabolism, utilizing a fairly broad range of experimental approaches. These include sequence

compilations²⁴⁰, substrate specificity studies¹⁸⁶, domain swapping and site-directed mutagenesis¹⁸⁸, and elucidation of 3 dimensional structures²⁵¹. Of particular relevance to the current work has been the extensive characterization of two monoterpene hydroxylases. Limonene-3-hydroxylase and limonene - 6 hydroxylase catalyze regio- and stereo –specific hydroxylations at the C3 and C6 positions of the six-membered olefin ring of limonene in what appears to be highly homologous reactions by enzymes that share 70% amino acid sequence identity and over 85% sequence similarity^{252,253}. The substrate specificity of these enzymes was also carefully examined by Wüst et al.¹⁸⁶. Both enzymes were capable of hydroxylating the 2 enantiomeric forms of limonene with greater than 85% accuracy in the trans-facial insertion of the hydroxyl group. The apparent binding constants, catalytic activity and product profile of the hydroxylases towards a wide range of substrate analogs and fluorinated derivatives likewise demonstrated enzyme specificity and indicated that substrate binding and orientation were precisely controlled, possibly mediated by hydrophobic interactions between substrate and active site residues. This suggestion is consistent with an earlier report demonstrating that a single point mutation, changing a phenylalanine at position 363 to an isoleucine, was sufficient to change the regiospecificity of the limonene C6-hydroxylase to a C3-hydroxylase¹⁸⁸.

Due to the limited availability of sesquiterpene substrate analogs for the EAH enzyme and the difficulty associated with generating such compounds using traditional synthetic means, we sought an alternative approach for testing the substrate specificity and catalytic activity of the tobacco dihydroxylase. The coupled assay described here consists of generating different sesquiterpene skeletons using sesquiterpene synthases, then assessing the suitability of these hydrocarbons to serve as substrates and substrate analogs for the cytochrome P450 hydroxylase. The assay as validated here cannot be used to measure several important kinetic parameters of catalysis often reported for enzymes, such as the substrate affinity (K_m) or maximum reaction velocity (V_{max}), and therefore the turnover rate (K_{cat}) calculated from these constants cannot be reported. However, the assays more closely approximate the physiological conditions wherein the synthase and hydroxylase enzymes cooperate during catalysis (i.e. channeling effects), and can be used to examine substrate specificity in a different, but quantitative

manner, giving rise to a relative value for how efficient a substrate or substrate analog is hydroxylated. For instance, the native sesquiterpene synthase (EAS) and hydroxylase (EAH) coupled assay was optimized such that a significant proportion of FPP turned over to the hydrocarbon skeleton *5-epi-aristolochene* was converted to the final hydroxylated product capsidiol. Using identical experimental conditions, the turnover of other in vitro synthesized sesquiterpenes can be measured relative to the EAS/EAH assay. In the work presented here, about 62% of the total radioactivity recovered (hydrocarbon plus hydroxylated) in the EAS/EAH assays was incorporated into capsidiol and deoxycapsidiol, while only 9% of the incorporated radioactivity from the C440A/EAH assay and 20% of the incorporated radioactivity from the HPS/EAH assay were associated with hydroxylated products. This type of information can be used to suggest that the germacrene A reaction product (derived from Y520F) was metabolized at approximately 14% ($9\% \text{ conversion} / 64\% \text{ conversion} \cdot 100$) the efficiency of aristolochene (derived from EAS), while the premnaspirodiene derived from HPS was used 34% ($20\% \text{ conversion} / 64\% \text{ conversion}$) as efficient as *5-epi-aristolochene*.

The results obtained in the coupled assays can also be used to infer new features about the catalytic mechanism of EAH (Scheme 6.2). The EAH enzyme appears to contain a single heme-oxygen binding region based on the predicted amino acid sequence comparison to other well described P450s^{240,251} and, is capable of catalyzing the specific insertion of hydroxyls at the C1 and C3 positions of aristolochene on opposite faces of the sesquiterpene ring structure, yet does not release appreciable amounts of mono-hydroxylated *5-epi-aristolochene* (²⁴¹ and Figs 6.1 & 6.2). These results suggest that initial substrate binding proceeds in a manner to present either C1 or C3 of *5-epi-aristolochene* to the activated heme moiety, followed by the transfer of the hydroxyl group from the heme iron to C1 or C3. Because P450 mediated hydroxylations have demonstrated preference for positions allylic to the carbon-carbon double bonds²³⁸, we speculate that C1 might be the initial position for hydroxylation for *5-epi-aristolochene*. The mono-hydroxylate intermediate must then flip or rotate within the pocket (without intermediate release) to re-position the second site into proper proximity to the heme for the next round of hydroxylation to occur. The current observations that the EAH enzyme is able to hydroxylate the germacrene A and

premnaspirodiene hydrocarbon skeletons provide additional insight into the hydroxylase reaction.

The migration of the metabolized germacrene A product by TLC is consistent with a dihydroxylated germacrene. By reference to the hydroxylation pattern of *5-epi-aristolochene*, we hypothesize that hydroxylation at C2 occurs first since this carbon is allylic to the C1-C10 double bond. Following rotation and a second hydroxylation event, which we speculate occurs at C3, the analogous position as in *5-epi-aristolochene*, a di-hydroxylated form of germacrene is formed and released. This anticipated compound, 2,3-dihydroxygermacrene, was previously isolated from *Datura stramonium*²⁵⁴. Important to note, however, is that the relative hydroxylation efficiency of germacrene A is quite low relative to *5-epi-aristolochene*. While this is somewhat surprising given the overall similarity between these two substrates, the lower efficiency may be related to the more relaxed geometry of germacrene A, which is not as constrained by an internal ring bond as *5-epi-aristolochene*.

In contrast to the *5-epi-aristolochene* and germacrene A reactions, multiple NADPH-dependent reaction products are generated by the action of EAH on the premnaspirodiene skeleton. The parent ions observed in the mass spectra for these clearly indicate mono-hydroxylated forms (m/z 220) and a ketone form (m/z 218)²⁵⁵. The mass spectrum for the former is consistent with that for solavetivol while the latter is essentially identical to solavetivone (NIST library). Hence, we suspect that the conversion of premnaspirodiene to solavetivone might occur along a reaction pathway similar to pathway C shown in Scheme II and that the accumulation of solavetivol represents the release of an intermediate from an incomplete cycle of catalysis. Precedence for the generation of more oxidized functional groups (ketones, aldehydes and acids) within hydrocarbon structures via sequential cycles of catalysis by mixed function oxidases is well established²³⁸. Alternatively, the two reaction products (solavetivol and solavetivone) may arise from separate catalytic mechanisms. For example, EAH may catalyze the initial hydroxylation, while a non-specific yeast oxidase might catalyze the oxidation step. We consider this possibility unlikely since we have never observed ketone or aldehyde derivatives upon incubation of control yeast microsomes with synthetic mono-hydroxylate sesquiterpenes (deoxycapsidiol,²⁴¹).

In either case, rotation of the spirane within the reaction pocket appears to be sterically hindered, which is probably a consequence of the different geometric orientation of the rings and isopropenyl groups within the spirane substrate versus the more planar configuration associated with the 5-*epi*-aristolochene and germacrene A structures.

A final speculation from the current results arises from the observation that the EAH enzyme converts premnaspirodiene to solavetivone, albeit at very low rates. Although the EAH enzyme has specificity for the conversion of eremophilane hydrocarbons to dihydroxylated species, it follows that the *Hyoscyamus muticus* P450 hydroxylase responsible for generating ketone functions in the sesquiterpene vetispiranes might also have residual activity for dihydroxylating eremophilanes. Furthermore, structural and functional comparisons between these two hydroxylases might also reveal features important for mediating these enzymatic specificities, similar to studies performed with limonene hydroxylases¹⁸⁸.

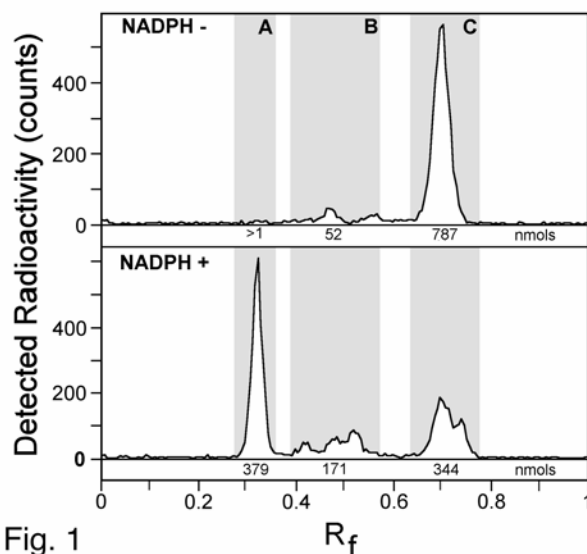


Fig. 1

Figure 6.1 Capsidiol formation in a coupled assay with 5-*epi*-aristolochene synthase and 5-*epi*-aristolochene dihydroxylase.

Capsidiol formation in a coupled assay with 5-*epi*-aristolochene synthase and 5-*epi*-aristolochene dihydroxylase. Purified EAS (1.5 μg) was pre-incubated with ^3H -FPP for 30 min before the addition of microsomes (68 μg microsomal protein) from yeast over-expressing the 5-*epi*-aristolochene dihydroxylase gene. Where indicated, 50 μM NADPH was added together with the microsomes (lower graph). After a further 30 min incubation at room temperature, the reaction products were extracted into ethyl acetate and aliquots of the extracts subjected directly to TLC analysis. Zones A, B and C correlate with the migration of authentic capsidiol (A), farnesol and 3-deoxycapsidiol (B), and 5-*epi*-aristolochene (C).

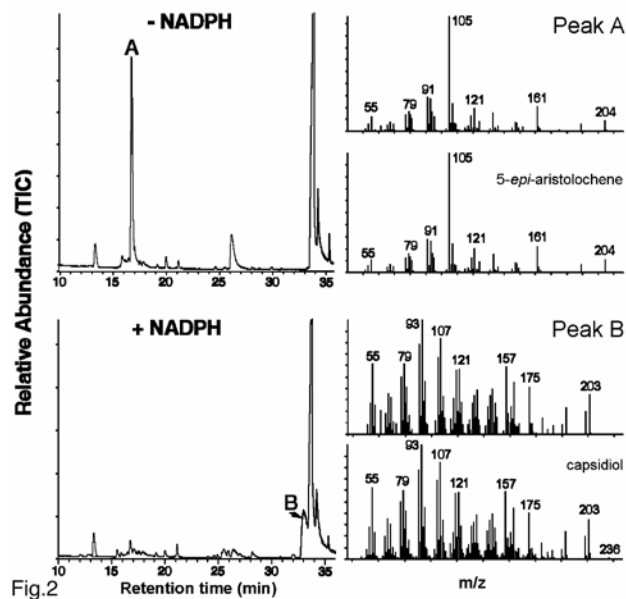


Figure 6.2 Verification of capsidiol as the dominant product of the coupled assay with 5-*epi*-aristolochene synthase and 5-*epi*-aristolochene dihydroxylase.

Verification of capsidiol as the dominant product of the coupled assay with 5-*epi*-aristolochene synthase and 5-*epi*-aristolochene dihydroxylase. Purified EAS (15 μ g protein) was incubated with non-radioactive FPP for 30 min, followed by the addition of microsomes (680 μ g microsomal protein) from yeast over-expressing the EAH gene and a second 30 min incubation. Duplicate assays were performed with one of the reactions being adjusted to 50 μ M NADPH (+NADPH) at the time of microsome addition, while the other received only buffer (-NADPH). Reactions were terminated by ethyl acetate extraction, the extracts concentrated under N_2 , and subjected to GC-MS analysis. The mass spectra for peaks A and B in the chromatograms are shown in the adjacent panels, along with spectra for authentic 5-*epi*-aristolochene and capsidiol.

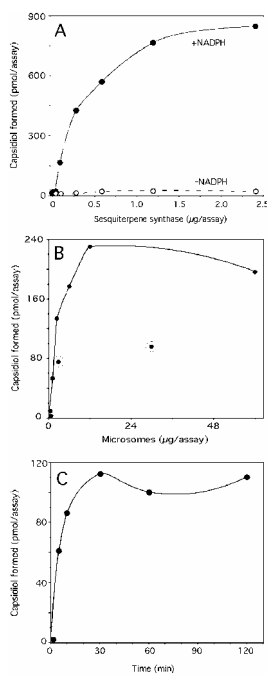


Figure 3

Figure 6.3 Optimization of the EAS/EAH coupled assay.

Optimization of the EAS/EAH coupled assay. Assays were performed with a 30 min incubation of variable amounts of EAS with ^3H -FPP, followed by the addition of microsomes (68 μg microsomal protein) from yeast over-expressing the EAH gene for a second 30 min period (A); incubation of 1.5 μg of EAS with ^3H -FPP for 30 min, followed by the addition of variable amounts of yeast microsomes for a second 30 min period (B); or incubation of 0.375 μg of EAS with ^3H -FPP for 30 min, followed by the addition of yeast microsomes (60 μg of microsomal protein) and the reactions terminated at the indicated time points (C). Reactions were terminated by ethyl acetate extraction and aliquots of the organic extracts separated directly by TLC. The zones of the TLC plate corresponding to the position where authentic capsidiol migrated were scraped and the radioactivity determined by scintillation counting. Except where indicated, NADPH was added to a final concentration of 50 μM at the time of microsome addition.

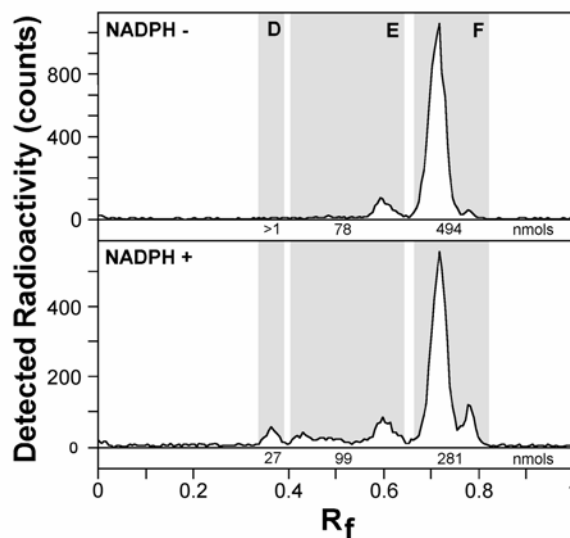


Fig. 4

Figure 6.4 5-*epi*-aristolochene dihydroxylase hydroxylates germacrene A, the sesquiterpene reaction product synthesized by the C440A mutant of EAS.

5-*epi*-aristolochene dihydroxylase hydroxylates germacrene A, the sesquiterpene reaction product synthesized by the C440A mutant of EAS. Purified EAS-C440A mutant synthase (1.5 μ g) was pre-incubated with ^3H -FPP for 30 min before the addition of microsomes (68 μ g microsomal protein) from yeast over-expressing the EAH gene. Where indicated, 50 μ M NADPH was added together with the microsomes (lower graph). After a further 30 min incubation at room temperature, the reaction products were extracted into ethyl acetate and aliquots of the extracts subjected directly to TLC analysis. Zones D, E and F correlate with the migration of authentic capsidiol (D), farnesol and 3-deoxycapsidiol (E), and aristolochene (F).

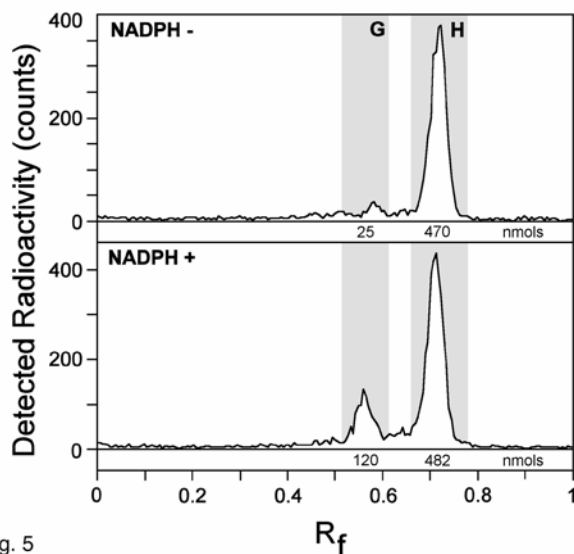


Fig. 5

Figure 6.5 Novel reaction products are formed in a coupled assay with *Hyoscyamus premnaspirodiene synthase (HPS)* and *5-epi-aristolochene dihydroxylase*.

Novel reaction products are formed in a coupled assay with *Hyoscyamus premnaspirodiene synthase (HPS)* and *5-epi-aristolochene dihydroxylase*. Purified HPS (1.5 μg) was pre-incubated with ^3H -FPP for 30 min before the addition of microsomes (68 μg microsomal protein) from yeast over-expressing the EAH gene. Where indicated, 50 μM NADPH was added together with the microsomes (lower graph). After a further 30 min incubation at room temperature, the reaction products were extracted into ethyl acetate and aliquots of the extracts subjected directly to TLC analysis. Zones G and H correlate with the migration of authentic farnesol and 3-deoxycapsidiol (G) and aristolochene (H).

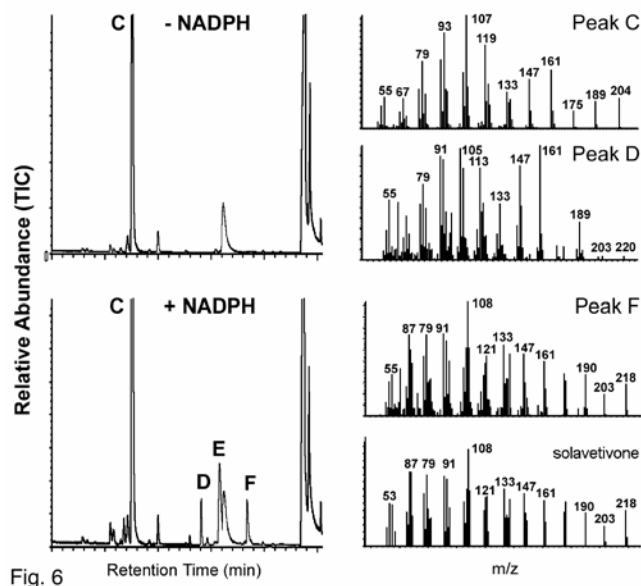
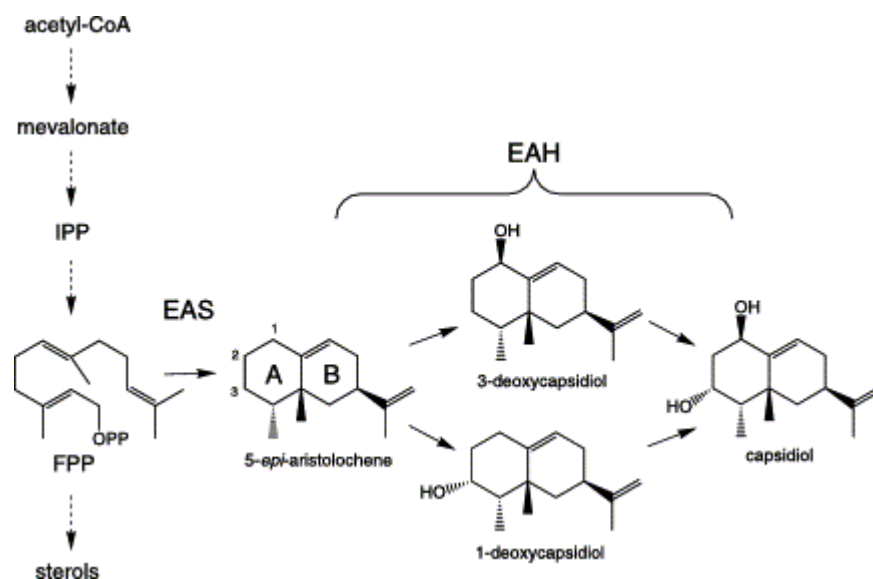


Fig. 6

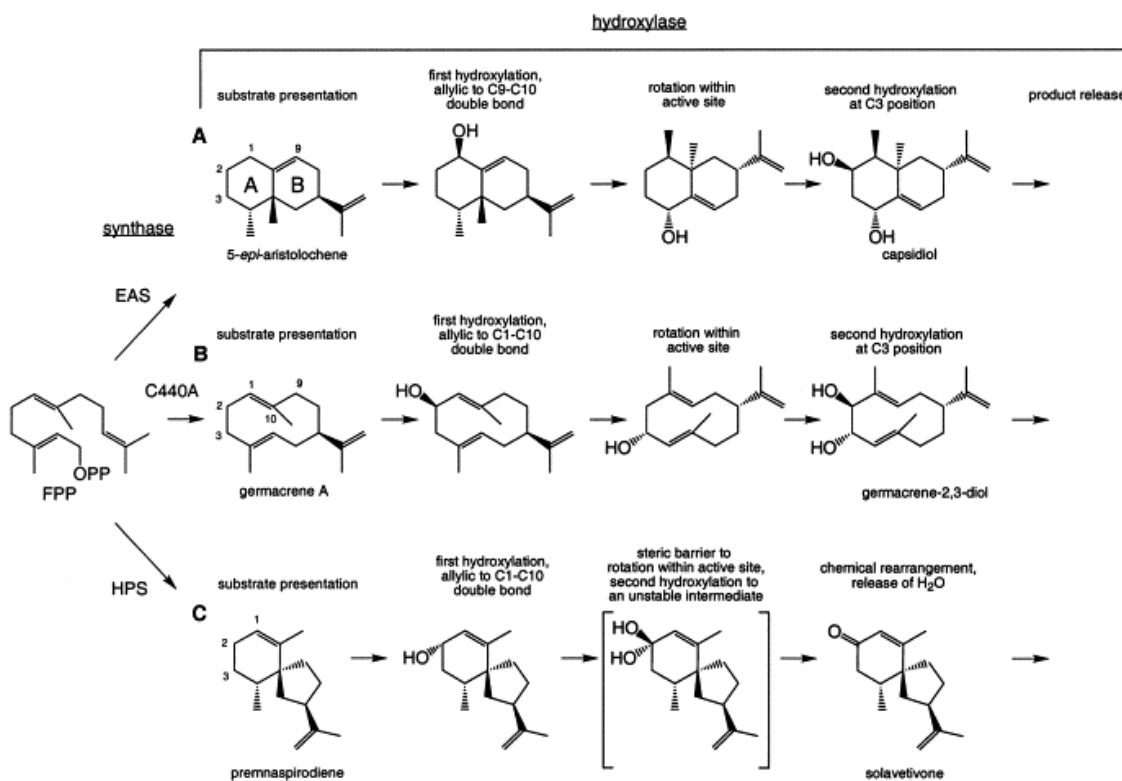
Figure 6.6 GC-MS analysis of the reaction products synthesized in the premnaspirodiene synthase/5-*epi*-aristolochene dihydroxylase coupled assay.

GC-MS analysis of the reaction products synthesized in the premnaspirodiene synthase/5-*epi*-aristolochene dihydroxylase coupled assay. Purified HPS (15 μ g protein) was incubated with non-radioactive FPP for 30 min, followed by the addition of microsomes (680 μ g microsomal protein) from yeast over-expressing the EAH gene and a second 30 min incubation. Duplicate assays were performed with one reaction adjusted to 50 μ M NADPH at the time of microsome addition (+NADPH) while the other reaction received only buffer (-NADPH). Reactions were terminated by ethyl acetate extraction, the extracts concentrated under N_2 , and analyzed by GC-MS. The mass spectra for peaks C, D and F in the chromatograms are shown in the adjacent panels, along with the spectrum for authentic solavetivone (NIST library).



Scheme 6.1 The elicitor-inducible branch pathway for capsidiol biosynthesis in *Nicotiana tabacum* cells consists of two enzymatic steps.

The elicitor-inducible branch pathway for capsidiol biosynthesis in *Nicotiana tabacum* cells consists of two enzymatic steps. 5-*epi*-aristolochene synthase (EAS) catalyzes the initial cyclization reaction of farnesyl diphosphate (FPP)²⁴², while 5-*epi*-aristolochene dihydroxylase (EAH) introduces 2 hydroxyl functions into the cyclized sesquiterpene ring structure in a NADPH-dependent reaction²⁴¹. The induction of this branch pathway has been correlated with a suppression in sterol biosynthesis and interpreted as a diversion of farnesyl diphosphate (FPP) from the central mevalonate biosynthetic pathway towards the biosynthesis of the anti-microbial compound capsidiol^{91,256}.



Scheme 6.2 A chemical and mechanistic rationalizations for product of coupled assays.

A chemical and mechanistic rationalization for the reaction products observed when 5-*epi*-aristolochene dihydroxylase (EAH) is presented with different sesquiterpene substrates biosynthesized by 5-*epi*-aristolochene synthase (EAS) (pathway A), a C440A mutant of EAS (pathway B) and *Hyoscyamus muticus* premnaspirodiene synthase (HPS) (pathway C).

CHAPTER 7 Conclusions and Perspectives

Isoprenoid biochemistry has been replete with interesting puzzles. The origin of cholesterol and related compounds was mysterious until the very simple concept that isoprenoids are made up of polymers of isoprene was introduced. However, the origin of eremophilene, suggested an anomaly to the rule. The recognition that electrophilic chemistry drives catalysis in terpene synthases resolves this problem when an electrophilic methyl migration is invoked. However, the question now turns on how an enzyme actually controls the stereochemical course of a reaction involving highly reactive carbocations.

This thesis has attempted to find some of the answers to the problems concerning the biosynthesis of terpenoids. Substrate specificity of sesquiterpene synthases was shown to be highly dependent on metal ion identities and concentrations. This raises interesting questions as to whether discrimination is exerted *in vivo* mainly by compartmentalization and what is the true substrate *in vivo*, Mn₂-FPP or Mg₂-FPP? It seems possible that nature might make use of the two to three fold improvement in synthetic rates afforded by manganese.

Evidence that TEAS proceeds without isomerization to NPP was provided in this thesis. Because theoretical schemes do not require this, my result is not particularly surprising. However, in considering the enzymology of TEAS, it is important to map and dissect every step in a round of catalysis. Isomerization to NPP seemed a perfectly reasonable step in TEAS catalysis. The suggestion that this does not happen helps interpret kinetic, structural, and mechanistic models, and forms the basis for testable hypotheses for enzymatic control of trans to cis bond isomerization in terpene synthases. Moreover, the assay developed in this work may allow further experiments that test structure-function hypotheses via a combined site-directed mutagenesis – substrate analog strategy which may help reveal the role of amino acid residues that cannot be tested using the fully reactive native substrate.

The TEAS derivatives, 4-epi-eremophilene synthase (TEAS-T402S/V516I), TEAS-C440S and TEAS-C440A, and TEAS-M9 are catalytically robust synthases relative to TEAS, and therefore provide a basis for understanding the enzymology of the sesquiterpene synthases. The change between TEAS and EES is extremely subtle

and has implicated a basis for acid-base chemistry within the catalyzed reaction of terpene synthases that is unprecedented. The implications of C440 roles in both the EES and the native enzyme may be amenable to examination by NMR using a substituted selenocysteine for cysteine to establish the protonation states for the C440 residue. EES also lends itself to other interesting challenges. Can the kinetic constants be improved? Can the specificity for 4-epieremoplilene synthesis be improved? Another interesting aspect is what is the relationship between reaction velocity and product specificity as a function of pH? Equally intriguing, can EES be used in conjunction with the preliminary work from chapter 6 on coupling the terpene synthases with cytochrome P450 enzymes in development of entirely new biosynthetic pathways by using directed evolution to select for the biosynthesis of new antimicrobials?

The TEAS transmutant M9 will continue to stimulate further investigations. First, is the model for product specificity derived from the transmutation project applicable to other product specifications, particularly from other classes of isoprenoids? In a related sense, are all terpenoids derived from Class I terpene synthases specified by the limited region of space in the center of the alpha-barrel structure just behind the active site? Are loops, particularly the JK loop which provides numerous active site residues, ever important for product specificity? HPS does crystallize but does not diffract X-rays well. Hence, resolution of the HPS structure is relatively poor. Perhaps it will be possible to compare the structures of the eremophilane specific active site of EES to TEAS since the surface residues of M9 are the same as TEAS, which should facilitate crystallization and diffraction. The results and model presented in this thesis predict that there will be little if any differences in the active site under crystallization conditions. Studies on the interactions between terpene synthase and cytochrome P450 enzymes will also be facilitated with the M9 mutant, which has identical surface residues to TEAS but product specificity more similar to HPS. The M9 mutant in combination with the TEAS and HPS enzymes should therefore help differentiate and tease out those components of these proteins that mediate their interaction with the P450 enzymes.

Two greater challenges for understanding terpene synthase enzymology emerge from my studies. First, can an enzyme like TEAS be converted into a prenyltransferase by a limited number of mutations? There may even be a low level of prenyltransferase activity, but this has not been tested to my knowledge. Secondly, the amino terminal region for the class I terpene synthases have been dismissed as functionally insignificant. Both stability and protein-protein interactions have been mentioned as possible roles played by this region without any experimental basis. Yet, the N-terminal domain has striking homology to glycosyl hydrolases¹⁰¹. Does this region actually bind sugars? Does it have an independent enzymatic activity? Could a stable terpene synthase be produced without it (akin to the bacterial and fungal terpene synthases which do not bear this domain), and if so, would function normally within a plant cell? Overall, the primary lesson from this thesis is that one assay, one enzyme, and one structure is not enough - and the variations found in nature may serve as an excellent guide to the secrets of isoprenoid diversity.

REFERENCES

1. Szkopinska, A. Ubiquinone. Biosynthesis of quinone ring and its isoprenoid side chain. Intracellular localization. *Acta Biochim Pol* **47**, 469-80 (2000).
2. Kessler, A. & Baldwin, I. T. Defensive Function of Herbivore-Induced Plant Volatile Emissions in Nature. *Science* **291**, 2141-2144 (2001).
3. Dudareva, N. & Pichersky, E. Biochemical and Molecular Genetic Aspects of Floral Scents. *Plant Physiol.* **122**, 627-634 (2000).
4. Bowers, W. S., Webb, R. E., Nault, L. R. & Dutky, S. R. Aphid Alarm Pheromone - Isolation, Identification, Synthesis. *Science* **177**, 1121-& (1972).
5. Bowers, W. S., Nishino, C., Montgomery, M. E., Nault, L. R. & Nielson, M. W. Sesquiterpene progenitor, germacrene A: an alarm pheromone in aphids. *Science* **196**, 680-1 (1977).
6. Milborrow, B. V. The pathway of biosynthesis of abscisic acid in vascular plants: a review of the present state of knowledge of ABA biosynthesis. *J. Exp. Bot.* **52**, 1145-1164 (2001).
7. Astot, C. et al. An alternative cytokinin biosynthesis pathway. *PNAS* **97**, 14778-14783 (2000).
8. Kasahara, H. et al. Contribution of the Mevalonate and Methylerythritol Phosphate Pathways to the Biosynthesis of Gibberellins in Arabidopsis. *J. Biol. Chem.* **277**, 45188-45194 (2002).
9. Creelman, R. A. & Mullet, J. E. Oligosaccharins, Brassinolides, and Jasmonates: Nontraditional Regulators of Plant Growth, Development, and Gene Expression. *Plant Cell* **9**, 1211-1223 (1997).
10. Fujioka, S. & Yokota, T. BIOSYNTHESIS AND METABOLISM OF BRASSINOSTEROIDS. *Annu. Rev. Plant Biol.* **54**, 137-164 (2003).
11. Benveniste, P. Sterol Biosynthesis. *Annual Review of Plant Physiology and Plant Molecular Biology* **37**, 275-308 (1986).
12. Pogson, B. J. & Rissler, H. M. Genetic manipulation of carotenoid biosynthesis and photoprotection. *Philosophical Transactions of the Royal Society of London Series B-Biological Sciences* **355**, 1395-1403 (2000).
13. Carroll, K. K., Guthrie, N. & Ravi, K. Dolichol - Function, Metabolism, and Accumulation in Human Tissues. *Biochemistry and Cell Biology-Biochimie Et Biologie Cellulaire* **70**, 382-384 (1992).
14. Waechter, C. J. & Lennarz, W. J. Role of Polyprenol-Linked Sugars in Glycoprotein Synthesis. *Annual Review of Biochemistry* **45**, 95-112 (1976).
15. Porter, J. W. (ed.) *Biosynthesis of Isoprenoid Compounds* (John Wiley and Sons, New York, 1981).
16. Rodriguez-Concepcion, M. et al. Genetic evidence of branching in the isoprenoid pathway for the production of isopentenyl diphosphate and dimethylallyl diphosphate in Escherichia coli. *FEBS Lett* **473**, 328-32 (2000).
17. Rohmer, M., Seemann, M., Horbach, S., BringerMeyer, S. & Sahn, H. Glyceraldehyde 3-phosphate and pyruvate as precursors of isoprenic units in an alternative non-mevalonate pathway for terpenoid biosynthesis. *Journal of the American Chemical Society* **118**, 2564-2566 (1996).

18. Rohmer, M., Knani, M., Simonin, P., Sutter, B. & Sahn, H. Isoprenoid biosynthesis in bacteria: a novel pathway for the early steps leading to isopentenyl diphosphate. *Biochem J* **295** (Pt 2), 517-24 (1993).
19. Hoeffler, J. F., Hemmerlin, A., Grosdemange-Billiard, C., Bach, T. J. & Rohmer, M. Isoprenoid biosynthesis in higher plants and in *Escherichia coli*: on the branching in the methylerythritol phosphate pathway and the independent biosynthesis of isopentenyl diphosphate and dimethylallyl diphosphate. *Biochem J* **366**, 573-83 (2002).
20. Seemann, M. et al. Isoprenoid biosynthesis through the methylerythritol phosphate pathway: the (E)-4-hydroxy-3-methylbut-2-enyl diphosphate synthase (GcpE) is a [4Fe-4S] protein. *Angew Chem Int Ed Engl* **41**, 4337-9 (2002).
21. Hoeffler, J. F., Tritsch, D., Grosdemange-Billiard, C. & Rohmer, M. Isoprenoid biosynthesis via the methylerythritol phosphate pathway. Mechanistic investigations of the 1-deoxy-D-xylulose 5-phosphate reductoisomerase. *Eur J Biochem* **269**, 4446-57 (2002).
22. Wolff, M. et al. Isoprenoid biosynthesis via the methylerythritol phosphate pathway: the (E)-4-hydroxy-3-methylbut-2-enyl diphosphate reductase (LytB/IspH) from *Escherichia coli* is a [4Fe-4S] protein. *FEBS Lett* **541**, 115-20 (2003).
23. Eisenreich, W. et al. The deoxyxylulose phosphate pathway of terpenoid biosynthesis in plants and microorganisms. *Chem Biol* **5**, R221-33 (1998).
24. Rohdich, F. et al. The deoxyxylulose phosphate pathway of isoprenoid biosynthesis: studies on the mechanisms of the reactions catalyzed by IspG and IspH protein. *Proc Natl Acad Sci U S A* **100**, 1586-91 (2003).
25. Fellermeier, M. et al. Studies on the nonmevalonate pathway of terpene biosynthesis. The role of 2C-methyl-D-erythritol 2,4-cyclodiphosphate in plants. *Eur J Biochem* **268**, 6302-10 (2001).
26. Rohdich, F. et al. Studies on the nonmevalonate terpene biosynthetic pathway: metabolic role of IspH (LytB) protein. *Proc Natl Acad Sci U S A* **99**, 1158-63 (2002).
27. Radykewicz, T. et al. Biosynthesis of terpenoids: 1-deoxy-D-xylulose-5-phosphate reductoisomerase from *Escherichia coli* is a class B dehydrogenase. *FEBS Lett* **465**, 157-60 (2000).
28. Hecht, S. et al. Studies on the nonmevalonate pathway to terpenes: the role of the GcpE (IspG) protein. *Proc Natl Acad Sci U S A* **98**, 14837-42 (2001).
29. Adam, P. et al. Biosynthesis of terpenes: studies on 1-hydroxy-2-methyl-2-(E)-butenyl 4-diphosphate reductase. *Proc Natl Acad Sci U S A* **99**, 12108-13 (2002).
30. Arigoni, D. et al. Terpenoid biosynthesis from 1-deoxy-D-xylulose in higher plants by intramolecular skeletal rearrangement. *Proc Natl Acad Sci U S A* **94**, 10600-5 (1997).
31. Lichtenthaler, H. K., Rohmer, M. & Schwender, J. Two independent biochemical pathways for isopentenyl diphosphate and isoprenoid biosynthesis in higher plants. *Physiologia Plantarum* **101**, 643-652 (1997).
32. Disch, A., Schwender, J., Muller, C., Lichtenthaler, H. K. & Rohmer, M. Distribution of the mevalonate and glyceraldehyde phosphate/pyruvate

- pathways for isoprenoid biosynthesis in unicellular algae and the cyanobacterium *Synechocystis* PCC 6714. *Biochemical Journal* **333**, 381-388 (1998).
33. Lichtenthaler, H. K., Schwender, J., Disch, A. & Rohmer, M. Biosynthesis of isoprenoids in higher plant chloroplasts proceeds via a mevalonate-independent pathway. *Febs Letters* **400**, 271-274 (1997).
 34. Lichtenthaler, H. K., Schwender, J., Seemann, M. & Rohmer, M. Biosynthesis of carotenoids and other isoprenoids via a non-mevalonate pathway in *Scenedesmus obliquus*. *Plant Physiology* **111**, 588-588 (1996).
 35. Schwender, J., Seemann, M., Lichtenthaler, H. K. & Rohmer, M. Biosynthesis of isoprenoids (carotenoids, sterols, prenyl side-chains of chlorophylls and plastoquinone) via a novel pyruvate/glyceraldehyde 3-phosphate non-mevalonate pathway in the green alga *Scenedesmus obliquus*. *Biochemical Journal* **316**, 73-80 (1996).
 36. Rohmer, M. The discovery of a mevalonate-independent pathway for isoprenoid biosynthesis in bacteria, algae and higher plants. *Nat Prod Rep* **16**, 565-74 (1999).
 37. Lichtenthaler, H. K. THE 1-DEOXY-D-XYLULOSE-5-PHOSPHATE PATHWAY OF ISOPRENOID BIOSYNTHESIS IN PLANTS. *standard.dtl Annu. Rev. Plant Physiol. Plant Mol. Biol.* **50**, 47-65 (1999).
 38. Rodriguez-Concepcion, M. & Boronat, A. Elucidation of the Methylerythritol Phosphate Pathway for Isoprenoid Biosynthesis in Bacteria and Plastids. A Metabolic Milestone Achieved through Genomics. *Plant Physiol.* **130**, 1079-1089 (2002).
 39. Guterman, I. et al. Rose Scent: Genomics Approach to Discovering Novel Floral Fragrance-Related Genes. *Plant Cell* **14**, 2325-2338 (2002).
 40. Chappell, J., Nable, R., Fleming, P., Andersen, R. A. & Burton, H. R. Accumulation of Capsidiol in Tobacco Cell-Cultures Treated with Fungal Elicitor. *Phytochemistry* **26**, 2259-2260 (1987).
 41. Zook, M. & Kuc, J. Elicitation of Sesquiterpenoid Stress Metabolites in Potato-Tuber Slices by *Helminthosporium-Carbonum*. *Phytopathology* **74**, 849-849 (1984).
 42. Zook, M. N. & Kuc, J. A. Induction of Sesquiterpene Cyclase and Suppression of Squalene Synthetase-Activity in Elicitor-Treated or Fungal-Infected Potato-Tuber Tissue. *Physiological and Molecular Plant Pathology* **39**, 377-390 (1991).
 43. Zook, M. N., Chappell, J. & Kuc, J. A. Characterization of Elicitor-Induction of Sesquiterpene Cyclase Activity in Potato-Tuber Tissue. *Phytochemistry* **31**, 3441-3445 (1992).
 44. Shaw, P. E. & Wilson, C. W. Importance of Nootkatone to the Aroma of Grapefruit Oil and the Flavor of Grapefruit Juice. *Journal of Agricultural and Food Chemistry* **29**, 677-679 (1981).
 45. Berry, R. E., Wagner, C. J. & Moshonas, M. G. Flavor Studies of Nootkatone in Grapefruit Juice. *Journal of Food Science* **32**, 75-& (1967).
 46. Macleod, W. D. & Buigues, N. M. Sesquiterpenes .1. Nootkatone New Grapefruit Flavor Constituent. *Journal of Food Science* **29**, 565-& (1964).

47. Klayman, D. L. Qinghaosu (artemisinin): an antimalarial drug from China. *Science* **228**, 1049-55 (1985).
48. Neukirch, H., Kaneider, N. C., Wiedermann, C. J., Guerriero, A. & D'Ambrosio, M. Parthenolide and its photochemically synthesized 1(10)Z isomer: chemical reactivity and structure-activity relationship studies in human leucocyte chemotaxis. *Bioorg Med Chem* **11**, 1503-10 (2003).
49. Li-Weber, M., Giaisi, M., Treiber, M. K. & Krammer, P. H. The anti-inflammatory sesquiterpene lactone parthenolide suppresses IL-4 gene expression in peripheral blood T. *Eur J Immunol* **32**, 3587-97 (2002).
50. Beranek, J. T. Sesquiterpene lactone parthenolide, an inhibitor of IkappaB kinase complex and nuclear factor-kappaB, exerts beneficial effects in myocardial reperfusion injury. *Shock* **17**(2):127-134, 2002. *Shock* **19**, 191-2; author reply 192 (2003).
51. Fiebich, B. L., Lieb, K., Engels, S. & Heinrich, M. Inhibition of LPS-induced p42/44 MAP kinase activation and iNOS/NO synthesis by parthenolide in rat primary microglial cells. *J Neuroimmunol* **132**, 18-24 (2002).
52. Li-Weber, M., Giaisi, M., Baumann, S., Treiber, M. K. & Krammer, P. H. The anti-inflammatory sesquiterpene lactone parthenolide suppresses CD95-mediated activation-induced-cell-death in T-cells. *Cell Death Differ* **9**, 1256-65 (2002).
53. Uchi, H., Arrighi, J. F., Aubry, J. P., Furue, M. & Hauser, C. The sesquiterpene lactone parthenolide inhibits LPS- but not TNF-alpha-induced maturation of human monocyte-derived dendritic cells by inhibition of the p38 mitogen-activated protein kinase pathway. *J Allergy Clin Immunol* **110**, 269-76 (2002).
54. Wen, J., You, K. R., Lee, S. Y., Song, C. H. & Kim, D. G. Oxidative stress-mediated apoptosis. The anticancer effect of the sesquiterpene lactone parthenolide. *J Biol Chem* **277**, 38954-64 (2002).
55. Kang, S. N. et al. Enhancement of 1 alpha,25-dihydroxyvitamin D(3)-induced differentiation of human leukaemia HL-60 cells into monocytes by parthenolide via inhibition of NF-kappa B activity. *Br J Pharmacol* **135**, 1235-44 (2002).
56. Zingarelli, B., Hake, P. W., Denenberg, A. & Wong, H. R. Sesquiterpene lactone parthenolide, an inhibitor of IkappaB kinase complex and nuclear factor-kappaB, exerts beneficial effects in myocardial reperfusion injury. *Shock* **17**, 127-34 (2002).
57. Mitra, S., Datta, A., Singh, S. K. & Singh, A. 5-Hydroxytryptamine-inhibiting property of Feverfew: role of parthenolide content. *Acta Pharmacol Sin* **21**, 1106-14 (2000).
58. Kwok, B. H., Koh, B., Ndubuisi, M. I., Elofsson, M. & Crews, C. M. The anti-inflammatory natural product parthenolide from the medicinal herb Feverfew directly binds to and inhibits IkappaB kinase. *Chem Biol* **8**, 759-66 (2001).
59. Kang, B. Y., Chung, S. W. & Kim, T. S. Inhibition of interleukin-12 production in lipopolysaccharide-activated mouse macrophages by parthenolide, a predominant sesquiterpene lactone in Tanacetum parthenium: involvement of nuclear factor-kappaB. *Immunol Lett* **77**, 159-63 (2001).

60. Patel, N. M. et al. Paclitaxel sensitivity of breast cancer cells with constitutively active NF-kappaB is enhanced by IkappaBalpha super-repressor and parthenolide. *Oncogene* **19**, 4159-69 (2000).
61. Fukuda, K. et al. Inhibition by parthenolide of phorbol ester-induced transcriptional activation of inducible nitric oxide synthase gene in a human monocyte cell line THP-1. *Biochem Pharmacol* **60**, 595-600 (2000).
62. Hehner, S. P., Hofmann, T. G., Droge, W. & Schmitz, M. L. The antiinflammatory sesquiterpene lactone parthenolide inhibits NF-kappa B by targeting the I kappa B kinase complex. *J Immunol* **163**, 5617-23 (1999).
63. Tournier, H. et al. Effect of the chloroform extract of *Tanacetum vulgare* and one of its active principles, parthenolide, on experimental gastric ulcer in rats. *J Pharm Pharmacol* **51**, 215-9 (1999).
64. Ross, J. J., Arnason, J. T. & Birnboim, H. C. Low concentrations of the feverfew component parthenolide inhibit in vitro growth of tumor lines in a cytostatic fashion. *Planta Med* **65**, 126-9 (1999).
65. Groenewegen, W. A. & Heptinstall, S. A comparison of the effects of an extract of feverfew and parthenolide, a component of feverfew, on human platelet activity in-vitro. *J Pharm Pharmacol* **42**, 553-7 (1990).
66. Fraga, B. M. Natural sesquiterpenoids. *Natural Product Reports* **19**, 650-672 (2002).
67. Fraga, B. N. Natural sesquiterpenoids. *Natural Product Reports* **18**, 650-673 (2001).
68. Fraga, B. M. Natural sesquiterpenoids. *Natural Product Reports* **17**, 483-504 (2000).
69. Fraga, B. M. Natural sesquiterpenoids. *Natural Product Reports* **16**, 711-730 (1999).
70. Fraga, B. M. Natural sesquiterpenoids. *Natural Product Reports* **16**, 21-38 (1999).
71. Fraga, B. M. Natural sesquiterpenoids. *Natural Product Reports* **15**, 73-92 (1998).
72. Fraga, B. M. Natural sesquiterpenoids. *Natural Product Reports* **14**, 145-162 (1997).
73. Fraga, B. M. Natural sesquiterpenoids. *Natural Product Reports* **13**, 307-326 (1996).
74. Fraga, B. M. Natural Sesquiterpenoids. *Natural Product Reports* **12**, 303-320 (1995).
75. Fraga, B. M. Natural Sesquiterpenoids. *Natural Product Reports* **11**, 533-554 (1994).
76. Dudareva, N., Cseke, L., Blanc, V. M. & Pichersky, E. Evolution of floral scent in *Clarkia*: novel patterns of S-linalool synthase gene expression in the *C. breweri* flower. *Plant Cell* **8**, 1137-48 (1996).
77. Ralston, L. et al. Cloning, heterologous expression, and functional characterization of 5-epi-aristolochene-1,3-dihydroxylase from tobacco (*Nicotiana tabacum*). *Arch Biochem Biophys* **393**, 222-35 (2001).
78. Lupien, S., Karp, F., Wildung, M. & Croteau, R. Regiospecific cytochrome P450 limonene hydroxylases from mint (*Mentha*) species: cDNA isolation,

- characterization, and functional expression of (-)-4S-limonene-3-hydroxylase and (-)-4S-limonene-6-hydroxylase. *Arch Biochem Biophys* **368**, 181-92 (1999).
79. Helliwell, C. A., Poole, A., Peacock, W. J. & Dennis, E. S. Arabidopsis entkaurene oxidase catalyzes three steps of gibberellin biosynthesis. *Plant Physiology* **119**, 507-510 (1999).
 80. Podust, L. M., Stojan, J., Poulos, T. L. & Waterman, M. R. Substrate recognition sites in 14 alpha-sterol demethylase from comparative analysis of amino acid sequences and X-ray structure of Mycobacterium tuberculosis CYP51. *Journal of Inorganic Biochemistry* **87**, 227-235 (2001).
 81. Polzin, J. P. & Rorrer, G. L. Halogenated monoterpene production by microplantlets of the marine red alga *Ochtodes secundiramea* within an airlift photobioreactor under nutrient medium perfusion. *Biotechnology and Bioengineering* **82**, 415-428 (2003).
 82. Crews, P. Monoterpene Halogenation by Red Alga *Plocamium-Oregonum*. *Journal of Organic Chemistry* **42**, 2634-2636 (1977).
 83. Argandona, V. H. et al. Antifeedant effects of marine halogenated monoterpenes. *Journal of Agricultural and Food Chemistry* **50**, 7029-7033 (2002).
 84. Steele, C. L., Katoh, S., Bohlmann, J. & Croteau, R. Regulation of oleoresinosis in grand fir (*Abies grandis*). Differential transcriptional control of monoterpene, sesquiterpene, and diterpene synthase genes in response to wounding. *Plant Physiol* **116**, 1497-504 (1998).
 85. Funk, C., Lewinsohn, E., Vogel, B. S., Steele, C. L. & Croteau, R. Regulation of Oleoresinosis in Grand Fir (*Abies grandis*) (Coordinate Induction of Monoterpene and Diterpene Cyclases and Two Cytochrome P450-Dependent Diterpenoid Hydroxylases by Stem Wounding). *Plant Physiol* **106**, 999-1005 (1994).
 86. Turner, G. W., Gershenzon, J. & Croteau, R. B. Development of Peltate Glandular Trichomes of Peppermint. *Plant Physiol*. **124**, 665-680 (2000).
 87. Guo, Z. H. & Wagner, G. J. Biosynthesis of Labdenediol and Sclareol in Cell-Free-Extracts from Trichomes of *Nicotiana-Glutinosa*. *Planta* **197**, 627-632 (1995).
 88. Wagner, M. R., Benjamin, D. M., Clancy, K. M. & Schuh, B. A. Influence of Diterpene Resin Acids on Feeding and Growth of Larch Sawfly, *Pristiphora-Erichsonii* (Hartig). *Journal of Chemical Ecology* **9**, 119-127 (1983).
 89. Altman, D. W., Stipanovic, R. D. & Bell, A. A. Terpenoids in Foliar Pigment Glands of a, D, and Ad Genome Cottons - Introgression Potential for Pest Resistance. *Journal of Heredity* **81**, 447-454 (1990).
 90. Vogeli, U. & Chappell, J. Regulation of a Sesquiterpene Cyclase in Cellulase-Treated Tobacco Cell-Suspension Cultures. *Plant Physiology* **94**, 1860-1866 (1990).
 91. Threlfall, D. R. & Whitehead, I. M. Coordinated Inhibition of Squalene Synthetase and Induction of Enzymes of Sesquiterpenoid Phytoalexin Biosynthesis in Cultures of *Nicotiana-Tabacum*. *Phytochemistry* **27**, 2567-2580 (1988).

92. Devarenne, T. P., Ghosh, A. & Chappell, J. Regulation of squalene synthase, a key enzyme of sterol biosynthesis, in tobacco. *Plant Physiol* **129**, 1095-1106 (2002).
93. Yin, S., Mei, L., Newman, J., Back, K. & Chappell, J. Regulation of sesquiterpene cyclase gene expression. Characterization of an elicitor- and pathogen-inducible promoter. *Plant Physiol* **115**, 437-51 (1997).
94. Wendt, K. U., Schulz, G. E., Corey, E. J. & Liu, D. R. Enzyme Mechanisms for Polycyclic Triterpene Formation. *Angew Chem Int Ed Engl* **39**, 2812-2833 (2000).
95. Cane, D. E. Enzymatic Formation of Sesquiterpenes. *Chemical Reviews* **90**, 1089-1103 (1990).
96. Greenhagen, B. & Chappell, J. Molecular scaffolds for chemical wizardry: learning nature's rules for terpene cyclases. *Proc Natl Acad Sci U S A* **98**, 13479-81 (2001).
97. Croteau, R. Biosynthesis and catabolism of monoterpenoids. *Chemical Reviews* **87**, 929-954 (1987).
98. Davis, E. M. & Croteau, R. Cyclization enzymes in the biosynthesis of monoterpenes, sesquiterpenes, and diterpenes. *Biosynthesis: Aromatic Polyketides, Isoprenoids, Alkaloids* **209**, 53-95 (2000).
99. Abe, I., Rohmer, M. & Prestwich, G. D. Enzymatic Cyclization of Squalene and Oxidosqualene to Sterols and Triterpenes. *Chemical Reviews* **93**, 2189-2206 (1993).
100. Corey, E., Matsuda, S. & Bartel, B. Isolation of an Arabidopsis thaliana Gene Encoding Cycloartenol Synthase by Functional Expression in a Yeast Mutant Lacking Lanosterol Synthase by the Use of a Chromatographic Screen. *PNAS* **90**, 11628-11632 (1993).
101. Starks, C. M., Back, K., Chappell, J. & Noel, J. P. Structural basis for cyclic terpene biosynthesis by tobacco 5-epi-aristolochene synthase. *Science* **277**, 1815-20 (1997).
102. Lesburg, C. A., Zhai, G., Cane, D. E. & Christianson, D. W. Crystal structure of pentalenene synthase: mechanistic insights on terpenoid cyclization reactions in biology. *Science* **277**, 1820-4 (1997).
103. Tarshis, L. C., Yan, M., Poulter, C. D. & Sacchettini, J. C. Crystal structure of recombinant farnesyl diphosphate synthase at 2.6-Å resolution. *Biochemistry* **33**, 10871-7 (1994).
104. Wendt, K. U., Poralla, K. & Schulz, G. E. Structure and function of a squalene cyclase. *Science* **277**, 1811-5 (1997).
105. Wendt, K. U., Lenhart, A. & Schulz, G. E. The structure of the membrane protein squalene-hopene cyclase at 2.0 Å resolution. *J Mol Biol* **286**, 175-87 (1999).
106. Caruthers, J. M., Kang, I., Rynkiewicz, M. J., Cane, D. E. & Christianson, D. W. Crystal Structure Determination of Aristolochene Synthase from the Blue Cheese Mold, *Penicillium roqueforti**. *J. Biol. Chem.* **275**, 25533-25539 (2000).
107. Rynkiewicz, M. J., Cane, D. E. & Christianson, D. W. Structure of trichodiene synthase from *Fusarium sporotrichioides* provides mechanistic inferences on the

- terpene cyclization cascade. *Proceedings of the National Academy of Sciences of the United States of America* **98**, 13543-13548 (2001).
108. Rynkiewicz, M. J., Cane, D. E. & Christianson, D. W. X-ray crystal structures of D100E trichodiene synthase and its pyrophosphate complex reveal the basis for terpene product diversity. *Biochemistry* **41**, 1732-1741 (2002).
 109. Whittington, D. A. et al. Bornyl diphosphate synthase: Structure and strategy for carbocation manipulation by a terpenoid cyclase. *PNAS* **99**, 15375-15380 (2002).
 110. Pandit, J. et al. Crystal Structure of Human Squalene Synthase. A KEY ENZYME IN CHOLESTEROL BIOSYNTHESIS *J. Biol. Chem.* **275**, 30610-30617 (2000).
 111. Rao, C. B., Raju, G. V. S. & Krishna, P. G. Chemical Examination of Premna Species .8. Spirosesquiterpenes from Premna-Latifolia Roxb and Var Cuneata. *Indian Journal of Chemistry Section B-Organic Chemistry Including Medicinal Chemistry* **21**, 267-268 (1982).
 112. Vogeli, U., Freeman, J. W. & Chappell, J. Purification and Characterization of an Inducible Sesquiterpene Cyclase from Elicitor-Treated Tobacco Cell-Suspension Cultures. *Plant Physiology* **93**, 182-187 (1990).
 113. Back, K., Yin, S. & Chappell, J. Expression of a plant sesquiterpene cyclase gene in Escherichia coli. *Arch Biochem Biophys* **315**, 527-32 (1994).
 114. Whitehead, I. M., Threlfall, D. R. & Ewing, D. F. 5-epi-aristolochene is a common precursor of the sesquiterpenoid phytoalexins capsidiol and debneyol. *Phytochemistry* **28**, 775-779 (1989).
 115. Back, K. & Chappell, J. Identifying functional domains within terpene cyclases using a domain-swapping strategy. *Proc Natl Acad Sci U S A* **93**, 6841-5 (1996).
 116. Hohn, T. M. & Plattner, R. D. Purification and characterization of the sesquiterpene cyclase aristolochene synthase from Penicillium roqueforti. *Arch Biochem Biophys* **272**, 137-43 (1989).
 117. Dehal, S. S. & Croteau, R. Partial purification and characterization of two sesquiterpene cyclases from sage (Salvia officinalis) which catalyze the respective conversion of farnesyl pyrophosphate to humulene and caryophyllene. *Arch Biochem Biophys* **261**, 346-56 (1988).
 118. Cane, D. E. & Pargellis, C. Partial purification and characterization of pentalenene synthase. *Arch Biochem Biophys* **254**, 421-9 (1987).
 119. Hohn, T. M. & VanMiddlesworth, F. Purification and characterization of the sesquiterpene cyclase trichodiene synthetase from Fusarium sporotrichodes. *Arch Biochem Biophys* **251**, 756-61 (1986).
 120. Lewinsohn, E., Gijzen, M. & Croteau, R. Wound-inducible pinene cyclase from grand fir: purification, characterization, and renaturation after SDS-PAGE. *Arch Biochem Biophys* **293**, 167-73 (1992).
 121. Savage, T. J., Hatch, M. W. & Croteau, R. Monoterpene synthases of Pinus contorta and related conifers. A new class of terpenoid cyclase. *J Biol Chem* **269**, 4012-20 (1994).
 122. Bohlmann, J., Steele, C. L. & Croteau, R. Monoterpene synthases from grand fir (Abies grandis). cDNA isolation, characterization, and functional expression of

- myrcene synthase, (-)-(4S)-limonene synthase, and (-)-(1S,5S)-pinene synthase. *J Biol Chem* **272**, 21784-92 (1997).
123. Chappell, J.
 124. Rupasinghe, H. P. V., Paliyath, G. & Murr, D. P. Sesquiterpene alpha-farnesene synthase: Partial purification, characterization, and activity in relation to superficial scald development in apples. *Journal of the American Society for Horticultural Science* **125**, 111-119 (2000).
 125. Wang, J., Evangelou, B. P., Nielsen, M. T. & Wagner, G. J. Computer, Simulated Evaluation of Possible Mechanisms for Sequestering Metal-Ion Activity in Plant Vacuoles .2. Zinc. *Plant Physiology* **99**, 621-626 (1992).
 126. Wang, J., Evangelou, B. P., Nielsen, M. T. & Wagner, G. J. Computer-Simulated Evaluation of Possible Mechanisms for Quenching Heavy-Metal Ion Activity in Plant Vacuoles. *Plant Physiology* **97**, 1154-1160 (1991).
 127. Krotz, R. M., Evangelou, B. P. & Wagner, G. J. Relationships between Cadmium, Zinc, Cd-Peptide, and Organic- Acid in Tobacco Suspension Cells. *Plant Physiology* **91**, 780-787 (1989).
 128. Lin, W., Wagner, G. J., Siegelman, H. W. & Hind, G. Membrane-bound ATPase of intact vacuoles and tonoplasts isolated from mature plant tissue. *Biochimica et Biophysica Acta (BBA) - Biomembranes* **465**, 110-117 (1977).
 129. Whittington, D. A. et al. Bornyl diphosphate synthase: Structure and strategy for carbocation manipulation by a terpenoid cyclase. *Proc Natl Acad Sci U S A* **99**, 15375-15380 (2002).
 130. King, H. L. & Rilling, H. C. Avian Liver Prenyltransferase - Role of Metal in Substrate Binding and Orientation of Substrates During Catalysis. *Biochemistry* **16**, 3815-3819 (1977).
 131. Brenner, S. Phosphotransferase sequence homology. *Nature* **329**, 21 (1987).
 132. Ashby, M. & Edwards, P. Elucidation of the deficiency in two yeast coenzyme Q mutants. Characterization of the structural gene encoding hexaprenyl pyrophosphate synthetase. *J. Biol. Chem.* **265**, 13157-13164 (1990).
 133. Ashby, M., Kutsunai, S., Ackerman, S., Tzagoloff, A. & Edwards, P. COQ2 is a candidate for the structural gene encoding para-hydroxybenzoate:polyprenyltransferase. *J. Biol. Chem.* **267**, 4128-4136 (1992).
 134. Proctor, R. H. & Hohn, T. M. Aristolochene synthase. Isolation, characterization, and bacterial expression of a sesquiterpenoid biosynthetic gene (Ari1) from *Penicillium roqueforti*. *J Biol Chem* **268**, 4543-8 (1993).
 135. Cane, D. E. & Watt, R. M. Expression and mechanistic analysis of a germacradienol synthase from *Streptomyces coelicolor* implicated in geosmin biosynthesis. *PNAS* **100**, 1547-1551 (2003).
 136. Cane, D. E. & Xue, Q. Trichodiene synthase. Enzymatic formation of multiple sesquiterpenes by alteration of the cyclase active site. *Journal of the American Chemical Society* **118**, 1563-1564 (1996).
 137. Little, D. B. & Croteau, R. B. Alteration of product formation by directed mutagenesis and truncation of the multiple-product sesquiterpene synthases delta-selinene synthase and gamma-humulene synthase. *Arch Biochem Biophys* **402**, 120-35 (2002).

138. Seemann, M. et al. Pentalenene synthase. Analysis of active site residues by site-directed mutagenesis. *Journal of the American Chemical Society* **124**, 7681-7689 (2002).
139. Cane, D. E., Xue, Q. & Fitzsimons, B. C. Trichodiene synthase. Probing the role of the highly conserved aspartate-rich region by site-directed mutagenesis. *Biochemistry* **35**, 12369-12376 (1996).
140. Cane, D. E., Xue, Q. & VanEpp, J. E. Enzymatic formation of isochamigrene, a novel sesquiterpene, by alteration of the aspartate-rich region of trichodiene synthase. *Journal of the American Chemical Society* **118**, 8499-8500 (1996).
141. Davisson, V. J., Neal, T. R. & Poulter, C. D. Farnesylpyrophosphate Synthetase - a Case for Common Electrophilic Mechanisms for Prenyltransferases and Terpene Cyclases. *Journal of the American Chemical Society* **107**, 5277-5279 (1985).
142. Saito, A. & Rilling, H. C. The Formation of Cyclic Sesquiterpenes from Farnesyl Pyrophosphate by Prenyltransferase. *Archives of Biochemistry and Biophysics* **208**, 508-511 (1981).
143. Davisson, V. J., Neal, T. R. & Poulter, C. D. Farnesyl-Diphosphate Synthase - Catalysis of an Intramolecular Prenyl Transfer with Bisubstrate Analogs. *Journal of the American Chemical Society* **115**, 1235-1245 (1993).
144. Poulter, C. D., Argyle, J. C. & Mash, E. A. Letter: Prenyltransferase. New evidence for an ionization-condensation-elimination mechanism with 2-fluorogeranyl pyrophosphate. *J Am Chem Soc* **99**, 957-9 (1977).
145. Poulter, C. D., Wiggins, P. L. & Le, A. T. Farnesylpyrophosphate Synthetase - a Stepwise Mechanism for the 1'-4 Condensation Reaction. *Journal of the American Chemical Society* **103**, 3926-3927 (1981).
146. Poulter, C. D., Satterwhite, D. M. & Rilling, H. C. Letter: Prenyltransferase. The mechanism of the reaction. *J Am Chem Soc* **98**, 3376-7 (1976).
147. Mash, E. A., Gurria, G. M. & Poulter, C. D. Farnesylpyrophosphate Synthetase - Evidence for a Rigid Geranyl Cation-Pyrophosphate Anion Pair. *Journal of the American Chemical Society* **103**, 3927-3929 (1981).
148. Croteau, R. Evidence for the ionization steps in monoterpene cyclization reactions using 2-fluorogeranyl and 2-fluorolinalyl pyrophosphates as substrates. *Arch Biochem Biophys* **251**, 777-82 (1986).
149. Brems, D. N. & Rilling, H. C. On the mechanism of the prenyltransferase reaction. Metal ion dependent solvolysis of an allylic pyrophosphate. *Journal of the American Chemical Society* **99**, 8351-8352 (1977).
150. Rittersdorf, W. & Cramer, F. Cyclization of Nerol and Linalool on Solvolysis of Their Phosphate Esters. *Tetrahedron* **24**, 43-& (1968).
151. Allinger, N. L. & Siefert, J. H. Organic Quantum Chemistry .33. Electronic-Spectra and Rotational Barriers of Vinylborane, Allyl Cation, and Related Compounds. *Journal of the American Chemical Society* **97**, 752-760 (1975).
152. Cane, D. E., Pawlak, J. L., Horak, R. M. & Hohn, T. M. Studies of the Cryptic Allylic Pyrophosphate Isomerase Activity of Trichodiene Synthase Using the Anomalous Substrate 6,7-Dihydrofarnesyl Pyrophosphate. *Biochemistry* **29**, 5476-5490 (1990).

153. Cane, D. E. & Ha, H. J. Trichodiene Biosynthesis and the Role of Nerolidyl Pyrophosphate in the Enzymatic Cyclization of Farnesyl Pyrophosphate. *Journal of the American Chemical Society* **110**, 6865-6870 (1988).
154. Cane, D. E. & Ha, H. J. Trichodiene Biosynthesis and the Enzymatic Cyclization of Nerolidyl Pyrophosphate. *Journal of the American Chemical Society* **108**, 3097-3099 (1986).
155. Cane, D. E., Chiu, H. T., Liang, P. H. & Anderson, K. S. Pre-steady-state kinetic analysis of the trichodiene synthase reaction pathway. *Biochemistry* **36**, 8332-8339 (1997).
156. Benedict, C. R. et al. The cyclization of farnesyl diphosphate and nerolidyl diphosphate by a purified recombinant delta-cadinene synthase. *Plant Physiol* **125**, 1754-65 (2001).
157. Jenson, C. & Jorgensen, W. L. Computational investigations of carbenium ion reactions relevant to sterol biosynthesis. *Journal of the American Chemical Society* **119**, 10846-10854 (1997).
158. Ma, J. C. & Dougherty, D. A. The Cation-pi Interaction. *Chem Rev* **97**, 1303-1324 (1997).
159. Dougherty, D. A. & Stauffer, D. A. Acetylcholine binding by a synthetic receptor: implications for biological recognition. *Science* **250**, 1558-60 (1990).
160. Rising, K. A., Starks, C. M., Noel, J. P. & Chappell, J. Demonstration of germacrene A as an intermediate in 5-epi-aristolochene synthase catalysis. *Journal of the American Chemical Society* **122**, 1861-1866 (2000).
161. Weinheim.Aj, Youngblo.Ww, Washeche.Ph, Karns, T. K. B. & Ciereszk.Ls. Isolation of Elusive (-)-Germacrene-a from Gorgonian, Eunicaea-Mammosa Chemistry of Colelenterates .18. *Tetrahedron Letters*, 497-& (1970).
162. Takeda, K. Stereospecific Cope Rearrangement of Germacrene-Type Sesquiterpenes. *Tetrahedron* **30**, 1525-1534 (1974).
163. Nishimura, H., Hasegawa, H., Seo, A., Nakano, H. & Mizutani, J. Acid-Catalyzed Stereoselective Cyclization of Germacrene-D. *Agricultural and Biological Chemistry* **43**, 2397-2398 (1979).
164. Itokawa, H., Matsumoto, H., Nagamine, S., Totsuka, N. & Watanabe, K. Sulfuric Acid-Catalyzed Cyclization of Germacrene-D to Eudesmane-4,6-Diol Cyclic Sulfate. *Chemical & Pharmaceutical Bulletin* **36**, 3161-3163 (1988).
165. Bulow, N. & Konig, W. A. The role of germacrene D as a precursor in sesquiterpene biosynthesis: investigations of acid catalyzed, photochemically and thermally induced rearrangements. *Phytochemistry* **55**, 141-168 (2000).
166. Huang, H. & Forsyth, C. J. Anti Selective Spirocarbomercuration - Synthesis and Stereochemistry of the Spirobicyclic Sesquiterpenes Spirojatamol and Erythrodiene. *Journal of Organic Chemistry* **60**, 2773-2779 (1995).
167. Baker, F. C. & Brooks, C. J. W. Biosynthesis of the sesquiterpenoid, capsidiol, in sweet pepper fruits inoculated with fungal spores. *Phytochemistry* **15**, 689-694 (1976).
168. Baker, F. C., Brooks, C. J. W. & Hutchinson, S. A. Biosynthesis of Capsidiol in Sweet Peppers (*Capsicum-Frutescens*) Infected with Fungi - Evidence for Methyl-Group Migration from C-13 Nuclear Magnetic-Resonance Spectroscopy. *Journal of the Chemical Society-Chemical Communications*, 293-294 (1975).

169. Whitehead, I. M., Ewing, D. F., Threlfall, D. R., Cane, D. E. & Prabhakaran, P. C. Synthesis of (+)-5-Epi-Aristolochene and (+)-1-Deoxycapsidiol from Capsidiol. *Phytochemistry* **29**, 479-482 (1990).
170. Schenk, D. in *Thesis* (University of Illinois, Urbana, 2000).
171. Storm, D. R. & Koshland, D. E. A Source for Special Catalytic Power of Enzymes - Orbital Steering. *Proceedings of the National Academy of Sciences of the United States of America* **66**, 445-& (1970).
172. Abdullah, M. I., Jackson, A. H., Lynch, P. P. & Record, K. A. F. Electrophilic Substitution in Indoles. 18. Hammett Correlations of the Coupling of Aryl Diazonium Tetrafluoroborates with Indole. *Heterocycles* **30**, 317-320 (1990).
173. Mathis, J. R. et al. Pre-steady-state study of recombinant sesquiterpene cyclases. *Biochemistry* **36**, 8340-8 (1997).
174. Greenhagen, B. T., Griggs, P., Takahashi, S., Ralston, L. & Chappell, J. Probing sesquiterpene hydroxylase activities in a coupled assay with terpene synthases. *Archives of Biochemistry and Biophysics* **409**, 385-394 (2003).
175. Lupien, S., Karp, F., Wildung, M. & Croteau, R. Regiospecific Cytochrome P450 Limonene Hydroxylases from Mint (*Mentha*) Species: cDNA Isolation, Characterization, and Functional Expression of (-)-4S-Limonene-3-hydroxylase and (-)-4S-Limonene-6-hydroxylase. *Archives of Biochemistry and Biophysics* **368**, 181-192 (1999).
176. Teutsch, H. G. et al. Isolation and sequence of a cDNA encoding the Jerusalem artichoke cinnamate 4-hydroxylase, a major plant cytochrome P450 involved in the general phenylpropanoid pathway. *Proceedings of the National Academy of Sciences of the United States of America* **90**, 4102-4106 (1993).
177. Koch, B. M., Sibbesen, O., Halkier, B. A., Svendsen, I. & Moller, B. L. The primary sequence of cytochrome P450^{tyr}, the multifunctional N-hydroxylase catalyzing the conversion of L-tyrosine to p-hydroxyphenylacetaldehyde oxime in the biosynthesis of the cyanogenic glucoside dhurrin in *Sorghum bicolor* (L.) Moench. *Archives of Biochemistry and Biophysics* **323**, 177-186 (1995).
178. Meyer, K., Cusumano, J. C., Somerville, C. & Chapple, C. C. S. Ferulate-5-hydroxylase from *Arabidopsis thaliana* defines a new family of cytochrome P450-dependent monooxygenases. *PNAS* **93**, 6869-6874 (1996).
179. Humphreys, J. M., Hemm, M. R. & Chapple, C. New routes for lignin biosynthesis defined by biochemical characterization of recombinant ferulate 5-hydroxylase, a multifunctional cytochrome P450-dependent monooxygenase. *Proceedings of the National Academy of Sciences of the United States of America* **96**, 10045-10050 (1999).
180. Schoendorf, A., Rithner, C. D., Williams, R. M. & Croteau, R. B. Molecular cloning of a cytochrome P450 taxane 10 beta-hydroxylase cDNA from *Taxus* and functional expression in yeast. *Proc Natl Acad Sci U S A* **98**, 1501-6 (2001).
181. Jennewein, S., Rithner, C. D., Williams, R. M. & Croteau, R. B. Taxol biosynthesis: Taxane 13alpha-hydroxylase is a cytochrome P450-dependent monooxygenase. *PNAS* **98**, 13595-13600 (2001).
182. Frey, M. et al. Analysis of a Chemical Plant Defense Mechanism in Grasses. *Science* **277**, 696-699 (1997).

183. Kaltenbach, M., Schroder, G., Schmelzer, E., Lutz, V. & Schroder, J. Flavonoid hydroxylase from *Catharanthus roseus*: cDNA, heterologous expression, enzyme properties and cell-type specific expression in plants. *Plant Journal* **19**, 183-193 (1999).
184. Holton, T. A. et al. Cloning and expression of cytochrome P450 genes controlling flower colour. *Nature* **366**, 276-279 (1993).
185. Kahn, R. A., Fahrendorf, T., Halkier, B. A. & Moller, B. L. Substrate Specificity of the Cytochrome P450 Enzymes CYP79A1 and CYP71E1 Involved in the Biosynthesis of the Cyanogenic Glucoside Dhurrin in *Sorghum bicolor*(L.) Moench. *Archives of Biochemistry and Biophysics* **363**, 9-18 (1999).
186. Wust, M., Little, D. B., Schalk, M. & Croteau, R. Hydroxylation of limonene enantiomers and analogs by recombinant (-)-limonene 3- and 6-hydroxylases from mint (*Mentha*) species: Evidence for catalysis within sterically constrained active sites. *Archives of Biochemistry and Biophysics* **387**, 125-136 (2001).
187. Gotoh, O. Substrate recognition sites in cytochrome P450 family 2 (CYP2) proteins inferred from comparative analyses of amino acid and coding nucleotide sequences. *J. BIOL. CHEM.* **267**, 83-90 (1992).
188. Schalk, M. & Croteau, R. A single amino acid substitution (F363I) converts the regiochemistry of the spearmint (-)-limonene hydroxylase from a C6- to a C3-hydroxylase. *PNAS* **97**, 11948-11953 (2000).
189. Hedstrom, L., Szilagyi, L. & Rutter, W. J. Converting trypsin to chymotrypsin: the role of surface loops. *Science* **255**, 1249-53 (1992).
190. Pettersson, P. L., Johansson, A.-S. & Mannervik, B. Transmutation of Human Glutathione Transferase A2-2 with Peroxidase Activity into an Efficient Steroid Isomerase. *J. Biol. Chem.* **277**, 30019-30022 (2002).
191. Hayes, R. J. et al. Combining computational and experimental screening for rapid optimization of protein properties. *PNAS* **99**, 15926-15931 (2002).
192. Oue, S., Okamoto, A., Yano, T. & Kagamiyama, H. Redesigning the substrate specificity of an enzyme by cumulative effects of the mutations of non-active site residues. *J Biol Chem* **274**, 2344-9 (1999).
193. Wojciechowski, C. L. & Kantrowitz, E. R. Altering of the metal specificity of *Escherichia coli* alkaline phosphatase. *Journal of Biological Chemistry* **277**, 50476-50481 (2002).
194. Babbitt, P. C. Reengineering the glutathione S-transferase scaffold: A rational design strategy pays off. *PNAS* **97**, 10298-10300 (2000).
195. Nilsson, L. O., Gustafsson, A. & Mannervik, B. Redesign of substrate-selectivity determining modules of glutathione transferase A1-1 installs high catalytic efficiency with toxic alkenal products of lipid peroxidation. *PNAS* **97**, 9408-9412 (2000).
196. Bertoldi, M., Gonsalvi, M., Contestabile, R. & Voltattorni, C. B. Mutation of Tyrosine 332 to Phenylalanine Converts Dopa Decarboxylase into a Decarboxylation-dependent Oxidative Deaminase. *J. Biol. Chem.* **277**, 36357-36362 (2002).
197. Bolon, D. N. & Mayo, S. L. From the Cover: Enzyme-like proteins by computational design. *PNAS* **98**, 14274-14279 (2001).

198. Penning, T. M. & Jez, J. M. Enzyme redesign. *Chemical Reviews* **101**, 3027-3046 (2001).
199. Kushiro, T., Shibuya, M. & Ebizuka, Y. Chimeric triterpene synthase. A possible model for multifunctional triterpene synthase. *Journal of the American Chemical Society* **121**, 1208-1216 (1999).
200. Moore, B. S. & Piel, J. Engineering biodiversity with type II polyketide synthase genes. *Antonie Van Leeuwenhoek* **78**, 397-8 (2000).
201. Ohnuma, S. et al. A pathway where polyprenyl diphosphate elongates in prenyltransferase. Insight into a common mechanism of chain length determination of prenyltransferases. *J Biol Chem* **273**, 26705-13 (1998).
202. Ohnuma, S., Hirooka, K., Ohto, C. & Nishino, T. Conversion from archaeal geranylgeranyl diphosphate synthase to farnesyl diphosphate synthase. Two amino acids before the first aspartate-rich motif solely determine eukaryotic farnesyl diphosphate synthase activity. *J Biol Chem* **272**, 5192-8 (1997).
203. Ohnuma, S. et al. Conversion of product specificity of archaeobacterial geranylgeranyl-diphosphate synthase. Identification of essential amino acid residues for chain length determination of prenyltransferase reaction. *J Biol Chem* **271**, 18831-7 (1996).
204. Ohnuma, S. et al. Conversion from farnesyl diphosphate synthase to geranylgeranyl diphosphate synthase by random chemical mutagenesis. *J Biol Chem* **271**, 10087-95 (1996).
205. Ohnuma, S. et al. A role of the amino acid residue located on the fifth position before the first aspartate-rich motif of farnesyl diphosphate synthase on determination of the final product. *J Biol Chem* **271**, 30748-54 (1996).
206. Kushiro, T., Shibuya, M., Masuda, K. & Ebizuka, Y. Mutational studies on triterpene syntheses: Engineering lupeol synthase into beta-amyrin synthase. *Journal of the American Chemical Society* **122**, 6816-6824 (2000).
207. Back, K. & Chappell, J. Cloning and bacterial expression of a sesquiterpene cyclase from *Hyoscyamus muticus* and its molecular comparison to related terpene cyclases. *J Biol Chem* **270**, 7375-81 (1995).
208. Colby, S. M., Crock, J., Dowdle-Rizzo, B., Lemaux, P. G. & Croteau, R. Germacrene C synthase from *Lycopersicon esculentum* cv. VFNT cherry tomato: cDNA isolation, characterization, and bacterial expression of the multiple product sesquiterpene cyclase. *Proc Natl Acad Sci U S A* **95**, 2216-21 (1998).
209. Bouwmeester, H. J. et al. Isolation and characterization of two germacrene A synthase cDNA clones from chicory. *Plant Physiol* **129**, 134-44 (2002).
210. Mercke, P., Crock, J., Croteau, R. & Brodelius, P. E. Cloning, expression, and characterization of epi-cedrol synthase, a sesquiterpene cyclase from *Artemisia annua* L. *Arch Biochem Biophys* **369**, 213-22 (1999).
211. Crock, J., Wildung, M. & Croteau, R. Isolation and bacterial expression of a sesquiterpene synthase cDNA clone from peppermint (*Mentha x piperita*, L.) that produces the aphid alarm pheromone (E)-beta-farnesene. *Proc Natl Acad Sci U S A* **94**, 12833-8 (1997).
212. Cai, Y. et al. A cDNA clone for beta-caryophyllene synthase from *Artemisia annua*. *Phytochemistry* **61**, 523-529 (2002).

213. Mercke, P., Bengtsson, M., Bouwmeester, H. J., Posthumus, M. A. & Brodelius, P. E. Molecular cloning, expression, and characterization of amorpha-4,11-diene synthase, a key enzyme of artemisinin biosynthesis in *Artemisia annua* L. *Arch Biochem Biophys* **381**, 173-80 (2000).
214. Chang, Y. J., Song, S. H., Park, S. H. & Kim, S. U. Amorpha-4,11-diene synthase of *Artemisia annua*: cDNA isolation and bacterial expression of a terpene synthase involved in artemisinin biosynthesis. *Archives of Biochemistry and Biophysics* **383**, 178-184 (2000).
215. Chen, X.-Y., Chen, Y., Heinstejn, P. & Davisson, V. J. Cloning, Expression, and Characterization of (+)-[delta]-Cadinene Synthase: A Catalyst for Cotton Phytoalexin Biosynthesis. *Archives of Biochemistry and Biophysics* **324**, 255-266 (1995).
216. Facchini, P. J. & Chappell, J. Gene family for an elicitor-induced sesquiterpene cyclase in tobacco. *Proc Natl Acad Sci U S A* **89**, 11088-92 (1992).
217. Steele, C. L., Crock, J., Bohlmann, J. & Croteau, R. Sesquiterpene synthases from grand fir (*Abies grandis*). Comparison of constitutive and wound-induced activities, and cDNA isolation, characterization, and bacterial expression of delta-selinene synthase and gamma-humulene synthase. *J Biol Chem* **273**, 2078-89 (1998).
218. Bohlmann, J., Crock, J., Jetter, R. & Croteau, R. Terpenoid-based defenses in conifers: cDNA cloning, characterization, and functional expression of wound-inducible (E)-alpha-bisabolene synthase from grand fir (*Abies grandis*). *Proc Natl Acad Sci U S A* **95**, 6756-61 (1998).
219. Cane, D. E. et al. Pentalenene Synthase - Purification, Molecular-Cloning, Sequencing, and High-Level Expression in *Escherichia-Coli* of a Terpenoid Cyclase from *Streptomyces* Uc5319. *Biochemistry* **33**, 5846-5857 (1994).
220. Hohn, T. M. & Beremand, P. D. Isolation and nucleotide sequence of a sesquiterpene cyclase gene from the trichothecene-producing fungus *Fusarium sporotrichioides*. *Gene* **79**, 131-8 (1989).
221. Wendt, K. U. & Schulz, G. E. Isoprenoid biosynthesis: manifold chemistry catalyzed by similar enzymes. *Structure* **6**, 127-33 (1998).
222. Wheeler, C. J. & Croteau, R. B. Direct demonstration of the isomerization component of the monoterpene cyclase reaction using a cyclopropylcarbiny pyrophosphate substrate analog. *Proc Natl Acad Sci U S A* **84**, 4856-9 (1987).
223. Cane, D. E. & Tsantrizos, Y. S. Aristolochene synthase. Elucidation of the cryptic germacrene A synthase activity using the anomalous substrate dihydrofarnesyl diphosphate. *Journal of the American Chemical Society* **118**, 10037-10040 (1996).
224. Schwab, W., Williams, D. C., Davis, E. M. & Croteau, R. Mechanism of monoterpene cyclization: stereochemical aspects of the transformation of noncyclizable substrate analogs by recombinant (-)-limonene synthase, (+)-bornyl diphosphate synthase, and (-)-pinene synthase. *Arch Biochem Biophys* **392**, 123-36 (2001).
225. Wheeler, C. J. & Croteau, R. Monoterpene cyclases: use of the noncyclizable substrate analog 6,7-dihydrogeranyl pyrophosphate to uncouple the

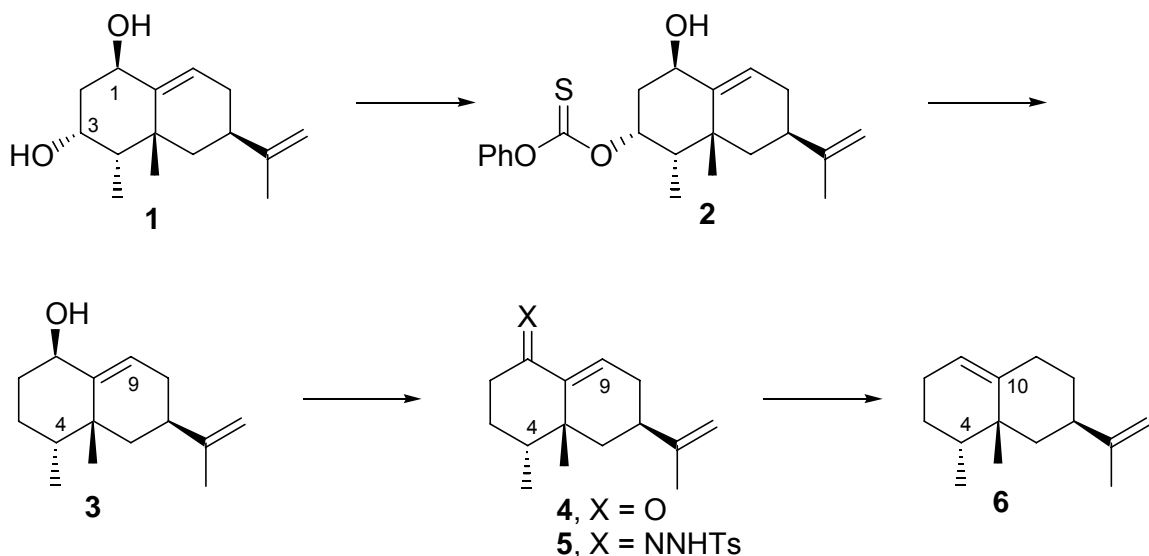
- isomerization step of the coupled isomerization-cyclization reaction. *Arch Biochem Biophys* **246**, 733-42 (1986).
226. Jia, J. W., Crock, J., Lu, S., Croteau, R. & Chen, X. Y. (3R)-linalool synthase from *Artemisia annua* L.: cDNA isolation, characterization, and wound induction. *Archives of Biochemistry and Biophysics* **372**, 143-149 (1999).
 227. Lewinsohn, E. et al. Enhanced levels of the aroma and flavor compound S-linalool by metabolic engineering of the terpenoid pathway in tomato fruits. *Plant Physiology* **127**, 1256-1265 (2001).
 228. Vial, M. V. et al. Enhancement of the hydrolysis of geranyl pyrophosphate by bivalent metal ions. A model for enzymic biosynthesis of cyclic monoterpenes. *Tetrahedron* **37**, 2351-2357 (1981).
 229. Segel, I. H. *Enzyme Kinetics* (John Wiley and Sons, Inc., New York, 1993).
 230. Colby, S. M., Alonso, W. R., Katahira, E. J., McGarvey, D. J. & Croteau, R. 4S-limonene synthase from the oil glands of spearmint (*Mentha spicata*). cDNA isolation, characterization, and bacterial expression of the catalytically active monoterpene cyclase. *J Biol Chem* **268**, 23016-24 (1993).
 231. Rojas, M. C., Chayet, L., Portilla, G. & Cori, O. Substrate and Metal Specificity in the Enzymic-Synthesis of Cyclic Monoterpenes from Geranyl and Neryl Pyrophosphate. *Archives of Biochemistry and Biophysics* **222**, 389-396 (1983).
 232. Stoessel, A., Stothers, J. B. & Ward, E. W. B. Sesquiterpenoid stress compounds of the solanaceae. *Phytochemistry* **15**, 855-872 (1976).
 233. Vogeli, U. & Chappell, J. Induction of Sesquiterpene Cyclase and Suppression of Squalene Synthetase Activities in Plant-Cell Cultures Treated with Fungal Elicitor. *Plant Physiology* **88**, 1291-1296 (1988).
 234. Donadio, S., Staver, M. J., McAlpine, J. B., Swanson, S. J. & Katz, L. Modular organization of genes required for complex polyketide biosynthesis. *Science* **252**, 675-9 (1991).
 235. McRee, D. E. (2001).
 236. Gordon, D. B., Marshall, S. A. & Mayo, S. L. Energy functions for protein design. *Current Opinion in Structural Biology* **9**, 509-513 (1999).
 237. Bennett, M. H., Mansfield, J. W., Lewis, M. J. & Beale, M. H. Cloning and expression of sesquiterpene synthase genes from lettuce (*Lactuca sativa* L.). *Phytochemistry* **60**, 255-261 (2002).
 238. Halkier, B. A. Catalytic reactivities and structure/function relationships of cytochrome P450 enzymes. *Phytochemistry* **43**, 1-21 (1996).
 239. Kahn, R. A., Fahrendorf, T., Halkier, B. A. & Moller, B. L. Substrate specificity of the cytochrome P450 enzymes CYP79A1 and CYP71E1 involved in the biosynthesis of the cyanogenic glucoside dhurrin in *Sorghum bicolor* (L.) Moench. *Archives of Biochemistry and Biophysics* **363**, 9-18 (1999).
 240. Gotoh, O. Substrate Recognition Sites in Cytochrome-P450 Family-2 (Cyp2) Proteins Inferred from Comparative Analyses of Amino-Acid and Coding Nucleotide-Sequences. *Journal of Biological Chemistry* **267**, 83-90 (1992).
 241. Ralston, L. et al. Cloning, heterologous expression, and functional characterization of 5-epi-aristolochene-1,3-dihydroxylase from tobacco (*Nicotiana tabacum*). *Archives of Biochemistry and Biophysics* **393**, 222-235 (2001).

242. Back, K. W. & Chappell, J. Identifying functional domains within terpene cyclases using a domain-swapping strategy. *Proceedings of the National Academy of Sciences of the United States of America* **93**, 6841-6845 (1996).
243. Back, K. & Chappell, J. Cloning and Bacterial Expression of a Sesquiterpene Cyclase from *Hyoscyamus-Muticus* and Its Molecular Comparison to Related Terpene Cyclases. *Journal of Biological Chemistry* **270**, 7375-7381 (1995).
244. Rising, K. A., Starks, C. M., Noel, J. P. & Chappell, J. Demonstration of germacrene A as an intermediate in 5-epi- aristolochene synthase catalysis (vol 122, pg 1861, 2000). *Journal of the American Chemical Society* **122**, 6526-6526 (2000).
245. Mathis, J. R. et al. Pre-steady-state study of recombinant sesquiterpene cyclases. *Biochemistry* **36**, 8340-8348 (1997).
246. Pompon, D., Louerat, B., Bronine, A. & Urban, P. Yeast expression of animal and plant P450s in optimized redox environments. *Cytochrome P450, Pt B* **272**, 51-64 (1996).
247. Urban, P., Mignotte, C., Kazmaier, M., Delorme, F. & Pompon, D. Cloning, yeast expression, and characterization of the coupling of two distantly related *Arabidopsis thaliana* NADPH-Cytochrome P450 reductases with P450 CYP73A5. *Journal of Biological Chemistry* **272**, 19176-19186 (1997).
248. Guedes, M. E. M., Kuc, J., Hammerschmidt, R. & Bostock, R. Accumulation of 6 Sesquiterpenoid Phytoalexins in Tobacco- Leaves Infiltrated with *Pseudomonas-Lachrymans*. *Phytochemistry* **21**, 2987-2988 (1982).
249. de Kraker, J. W., Franssen, M. C. R., de Groot, A., Shibata, T. & Bouwmeester, H. J. Germacrenes from fresh costus roots. *Phytochemistry* **58**, 481-487 (2001).
250. Eggers, M. D., Sinnwell, V. & Stahl-Biskup, E. (-)-Spirolepechinene, a spirosesquiterpene from *Lepechinia bullata* (Lamiaceae). *Phytochemistry* **51**, 987-990 (1999).
251. Williams, P. A., Cosme, J., Sridhar, V., Johnson, E. F. & McRee, D. E. Mammalian microsomal cytochrome P450 monooxygenase: Structural adaptations for membrane binding and functional diversity. *Molecular Cell* **5**, 121-131 (2000).
252. Lupien, S., Karp, F., Wildung, M. & Croteau, R. Regiospecific cytochrome P450 limonene hydroxylases from mint (*Mentha*) species: cDNA isolation, characterization, and functional expression of (-)-4S-limonene-3-hydroxylase and (-)- 4S-limonene-6-hydroxylase. *Archives of Biochemistry and Biophysics* **368**, 181-192 (1999).
253. Haudenschild, C., Schalk, M., Karp, F. & Croteau, R. Functional expression of regiospecific cytochrome P450 limonene hydroxylases from mint (*Mentha* spp.) in *Escherichia coli* and *Saccharomyces cerevisiae*. *Archives of Biochemistry and Biophysics* **379**, 127-136 (2000).
254. Stoessel, A., Stothers, J. B. & Ward, E. W. B. 2,3-Dihydroxygermacrene and Other Stress Metabolites of *Datura- Stramonium*. *Journal of the Chemical Society-Chemical Communications*, 431-432 (1975).
255. Dauben, W. G. General Method of Preparing Functionalized Spirocycles - Synthesis of Spirovetivane Sesquiterpenes. *Journal of the American Chemical Society* **99**, 7307-7314 (1977).

256. Vögeli, U. & Chappell, J. Induction of sesquiterpene cyclase and suppression of squalene synthetase activities in plant cell cultures treated with fungal elicitor. *Plant Physiology* **88**, 1291-1296 (1988).

APPENDIX: Synthesis of 4-epieremophilene

An authentic reference sample of the unknown 4-epieremophilene **6** was synthesized from capsidiol **1** in five steps (Scheme 1).² Regioselective formation of the less hindered phenylthiono carbonate **2** at the equatorial 3 position (PhOC(=S)Cl, pyr-CH₂Cl₂)³ followed by reductive cleavage with tin hydride ((Bu₃Sn)₂O, PHMS, AIBN, BuOH, Benzene, reflux)³ afforded (-)-3-deoxycapsidiol **3** (4-epieremophil-9-en-1-ol, [α]_D -12.7, 69%),⁴ a possible intermediate in the biosynthesis of capsidiol from epiaristolochene.⁵ Swern oxidation ((COCl)₂, DMSO, CH₂Cl₂, -78°C; Et₃N)⁶ provided (-)-4-epieremophil-9-en-1-one **4** ([α]_D -10.6, 98%), the tosylhydrazone (**5**) of which (TsNHNH₂, EtOH, reflux, 1 h, 56%)⁷ underwent conjugate reduction with catechol borane (0°C, 30 min)⁷ and sodium acetate-induced fragmentation (60°C, 50 min)⁷ to give 4-epieremophilene **6** (47 %).⁸



VITA

Bryan T. Greenhagen

BORN: April 14, 1971, Minneapolis, Minnesota

EDUCATION:

December 2000 **University of Kentucky**, Lexington, KY
B.S. in Biology. Conducted one year of undergraduate research while employed in Prof. Joe Chappell's laboratory.

September 1989-
May 1990 **Ithaca College**, Ithaca, NY

PUBLICATIONS:

- Greenhagen, B. and Chappell, J. (2001). Molecular scaffolds for chemical wizardry: Learning nature's rules for terpene cyclases. *Proc. Natl. Acad. Sci. U. S. A.* 98: 13479-13481. (Review)
- Greenhagen, B.T., Griggs, P Takahashi, S, Ralston, L., and Chappell, J. (2003) Probing Sesquiterpene Hydroxylase Activities in a Coupled Assay with Terpene Synthases. *Arch. Biochem. Biophys.* 409: 385-394.
- Greenhagen, B.T., Schoenbeck, M., Yeo, Y., Chappell, J. The Chemical Wizardry of Isoprenoid Metabolism in Plants. (Review) (In press, Recent Advances in Phytochemistry)

Bryan T. Greenhagen